AN ABSTRACT OF THE DISSERTATION OF

Stephen Koghan Ndzeidze for the degree of Doctor of Philosophy in Rangeland Ecology and Management on June 9, 2011
Title: Detecting Medusahead (*Taeniatherum caput-medusae (L.)* Nevski) Using High Frequency, Sequential, Globally Positioned Digital Images

Abstract approved: ____
Douglas E. Johnson

Invasive plant species are expanding and transforming vegetative communities across Oregon and throughout the United States. Over the past three decades remote sensing, geographic information system (GIS), and Global Positioning System (GPS) technologies have been integrated to detect and map the distribution of noxious rangeland plants. This study developed low-cost protocols to detect and map Medusahead (*Taeniatherum caput-medusae* (L.) Nevski) weed infestations using GPS loggers to track aircraft/camera position, altitude, and bearing, as well as Aerial Image Positioning Tool software to geographically rectify and project each aerial image. We then mapped the extent of medusahead in target areas and evaluated patterns of infestation. Flying in a single engine fixed-wing aircraft, images were collected every five seconds, with a total of 10,362 images obtained. All of the aerial images were processed and, on average, 23.9 % of the area was classified as medusahead infested, with 76.1 % without infestation. Each image covered 215 ha (531 acres), with 60% overlap, at a cost of \$ 0.54/km^2. Our study also employed mobile mapping technology to map medusahead on the ground by digitizing infestations using a laptop computer equipped with a GPS antenna and GIS software. Mobile mapping was also done from aircraft, but yielded coarser infestation

maps, as the observation distance was greater. These maps covered the full study area. Aerial reconnaissance and mobile survey is cost effective, because thousands of digital images were collected, automatically positioned, and stored.

Detecting Medusahead (*Taeniatherum caput-medusae (L.)* Nevski) Using High Frequency, Sequential, Globally Positioned Digital Images

by

Stephen Koghan Ndzeidze

A DISSERTATION

submitted to

Oregon State University

in partial fulfillment of
the requirements for the
degree of

Doctor of Philosophy

Presented June 9, 2011
Commencement June 2012

Doctor of Philosophy dissertation of Stephen Koghan Ndzeidze presented on June 9, 2011.

APPROVED:

Major Professor, representing Rangeland Ecology and Management

Head of the Department of Rangeland Ecology and Management

Dean of the Graduate School

I understand that my dissertation will become part of the permanent collection of Oregon State University libraries. My signature below authorizes release of my dissertation to any reader upon request.

Stephen Koghan Ndzeidze, Author

ACKNOWLEDGEMENTS

This work has been realized through concerted efforts made by different people at various levels. I wish to express my profuse gratitude first of Almighty God who gave me the provisions, will, strength and success to go through this program.

A special gratitude and recognition of my supervisor Professor Douglas E. Johnson for his unflinching devotion to the successful realization of this work. His valuable criticisms and immeasurable suggestions have immensely added value to this work and my intellectual ability carry out scientific research and writing. Worth gratifying are my committee members, Professor Jon Kimerling, Professor Michael Borman, Professor Larry Larson and Professor Steve Cook for accepting to serve as members of the committee of my dissertation. Their valuable corrections and directions gave this study the desired standard.

Special thanks go to the general staff of the Department of Rangeland Ecology and management. In particular, I call to mind Dr. Ricardo Mata-Gonzalez and Professor Steven Sharrow for imparting a great deal of knowledge to me that has greatly upgraded my educational standards. Connie Davis, Carolyn Dingus and Raquel Gonzalez made up a wonderful office staff during my stay in the range department.

The effort of Kipp Johnson in programming the Aerial Image Positioning Tool and Michael Johnson in programming VegMeasure2 is specially acknowledged for devoting their valuable time to producing these very important components of our study that greatly improved and enriched the work.

I am immensely indebted to my dear parents Maurice Moyika Ndzeidze and Irene

Lantom Viban for their wonderful moral and spiritual assistance. My brothers and sisters: Beri, Bongsheh, Mlimfenyuy, Verkutumni, Moyika, Njowir and Fonyuy are not left out especially as their prayers and love have encouraged me to come this far.

Whole-heartedly I acknowledge with special thanks the United States Institute of International Studies for awarding me the Fulbright scholarship to Oregon State University in the Department of Geosciences where I obtained my masters and the Department of Rangeland Ecology and Management where I am obtaining my PhD with funding from United State Department of Interior, Bureau of Land Management. This was through the Burns District Harney County Weed Management Area, and the Oregon Agricultural Experiment Station. They funded and supported the collection of data through Ms. Lesley Richman (USDI/BLM), who provided the guidance and technical support.

The mention of product names or corporations is for the convenience of the reader and does not constitute an official endorsement or approval by the US Department of Interior, Oregon State University or the Oregon Agricultural Experiment Station of any product or service to the exclusion of others that may be suitable.

CONTRIBUTION OF AUTHORS

Stephen K. Ndzeidze was involved with all the phases of fieldwork, including data collection protocol design, analysis, GIS and remote sensing analysis and image processing. Dr. Douglas E. Johnson was involved with all the phases of fieldwork including data collection protocol design, analysis, GIS and remote sensing analysis and image processing. Kipp Johnson wrote the Aerial Image positioning tool for image georectification and Michael Johnson wrote the Vegmeasure2 software for image processing and this was reviewed by Dr. Louhaichi Mounir. Mike Halbleib was involved with aerial image collection. Mike Iademarco helped read and edit manuscripts.

TABLE OF CONTENTS

Page

TABLE OF CONTENTS (Continued)

TABLE OF CONTENTS (Continued)

Page

TABLE OF CONTENTS (Continued)

LIST OF FIGURES

LIST OF FIGURES (Continued)

LIST OF FIGURES (Continued)

LIST OF FIGURES (Continued)

LIST OF TABLES

LIST OF APPENDICES

LIST OF EQUATIONS

DETECTING MEDUSAHEAD (*TAENIATHERUM CAPUT-MEDUSAE (L.)* NEVSKI) USING HIGH FREQUENCY, SEQUENTIAL, GLOBALLY POSITIONED DIGITAL IMAGES

CHAPTER 1: INTRODUCTION AND SCIENTIFIC BACKGROUND

REMOTE SENSING FOR THE DETECTION OF INVASIVE WEEDS

The spread of invasive weeds has long been recognized as one of the most significant environmental threats due to their ability to decrease biodiversity and alter ecosystem processes. The use of remote sensing to detect and map invasive weeds has become a high priority for rangeland resource managers and other natural resource researchers across the United States. Over the past three decades remote sensing, geographic information system (GIS), and Global Positioning System (GPS) technologies have been integrated for the detection and mapping of the distribution of noxious rangeland plants (Dewey *et al*., 1991; Anderson *et al*., 1996; Everitt *et al*., 1996; Everitt *et al*., 2001a). Remote observations in georeferenced formats help to monitor and assess the extent of infestations, to observe and track changes, to develop management strategies, and to evaluate control measures on noxious plant populations.

Invasive weeds not only compete with natives on a species scale, but can alter the primary productivity, decomposition, hydrology, geomorphology, nutrient cycling, and natural disturbance regimes in an ecosystem (Vitousek and Walker 1989, Mack *et al*., 2000). Interest in, and research on, invasive weeds on rangelands has accelerated as a result of increasing numbers of non-native species invading and threatening the physical and biological components of the rangeland ecosystem. Nonetheless, the ecological and economic impacts of non-native species continues to grow, raising the question of how to best apply science to the regulation and management of invasive plants (Sheley *et al*., 2010). Introduced species do not always become invasive in their new environment. Here we define a species as invasive when it readily propagates across landscapes with or without being facilitated by human or natural disturbances (e.g. fire, deforestation, hurricanes) (Asner *et al*., 2008). Remote sensing technology, such as aerial photography and satellite imagery, have evolved to have far reaching success in detecting many different invading species found in forests, rangelands, and pasture environments. The use of low flying aircraft, helicopters and balloons to aid in the collection of very high-resolution aerial photographs has helped to successfully distinguish targeted infestations (cf. Everitt *et al*., 1996: Anderson *et al*., 1996; Bellmund and Kitchens, 1997; Pearlstine *et al*., 1998). Multispectral satellite remote sensing studies have had success using broad and narrow band images to identify and distinguish some plant species, including noxious weeds (Anderson *et al*., 1993; Everitt *et al*., 1994; Carson *et al*., 1995; Lass *et al*., 1996, 2002; Lass and Callihan, 1997; Parker and Hunt, 2002).

Early work on weed detection in rangeland and pastures using aerial photographs has been generally limited to small areas due to the high cost of near-infrared image acquisition and photo interpretation (Arnold *et al*., 1985). Very little progress has been made over the years in the use of aerial photography to detect and map weeds in rangelands and pastures. The absence of quantitative data, the high cost of color-infrared film and processing, variable interpretations, and the requirement for manual scanning or digitizing to use information in a geographic information system (GIS) are some of the problems that need to be overcome (Arnold *et al*., 1985). Aerial photographs and camera-on-stick (camera mounted on a pole) and cross sectional ground-truth surveys provide the finest spatial resolution and capture the spatial and textural essence better than any other procedure (Tueller, 1989).

The use of digital cameras has greatly improved the spatial resolution of aerial photography and resulted in the use of color images for weed detection at both large and small scales. A major advantage of smaller size cameras is that they are lighter weight and can be attached to kites, balloons, and ultralite or unmanned aircraft (cf. Haefner, 2004; Lindholm, 2004). However, the principal problems with these images are complications from image rectification and co-registration with ground coordinates. Until now, this continues to limit their use to the more expensive systems that integrate pitch, roll, and yaw measurements with GPS data to determine location when imaging large areas.

We focused on creating a program to tag aerial photos with GPS coordinates using trigonometric functions to calculate scope and pixel size and correct for geometric error generated by aircraft heading and altitude while investigating the invasive weed Medusahead -*Taeniatherum caput-medusae (L.)* Nevski in central Oregon.

STUDY HYPOTHESIS AND OBJECTIVES

This study proposes to develop low-cost techniques that can detect, map, and monitor medusahead infestations based upon the GPS tracking and the VegMeasure 2 software, which was developed by Johnson *et al*. (2009). Using these techniques, we mapped the extent of medusahead in target areas. This information can be used to evaluate rates of spread, efficacy of control methods, and the success or failure of existing control programs.

STUDY HYPOTHESES

The utilization of high-resolution, automatically positioned, aerial imagery, with updated and improved software, for better tracking and positioning of imagery and mobile mapping system operational protocols, can provide easier low cost data acquisition and the efficient detection, mapping, classification and monitoring of weeds for better rangeland resource management.

STUDY OBJECTIVES

Objectives of this project are to develop sampling protocols for monitoring weed infestations, and improve on the equipment and software components of Aerial Image Positioning Tool, VegMeasure 2, Digital Charting, and GPS-enabled computer-based mobile mapping. These include:

- Refining the mobile mapping techniques used to identify infestations on the ground.
- Development of digital photographic charting protocols for documenting infestation density, cover, and diversity on the ground using better tracking hardware with easier data downloading.

- Creation of a low-cost and efficient data collection system for high-resolution aerial imagery with auto referencing (geographic registration) and processing, so that large numbers of images can be collected and easily processed and stored.
- Employment of better tracking hardware with easier data download, resulting in low cost and efficient data collection of high resolution aerial imagery and processing for better detection, monitoring and classification of medusahead.
- Update VegMeasure2 Software (Johnson *et al.*, 2009) with: 1) specific classification algorithms for medusahead, 2) more classification algorithms, and 3) four band (red, green, blue, and near infrared) analysis capabilities.
- Production of infestation maps for the Harney County Weed Management Area (approximately 667,077 ha or 2,575 mi^2 were photographed and classified).
- Field-testing and refinement of data collection protocols for medusahead distribution and spread on experimental locations in Harney County.
- Documentation of operational protocols that can be used countywide to detect, map, and monitor medusahead infestations.

While our project focused on the detection of medusahead, the technologies used are applicable to other visually distinct weed or vegetation types.

CHAPTER OUTLINES

This dissertation begins with Chapter 1, a general background of invasive weed detection by remote sensing. This research explores the literature available pertaining to invasive weeds in general, for both the geospatial and biological aspects of infestations and their distribution across landscapes. The second part of the introduction outlines the scientific background of the study. This section consists of the theoretical and conceptual framework of the study.

In Chapter 2, the socio-economic, environmental, and ecological implications of medusahead infestation are addressed. The chapter also focuses on the history of medusahead establishment in conterminous United States.

In Chapter 3, the persistent challenge of transferring aerial photographic imagery to planimetric base maps is discussed. It is for this purpose that the Aerial Image Positioning Tool is programmed for collecting and storing sequential digital aerial images for rapid Coarse Geo-referencing.

Chapter 4 addresses the mobile mapping of medusahead (*Taeniatherum caput-medusae* (L.) Nevski) infestations using road/trail surveys using a GPS-enabled computer, GIS software, and digital orthophotographic and topographic maps. This is the full spectrum of spatial analysis for infestations across the landscape with the associated geospatial techniques used in conjunction with currently available, commonly used geographic information systems (GIS) and associated hardware, including hand held computers, Global Positioning System receivers, mobile GIS, and computing software.

Chapter 5 focuses specifically on the use of sequential, GPS positioned digital color aerial photography collected within a strict protocol and analyzed with dedicated software as a means of mapping medusahead. In this chapter, we look at the development of digital photographic charting protocols for documenting infestation density, cover, and diversity on the ground by using improved tracking hardware with easier data download. In this chapter, we also discuss a low-cost and efficient data collection system for high-resolution aerial imagery with auto-geographic registration using the aerial image positioning tool and image processing with VegMeasure2.

Chapter 6 summarizes the arguments advanced in this dissertation and offers a roadmap for future research using new mapping protocols and the improved KRESS tracker in conjunction with the Aerial Image Positioning Tool.

LITERATURE REVIEW

REMOTE SENSING

Airborne Methods and Noxious Weed Detection

Although satellite imagery has been available for nearly 30 years, relatively few studies have reported its use for detecting noxious plants. The relatively coarse spatial resolution of satellite sensor data, as compared to aerial photography and videography, has limited its usefulness for this application. Nonetheless, satellite sensors have shown potential for detecting relatively large stands of weeds (Hunt *et al*., 2003).One of the most important factors for distinguishing noxious species is obtaining the aerial photographs at the proper phenological stage, usually during flowering (Hunt *et al*., 2003). Gausman *et al*. (1977b) conducted aerial photography research at Weslaco on the utilization of remote sensing for detecting noxious plants. They described the light reflectance of silverleaf sunflower (*Helianthus argophyllus* Torr. and A. Gray) and demonstrated that aerial color-infrared (CIR) (0.50 - to 0.90 - m) photography could be used to distinguish this annual weed on south Texas rangelands. The ability to remotely distinguish silverleaf sunflower was attributed to its white pubescent foliage that gave it higher visible (0.45 - to 0.75 - *m*m) reflectance than other associated species.

Aerial photographs are the most often used remote-sensing technique for detecting plant species. They can provide area estimates of plant populations, and have been used as a tool for quantitative assessment of infestations by alien plants and the dynamics of their spread (Mullerova, 2005; Everitt, 1998; Higgins and Richardson, 1999; McCormick, 1999; Stow *et al*., 2000; Higgins, Richardson and Cowling, 2001; Rouget *et al*., 2001, 2003; Shaw, 2005; Fuller and Boorman, 1977; Mast *et al*., 1997). Remote sensing studies have had success using broad and narrow band images to identify and distinguish some plant species, including noxious weeds (Anderson *et al*., 1993; Everitt *et al*., 1994; Carson *et al*., 1995; William, 2000; Lass *et al*., 1996, 2002; Lass and Callihan, 1997; Parker and Hunt, 2002). Aerial imaging has also been effectively used for weed detection in two ways (Shaw, 2005). First, the detection of invasive species in rangeland and natural areas has been shown for a number of species. Detecting these species does not require early recognition and control, and spatial resolutions of these systems are sufficient for detecting patches that are usually expected (Shaw, 2005). Key phenological differences (e.g, flower or leaf color) can often be determined at different points in the season, making it much easier to use the existing spectral bands to detect a given species (Rew *et al*., 2005; Lass *et al*., 2005).

Aerial photographs work best for weed detection when plants have unique growth patterns, different from surrounding vegetation and have been used to detect saltcedar

(*Tamarix ramosissima* Ledeb.), leafy spurge (*Euphorbia esula* L.), and Brazilian pepper (*Schinus terebinthifolius* Raddi) (cf. Lass *et al*., 2005; Everitt *et al*., 1996; Anderson *et al*., 1996; Bellmund and Kitchens, 1997; Pearlstine *et al*., 1998). Aerial photography has not been widely used for weed detection in rangeland and pastures due to the absence of quantitative data, the high cost of color-infrared film and processing, variable interpretations, and the requirement for manual scanning or digitizing before using the data in geographic information systems (Arnold *et al*., 1985). Recent technological advances in digital aerial photography have improved spatial resolution, and color images are once again being use for weed detection in limited areas.

Tang *et al.* (2001) developed a sensor-based, high resolution, real time, field-mapping system. Vegetation density, weed density, crop population, spectral information, in addition to incoming irradiance and global positioning, could be collected in real time. Cameras suspended 3.2 m above the soil surface (without shading) showed variations in camera performance due to the variable outdoor lighting.

Wood *et al*. (2006), while focusing on the utility of remote sensing for detecting weed infestations, argues that this depends upon the potential to map large areas accurately using automated techniques that process and classify imagery with relative technological ease. Both spatial and spectral resolutions impact the accuracy with which individual species are mapped (Wood *et al*., 2006). Moderate resolution satellite imagery is more suited to mapping at the community level as the spatial resolution is generally too coarse to distinguish individual species, unless represented as a monoculture (Dewey *et al*., 1991; Everitt and Escobar, 1996; Sohn and McCoy, 1997). Cochrane (2000), and Okin *et al*. (2001), identified the contrast between satellite imagery and aerial photography in that air photos are capable of producing very high spatial resolution, often less than 1 m. Anderson *et al*., (1996) did a study of airborne digital imagery and noted that it is possible to achieve spatial resolutions similar to aerial photography, and methods for processing and spectrally classifying the imagery can be automated, allowing for more efficient landscape-scale coverage. Most airborne digital imagery is multispectral, meaning that the electromagnetic energy is recorded in a few, distinct spectral bands, such as blue, green, red, and NIR (Lillesand and Kiefer, 2000 and Lass and Callihan, 1997). In Idaho, 4-band multispectral imagery captured from fixed wing aircraft with very high spatial resolution has been used to map several invasive plants (cf. Carson *et al*., 1995; Lass *et al*., 1996; Lass and Callihan, 1997).

GPS and Weed Mapping

The Global Positioning System is a satellite based navigation system made up of a network of 24 satellites placed into orbit by the U.S. Department of Defense. GPS was originally intended for military applications, but in the 1980s, the government made the system available for civilian use. GPS works in any weather condition, anywhere in the world, 24 hours a day. There are no subscription fees or setup charges to use GPS. GPS is one of the many technologies that make precision weed mapping effective by allowing rangeland managers to collect area, point, and line features for proper spatial display of referenced field information such as weed location. GPS allows the ground samples to be located and permits the integration of

GIS software. Studies on GPS use by Webster and Cardina (1997), Stafford et al. (1996), and Kvien *et al*. (1995) found that the GPS can be a very valuable instrument in agricultural research. For example, researchers can map a field using a GPS to explore spatial relationships between landscapes and weed invasion, growth, and extinction at a particular site. In addition, crop scouts can use a GPS to map weed infestations, locate environmentally sensitive areas, and monitor the effectiveness of management practices. One area where GPS techniques could aid in weed management is facilitating the study of spatial dynamics of perennial weed patches over time. Stafford et al. (1996) showed that a GPS with 1 to 2m accuracy estimated the area of a $100m^2$ patch to be within 92 to $126m^2$. However, because weed patches vary greatly, it was necessary to determine whether acceptable accuracy could be achieved over a range of patch sizes. Since weed research studies may be conducted in growers' fields over time, the GPS may be useful in relocating experiment units and in interfacing data to a geographic information system (GIS). He also noted that a compact hand-held data logger, based on a palm-top PC linked to a differential Global Positioning System (GPS) system in a backpack, has been developed to aid the farmer during field walking. It can record weed information and position, which is displayed on a screen map for later updating of a 'master' field weed map held on the farm PC (Stafford *et al*., 1996).

Other related work on GPS and remote sensing with aerial and satellite imagery for yield and weed mapping includes the work of Webster *et al.* (2000), who discussed expansion patterns, and mapping assessments for a hard to kill perennial weed *Apocynum cannabinum.* Webster *et al.* (2000), further indicated that identification of individual plants of this weed with remote sensing was difficult; however, the colonial nature of the weed would allow identification using remote sensing. Tillet *et al*. (2001) developed a computer vision system for estimating crop and weed plants. Rew and Cousens (2001) indicate that discrete sampling of weeds has been the most common method for weed identification and mapping. Van Wychen *et al*. (2002) analyzed the effectiveness of GPS-assisted mapping of wild oats in cereal and Lass and Callihan (1993) on GPS and GIS for weed surveys and management. Ndzeidze *et al.* (2010 a and b) examined mobile mapping of medusahead and detection using high frequency, sequential, GPS data.

This study will describe a mapping system that can be used to identify weed densities with specific geographic locations. This system will overlay GPS coordinates on a base map during a mobile drive-through using GIS software like Global Mapper and NAIP images. Automated GPS mapping of images with an indication of location (latitude and longitude) is a new method for monitoring weed infestations across the landscape (Stafford *et al*., 1996).

Mobile mapping and Ground-based systems

In contrast to aerial imaging, ground-based mobile mapping systems take a fundamentally different approach in that a GPS and a laptop computer mounted on a truck, with a drive through expedition, is conducted to detect and map weeds in the field. A significant and elaborate conceptual background of Mobile Mapping System has been reviewed by Grejner-Brzezinska (2004). Grejner-Brzezinska (2004) presented the Mobile Mapping: Operational Aspects with the concept of the Mobile Mapping System (MMS) dating back to the late 1980s, when The Ohio State

University Center for Mapping initiated the GPSVan™ project, leading to the development of the first directly georeferenced and fully digital land-based mapping system in 1991. A list of major existing land-based mobile mapping systems, and more details on the modern sensors and airborne systems, can be found in Grejner-Brzezinska (2001a; 2001b).

The capabilities and functionality of hand-held computers, mobile GIS, and related mobile location technology for scientific purposes are described by many researchers (Pundt and Brinkkötter-Runde, 2000; Vivoni and Camilli, 2003 and others). Wagtendonk and De Jeu (2007) provide convincing evidence that the application of mobile technology is very successful in the long term. In fact, critical reviews of mobile GIS methods are infrequent. Authors such as Clarke, (2004) and Nusser *et al*. (2004) propose the development of new models and methods for the use of mobile GIS and mobile computing in scientific data collection on the research agenda (Wagtendonk and De Jeu, 2007). Missing in this respect are sound methodological principles for the design and evaluation of mobile computing methods, prior to and after their application (Wagtendonk and De Jeu, 2007).

Georectification of aerial photographs and weeds mapping

Ever since aerial imagery was first used in 1858 by Gaspar Felix Tournachon to capture photographic images of his village from a balloon, complications from image rectification and co-registration have remained one of the major challenges in the scientific use of aerial photography. Up to date ground coordinates continue to limit use to the more expensive systems that integrate pitch, roll, and yaw measurements with global positioning system (GPS) data to determine location when imaging large areas. Since the mid 20th century, aerial photography has been widely used in rangeland assessment and management to detect changes in land cover and land use. Geo-rectifying these images for weed detection has remained a major challenge to range scientists. However, studies using very high-resolution images have been able to detect invasive weeds. Aerial photography has been used to successfully detect and map a number of rangeland and pasture weed species, including Dyers wood (*Isatis tinctoria* L.), yellow hawkweed (*Hieracium pratense*), yellow starthistle (*Centaurea*), and Ashe (*Juniperus*) (Dwey *et al*., 1991; Lass *et al*., 1996; Everitt *et al*., 2007). Lestak *et al*., (2007) geo-corrected aerial photographs of Barrow, Alaska, taken from 1948 to 2002 to map land cover and land use changes.

This study will aid in the development of a camera mount that can be used on several types of aircraft as well as software for automatic positioning and correction of aerial images for use in GIS.

Image processing software for invasive weeds

Image processing methods used to detect and classify invasive weeds depend on the researchers' experience with hyperspectral satellite images. Supervised classification techniques, including minimum distance, Mahalanobis distance, maximum likelihood, spectral angle mapper (SAM), and mixture tuned matched filtering (MTMF), were used to classify the images, with ENVI chosen as the image processing software (Yang and Everitt, 2010). These first three classifiers are traditionally used for multispectral image classification, while SAM and MTMF are used for hyperspectral image classification (Yang and Everitt, 2010). Other spectral un-mixing techniques to classify invasive weeds include the Parker and Hunt (2002) method for the estimation of leafy spurge cover from hyperspectral imagery using the mixture tuned matched filtering of Miao *et al*. (2006) for the estimation of yellow starthistle abundance through CASI-2 hyperspectral imagery with linear spectral mixture models. Hunt *et al*. (2003) provide a comprehensive review of the technology and algorithms used to process data for remote sensing of weeds in pasture and range, and a working example for the detection of spotted knapweed (*Centaurea maculosa Lam. Syn. C. biebersteinii DC. or C. stoebe L. subsp. microanthos (Gugler) Hayek)* and babysbreath *(Gypsophila paniculata L.)*.

Classifying images from remotely sensed data enhances detection of infestations (Hunt *et al*., 2003; Yang and Everitt, 2010). Booth *et al*. (2004) discussed the calibration of threshold levels in vegetation-cover classification software in rangelands. Johnson *et al*. (2004) developed an algorithm and protocols within a software package called VegMeasure2 (Johnson *et al*., 2009) that can be used to measure the percent cover of foliage, litter, and bare ground or other parameters of interest in electronically positioned and defined quadrats. Detection abilities have improved because sensor technology and classification techniques have become more sophisticated.

CONCEPTUAL FRAMEWORK

Conceptual and operational approaches for remote detection and mapping of biodiversity, especially invasive species, are currently lacking because we have an insufficient biophysical understanding of when remotely sensed signatures indicate the presence of unique species (native, introduced, or invasive) within and across ecosystems (Asner, 2008). By remote sensing signatures, we are referring generally to the spectral, temporal, angular, or spatial information contained in an observation, often obtained from airborne or space-borne instruments. For rangeland vegetation detection using aircraft mounted with a camera, these spectral signatures are determined by a combination of red, green, and blue reflection in the visible wavelengths of the electromagnetic spectrum. Other vegetation types can be detected using hyperspectral sensing of leaf biochemical and canopy structural properties that include pigment, water and N concentrations, specific leaf area (SLA; leaf area per unit mass), canopy leaf area index (LAI), leaf angle distributions and stem/branch architecture for the spectral signature (Asner, 2008). Our study is based on the spectral separability of medusahead, using a presence and absence classification on high spatial resolution aerial digital images.

The conceptual framework for detecting and mapping invasive weeds using high frequency, sequential, globally positioned digital images allows researchers to assess the effectiveness of weed monitoring and mapping strategies. This entails development and application of very low cost protocols for weed mapping. The management concern at this point is gathering data on weed location and making the information easily available for incorporation into management strategies. As a new management strategy, detection and mapping using low cost high frequency, sequential and globally positioned images, allows the development of immediate comprehensive plans to make weed locations and distributions available to control agents. The GPS and laptop computer with a large capacity external hard drive enables the sequential collection of aerial images, mobile mapping, and transect mapping of weeds across the landscape. Given the increasing need to limit the dispersal and spread of invasive weeds, this protocol may be applied widely in the future.

Most of the weed species that cause significant problems on rangelands, such as medusahead, have been introduced from other continents (DiTomaso, 2000). Management practices, particularly fire suppression and overgrazing, have increased the proportion of some weed and undesirable weed species. These natives reduce the overall forage quality or quantity (e.g., *Juniperus spp*, *Artemisia tridentata*, and *Gutierrezia*) and poison livestock (e.g., *Delphinium*, *Astragalus*, and *Amsinckia menziesii*. *intermedia*). They can be annuals (e.g., *Centaurea solstitialis, Crupina vulgaris, Bromus tectorum*), biennials (e.g., *Carduus nutans*, *Conium maculatum, Onopordum acanthium*), long-lived herbaceous perennials (e.g., *Convolvulus arvensis, Centaurea maculosa, Cirsium arvense*), shrubs (e.g., *Gutierrezia*., *Artemisia tridentata*), or trees (e.g., *Juniperus*spp., *Prosopis glandulosa*). Although several plant families are represented, the largest number of noxious species belongs to the *Asteraceae* (sunflower) family (DiTomaso, 2000).

This study also implemented hardware, software, and protocols for monitoring medusahead (*Taeniatherum caput-medusae (L.) Nevski*) and other weed infestations in Harney County, Oregon. These methods include both direct sampling and remote sensing technologies. The direct sampling process used Mobile Mapping (real-time mapping in the field with GIS software on GPS-equipped laptop computers), and Digital Photographic Charting (GPS registered digital photographs taken with a staff-mounted camera). Aerial reconnaissance was employed using GPS-positioned digital cameras. Aerial images taken downward vertically were obtained at 5-second intervals over target landscapes using a Canon camera mounted in the belly of a Cessna 182 aircraft. The aircraft and camera were tracked continuously at a one second interval with recording GPS loggers to determine the position of the camera (latitude, longitude, and altitude) for each photo. The GPS tracklogs were also used to determine the bearing and speed of the camera, which was used to orient the image. Approximately 10,000 high-resolution digital aerial images were taken over Harney County landscapes during this project.

Software (Aerial Image Positioning Tool) geo-referenced and converted these aerial photos into GIS-ready format. The images were rough corrected so as to be oriented, scaled, and positioned correctly. Terrain distortion and minor positional distortions may remain in the images; however, they are generally accurate to within 150 m.

VegMeasure2 was also used in this project. This program automatically extracts the spectral signatures (red, green and blue color space/pixel values) for objects of interest visible in photographs. VegMeasure2 allows the operator to set tolerance levels around color spaces and automatically classify all images taken under similar light conditions during a photo shoot. Single feature classification e.g, medusahead infestations) or multi-feature classifications, (e.g. medusahead, cheatgrass, bare soil, perennial grass, juniper, etc), can be generated using this software. Outputs can be in either Arc ASCII or bitmap formats.

The concept of detection, mapping, and image processing of medusahead infestations is based on a combination of GPS antenna, data logger, compass, level, staff, digital camera software and a computer system that permits the collection of photographic aerial images and quadrat data that can be analyzed in any of several image processing software packages (VegMeasure2, ERDAS, Global Mapper, ENVI, IDRISI, PCI etc.).

Over the course of the project, we surveyed and documented weed infestations by direct observation along 270 km of roadway with the subsequent digitization of 410 medusahead polygons. These areas were used as reference infestations so that spectral signatures could be extracted, permitting the identification of more remote infestations on high-resolution aerial images. As a result, we merged GPS, remote sensing (RS) and GIS technologies into a package that allows us to rapidly identify infestations over extensive landscapes.

CONCLUSION

The detection, mapping, and image processing for medusahead using high frequency, sequential, globally positioned digital images utilizes the application of remote sensing and GIS technologies for possible solutions to invasive weed detection and monitoring. Problem identification, definition, and information research are the first three steps that lead to the proper selection of appropriate remote sensing instruments and programs. High-resolution aerial images and image processing algorithms for classification provide the data to indicate the presence or absence of infestations across a landscape.

LITERATURE CITED

Anderson, G. L., J. H. Everitt, D. E. Escobar, N. R. Spencer, and R. J. Andrascik. 1996. Mapping leafy spurge (*Euphorbia esula*) infestations using aerial photography and geographic information systems. Geocarto International 11:81-89.

Anderson, G.L., C.W. Prosser, S. Haggar, and B. Foster, 1999. Change detection of leafy spurge infestations using aerial photography and geographic information systems, pp. 223-230, In: P. T. Tueller (ed.), Proceedings of the 17th Biennial Workshop Color Aerial Photography and Videography in Resource Assessment. American Society of Photogrammetry and Remote Sensing, Bethesda, MD.

Arnold, G. W., P. G. Ozanne, K. A. Galbraith, and F. Dandridge. 1985. The capeweed content of pastures in south-west Western Australia. Australian Journal of Experimental Agriculture 25:117-123.

Asner, G. P., M. O. Jones, R. E. Martin, D. E. Knapp and R. F. Hughes. 2008. Remote sensing of native and invasive species in Hawaiian forests. Remote Sensing of Environment 112:1912-1926.

Asner, G.P., C. A. Wessman, C. A. Bateson, and J. L. Privette. 2000. Impact of tissue, canopy and landscape factors on the hyperspectral reflectance variability of arid ecosystems. Remote Sensing of Environment 74:69-84.

Bethany A. B. and J. F. Mustard. 2006. Characterizing the Landscape Dynamics of an Invasive Plant and Risk of Invasion Using Remote Sensing. Ecological Applications 16(3):1132-1147.

Byers, J.E., S. Reichard, J. Randall, I. Parker. 2002. Directing research to reduce the impacts of nonindigenous species. Conservation Biology 16(3): 630-640

Booth, D. T., S.E. Cox, M. Louhaichi, and D. E. Johnson. 2004. Technical Note: Lightweight Camera Stand for Close-to-Earth Remote Sensing. Journal of Range Management 57:675-678.

Booth, D. T., S.E. Cox, and D.E. Johnson. 2004. Calibration of Threshold Levels in Vegetation-Cover Classification Software. 57th Annual Meeting for the Society for Range Management. 24th-30th January 2004 in Salt Lake City, USA.

D'Antonio, C.M., N.E. Jackson, C.C. Horvitz, and R. Hedberg. 2004. Invasive plants in wildland ecosystems: merging the study of invasion processes with management needs. Frontiers in Ecology and the Environment 2: 513-521.

Carson, H.W., L.W. Lass, and R.H. Callihan.1995. Detection of yellow hawkweed with high-resolution multispectral digital imagery. Weed Technology 9:477-483.

Cochrane, M. A. 2000. Using vegetation reflectance variability for species level classification of hyperspectral data. International Journal of Remote Sensing 21:2075-2087.

Daniel, D., D. K. Giles, D. C Slaughter. 2003. Ground based vision identification for weed mapping using DGPS. American Society of Agricultural and Biological engineers. Paper No: 031005. ASAE Annual International Meeting. July 27-30 Las Vegas, Nevada.

David, R. S. 2005. Remote sensing and site-specific weed management. Frontiers in Ecology and the Environment 3: 526-532.

Dewey, S.A., K.P. Price, and D. Ramsey. 1991. Satellite remote sensing to predict potential distribution of Dyers woad (*Isatis tinctoria*). Weed Technology 5:479-484.

DiPietro, D. Y. 2002. Mapping the Invasive Plant *Arundo donax* and Associated Riparian Vegetation Using Hyperspectral Remote Sensing. M.A. thesis. Davis, CA: University of California, Davis, 49 p.

DiTomaso, J. M. 2000. Invasive weeds in rangelands: species, impacts, and management. Weed Science 48:255-265.

Grejner-Brzezinska, D. A., R. Li, N. Haala, and C. Toth. 2004. From Mobile Mapping to Telegeoinformatics: Paradigm Shift in Geospatial Data Acquisition, Processing, and Management. Photogrammetric Engineering and Remote Sensing 70(2):197-210.

Grejner-Brzezinska, D. 2001a. "Mobile Mapping Technology: Ten Years Later (Part One), Surveying and Land Information Systems, 61(2):75-91.

Everitt, J.H., C. Yang, B.J. Racher, C.M. Britton and M.R. Davis. 2001. Remote sensing of redberry juniper in the Texas Rolling Plains. Journal of Range Management 54:254-259.

Everitt, J.H. and C.J. Deloach. 1990. Remote sensing of Chinese Tamarisk (*Tamarix chinensis*) and associated vegetation. Weed Science 38:273-278.

Everitt, J. H., and D. E. Escobar. 1996. Use of spatial information technologies for noxious plant detection and distribution on rangelands. Geocarto International *11*:63-80.

Everitt, J. H., D. E. Escobar, and M. R. Davis. 2001. Reflectance and image characteristics of selected noxious rangeland species. Journal of Range Management 54:A106–A120.

Everitt, J. H., D. E. Escobar, M. A. Alaniz, and M. R. Davis. 1987. Using airborne middle-infrared (1.45–2.0 mm) video imagery for distinguishing plant species and soil conditions. Remote Sensing of Environment 22: 423-428.

Everitt, J. H., D. E. Escobar, M. A. Alaniz, and M. R. Davis. 1991. Light reflectance characteristics and video remote-sensing of prickly pear. Journal of Range Management 44:587-592.

Everitt, J. H., D. E. Escobar, M. A. Alaniz, M. R. Davis, and J. V. Richerson. 1996. Using spatial information technologies to map Chinese tamarisk (*Tamarix* *chinensis*) infestations. Weed Science 44:194-201.

Everitt, J. H., M. A. Alaniz, and D. E. Escobar. 1992. Using remote sensing to distinguish common goldenweed (*Isocoma coronopifolia*) and Drummon goldenweed (*Isocoma drummondii*). Weed Science 40:621-628.

Everitt, J.H., G.L. Anderson, D.E. Escobar, M.R. Davis, N.R. Spencer and R.J. Andrascik.1995. Use of remote sensing for detecting and mapping leafy spurge (*Euphorbia esula*). Weed Technology 9:599-609.

Everitt, J.H., C.Yang and H.B. Johnson. (2007). Canopy spectra and remote sensing of Ashe juniper and associated vegetation. Environmental Monitoring and Assessment 130:403-413.

Everitt, J.H., C.Yang, M.A. Alaniz, and M.R. Davis. 2006. Using spatial information technologies to detect and map invasive weeds in Texas riparian zones and waterways. MAPPS/ASPRS Fall Conference, November 6-10, 2006 San Antonio, Texas.

Everitt, J.H., C.Yang, M.A. Alaniz, M.R. Davis, F.L. Nibling, and C.J. Deloach. 2004. Canopy spectra and remote sensing of giant reed and associated vegetation. Journal of Range Management 57:561-569.

Fuller, R.M. and L.A. Boorman.1977. The spread and development of *Rhododendron ponticum* L. on dunes at Winterton, Norfolk, in comparison with invasion by *Hippophaë rhamnoides* L. at Saltfleetby, Lincolnshire. Biological Conservation 12:83-94.

Haefner, S. 2004. Kite Aerial Photography. www.thehaefners.com/kap/?page5kites.

Higgins, S.I. and D.M. Richardson.1996. A review of models of alien plant spread. Ecological Modeling 87:249-265.

Hughes, M.L., P.F. Mcdowell and W.A. Marcus. 2006. Accuracy assessment of georectified aerial photographs: Implications for measuring lateral channel movement in a GIS. Geomorphology 74:1-16.

Hunt E. R. Jr., J.H. Everitt, J.C. Ritchie, M.S. Moran, D.T. Booth, G.L. Anderson, P.E. Clark, and M.S. Seyfried. 2003. Applications and Research Using Remote Sensing for Rangeland Management Photogrammetric Engineering & Remote Sensing. 69(6):675-693.

Joshi, C., J. de Leeuwand, I.C. Van Duren. 2004. Remote sensing and GIS applications for mapping and spatial modeling of invasive species. In: ISPRS 2004: Proceedings of the XXth ISPRS Congress: Geo-imagery bridging continents, 12-23 July 2004, Istanbul, Turkey. 7:669-677.

Ladd G. B., A. Nagchaudhuri, T. J. Earl, M. Mitra, G. L. Bland, G.M. Casady, R.S. Hanley, S.K. Seelan. 2005. Detection of Leafy Spurge (*Euphorbia esula*) Using Multidate High-Resolution Satellite Imagery. Weed Technology 19(2):462-467.

Ladd G. B., A. Nagchaudhuri, T. J. Earl, M. Mitra, G.L. Bland. 2006. Rectification, georeferencing and mosaicking of images acquired with remotely operated aerial platforms. ASPRS 2006 Annual Conference Reno, Nevada, May 1-5, 2006.

Lass, L.W. and D.C. Thill. 2000. Detecting yellow starthistle (*Centaurea solstitialis*) with hyperspectral remote sensing technology. Proceedings of Western Society. Weed Science. 53:11.

Lass, L.W. and R.H. Callihan. 1997. The effect of phenological stage on detectability of yellow hawkweed (*Hieracium partense*) and oxeye daisy (*Chrysanthemum leucanthemum*) with remote multispectral digital imagery. Weed Technology. 11:248–256.

Lass, L.W. and T.S. Prather. 2004. Detecting the locations of Brazilian pepper trees in the Everglades with a hyperspectral sensor. Weed Technology. 18:437-442.

Lass, L.W., and R.H. Callihan (1997). The effect of phenological stage on detectibility of yellow hawkweed (*Hieracium pratense*) and oxeye daisy (*Chrysanthemum leucanthemum*) with remote multispectral digital imagery. Weed Technology 11:248-256.

Lass, L.W., B. Shafii, W.J. Price, and D.C. Thill. 2000. Assessing agreement in multispectral images of yellow starthistle (*Centaurea solstitialis*) with ground truth data using a Bayesian methodology. Weed Technology 14:539–544.

Lass, L. W., D. C. Thill, B. Shafii, and T. S. Prather. 2002. Detecting spotted knapweed (*Centaurea maculosa*) with hyperspectral remote sensing technology. Weed Technology 16:426–432.

Lass, L. W., H. W. Carson, and R. H. Callihan. 1996. Detection of yellow starthistle (*Centaurea solstitialis*) and common St. Johnswort (*Hypericum perforatum*) with multispectral digital imagery. Weed Technology 10:466-474.

Lass, L.W., Timothy S.P., Nancy F. G., Keith T. W., Jacob, T. M., and Jeffery, P. (2005). A review of remote sensing of invasive weeds and example of the early detection of spotted knapweed (*Centaurea maculosa*) and babysbreath (*Gypsophila paniculata*) with a hyperspectral sensor Weed Science 53(2):242-251.

Lass, L.W., T.S. Prather, and N.F. Glenn. 2005. A review of remote sensing of invasive weeds and example of the early detection of spotted knapweed (*Centaurea maculosa*) and babysbreath (*Gypsophila paniculata*) with a hyperspectral sensor. Weed Science 53:242–51.

Lass, L.W and R.H. Callihan. 1993. GPS and GIS for weed surveys and management. Weed Technology. 1993. 7:249-254.

Lestak, L.R., W.F. Manley, P.M. Sturtevant, J.A. Maslanik, C.E. Tweedie, and J. Brown. 2007. High-resolution rectified aerial photography for collaborative research of environmental change at Barrow, Alaska, USA. *Boulder*, Colorado USA: National Snow and Ice Data Center. DVD.

Lillesand, T. M., and R. W. Kiefer. 2000. Remote sensing and image interpretation. Fourth edition. John Wiley and Sons, Inc., New York, NY. 724 pp.

Lindholm, S. 2004. Aerial Digital Photography from a Balloon for Fifty Dollars. www.stanford.edu/;lindholm/chpropbal.html.

Lodge, D. 1993. Biological invasions: lessons from ecology. Trends in Ecology and Evolution 8:133-137.

Mack, R.N., D. Simberloff, W. M. Lonsdale, H. Evans, M. Clout and F. A. Bazzaz. 2000. Biotic invasions: causes, epidemiology, global consequences, and control. Ecological Applications 10(3):689-710.

Mast, J.N., T.T. Veblen and M.E. Hodgson. 1997. Tree invasion within a pine/grassland ecotone: an approach with historic aerial photography and GIS modeling. Forest Ecology and Management 93:181-194.

Mathieu, M.G. and S. de Blois. 2005. Mapping the invasive species *Phragmites australis* in linear wetland corridors. Aquatic Botany. Volume 83, Issue 4, Pp 310 – 320.

MÜllerová, J., P. Pysek, V. Jarosík and J. Pergl. 2005. Aerial photographs as a tool for assessing the regional dynamics of the invasive plant species *Heracleum mantegazzianum.* Journal of Applied Ecology 42:1042-1053.

Mustafa, M., K. Steddom, G. J. Michels Jr. 2006. Estimating Biophysical Characteristics of Musk Thistle (*Carduus nutans*) With Three Remote Sensing Instruments. Rangeland Ecology and Management 59(1):44-54.

Naylor, B. J., B. A. Endress, and C. G. Parks. 2005. Multiscale detection of sulfur cinquefoil using aerial photography. Rangeland Ecology and Management 58:447-451.

Ndzeidze, S. K. M.D. Johnson, L.R. Richman, M. Louhaichi, and D.E. Johnson. 2010. Mobile mapping of medusahead (*Taeniatherum caput-medusae* (L.)

Nevski) infestations. Abstr. of Papers, 63rd annual meeting Soc. for Range Manage., Denver, Colorado, USA. February 7-11th, 2010.

Ndzeidze, S. K. M.D. Johnson, L.R. Richman, M. Louhaichi, M. Halbleib, and D.E. Johnson. 2010. Detection of medusahead (*Taeniatherum caput-medusae* (L.) Nevski) using high frequency, sequential, globally positioned digital images. Abstr. of Papers, 63rd annual meeting Soc. for Range Manage., Denver, Colorado, USA. February 7-11th, 2010.

Okin, G. S., D. A. Roberts, B. Murray, and W. J. Okin. 2001. Practical limits on hyperspectral vegetation discrimination in arid and semiarid environments. Remote Sensing of Environment 77:212-225.

Pearlstine, L., S. Smith, E. Walsh, and J. Stenberg. 1998. Aerial Sampling for Brazilian Pepper on Canaveral National Seashore. Gainesville, FL: USGS Biological Resources Division, Florida Cooperative Fish and Wildlife Research Unit.

Perez, A.J., F. Lopez, J.V. Benlloch and S. Christensen. 2000. Colour and shape analysis techniques for weed detection in cereal fields. Computerand Electronics in Agriculture 25:197-212.

Peters, A.J., B.C. Reed, and M.D. Eve. 1992. Remote sensing of broom snakeweed (*Gutierrezia sarothrae*) with NOAA-10 spectral image processing. Weed Technology 6:1015–1020.

Peterson, E.B. 2005. Estimating cover of an invasive grass (*Bromus tectorum*) using tobit regression and phenology derived from two dates of Landsat ETM plus data. International Journal of Remote Sensing 26:2491-2507.

Ponzetti, J. M. 1997. Assessment of medusahead and cheatgrass control techniques at Lawrence Memorial Grassland Pre-serve. The Nature Conservancy of Oregon, Portland, Oregon, USA.

Rew, L.J. and R.D. Cousens. 2001. Sptaila distribution of weeds in arable crops: are current sampling and analytical methods appropriate? Weed Research 41:1-18.

Rew, LJ, BD Maxwell, and R. Aspinall. 2005. Predicting the occurrence of non-indigenous species using environmental and remote sensed data. Weed Science 53:236-41.

RotorKraft. 2004. RotorKraft: Premium Radio Control Helicopters and Accessories. www.rotorkraft.com/index.htm.

Rouget, M., D.M. Richardson, S.J. Milton, and D. Polakow. 2001. Predicting invasion dynamics of four alien *Pinus* species in a highly fragmented semi-arid shrubland in South Africa. Plant Ecology 152:79-92.

Sheley, R., J. James, B. Smith, and E. Vasquez. 2010. Applying Ecologically Based Invasive-Plant Management. Rangeland Ecology and Management 63(6) 605-613.

Sheley, R. L. and J. K. Petroff, editors. (eds.). 1999. Biology and Management of Noxious Rangeland Weeds. Oregon State University Press. Corvallis.

Sohn, Y., and R. M. McCoy. 1997. Mapping desert shrub rangeland using spectral unmixing and modeling spectral mixtures with TM data. Photogrammetry Engineering Remote Sensing 63:707-716.

Stafford, J. V., J. M. Le Bars and B. Ambler. 1996. A hand-held data logger with integral GPS for producing weed maps by field walking. Computers and Electronics in Agriculture 14 (2-3):235-247.

Tang, L., Tian, L.H. Yao, and K. Thorp. 2001. A real-time in-field variability mapping system. ASAE Paper No. 011025. St. Joseph, MI: ASAE.

Theodore, M.W. and J. Cardina. 1997. Accuracy of a Global Positioning System (GPS) for Weed Mapping. Weed Technology. 11(4):782-786.

Underwood, E., S.L. Ustin, and D. DiPietro. 2003. Mapping nonnative plants using hyperspectral remote sensing. Remote Sensing of Environment 86:150–161.

Ustin S.L., D. DiPietro, K. Olmstead, E. Underwood, and G.J. Scheer. 2002. Hyperspectral Remote Sensing for Invasive Species Detection and Mapping. IEEE.

Van Wychen, L.R., E.C. Luschei, A.J. Bussan and B.D. Maxwell. 2002. Accuracy and cost effectiveness of GPS-assisted wild oat mapping in spring cereal crops. Weed Science. 50:120-129.

Webster, T.M. and J. Cardina. 1997. Accuracy of a global positioning system (GPS) for weed mapping. Weed Technology. 11:782-786.

Webster, T.M., J. Cardina and S.J. Woods. 2000. Spatial and temporal expansion patterns of *Apocynum cannabinum* patches. Weed Science. 48:728-733.

William, G. 2000. Remote Sensing of Vegetation, Plant Species Richness, and Regional Biodiversity Hotspots. Ecological Applications 10(6)1861-1870.

Wood, S.D., R.L. Lawrence, R.L. Sheley. 2006. Mapping invasive plants using hyperspectral imagery, classification trees, and classification thresholds. ASPRS 2006 Annual Conference Reno, Nevada, May 1-5, 2006.

Yang, C., J.H. Everitt, M.R. Davis and C. Mao. 2003. A CCD camera-based hyperspectral imaging system for stationary and airborne applications. Geocarto International Journal. 18:71-80.

Yang, C., J.H. Everitt and H.B. Johnson. (2009). Applying image transformation and classification techniques to airborne hyperspectral imagery for mapping Ashe juniper infestations. International Journal of Remote Sensing 30 (11):2741-2758.

Yang, C., and J. H. Everitt. 2010. Mapping three invasive weeds using airborne hyperspectral imagery. Ecological Informatics 5(5):429-439

CHAPTER 2: MEDUSAHEAD GERMINATION, ESTABLISHMENT AND GROWTH CHARACTERISTICS

INTRODUCTION

Medusahead rye (*Taeniatherum caput-medusae* [L.] Nevski) is an exotic, noxious winter annual grass that has invaded sagebrush steppe rangeland communities of the western United States and several eastern states (Figure 1). Medusahead invasion has reduced livestock forage by reducing grazing capacity by up to 80% (Davies and Svejcar, 2008; Amy, 2001). Medusahead also out-competes native vegetation, reduces land value, and creates a wildfire hazard (Young and Evans, 1970; Dahl and Tisdale, 1975; Davies, 2008). Its rapid spread in grassland, openings in chaparral, oak woodlands, and rangelands creates serious management concerns by degrading wildlife habitat and disturbing the ecological, biological and chemical functions of the ecosystem (Dahl and Tisdale, 1975; Lusk *et al*., 1961).

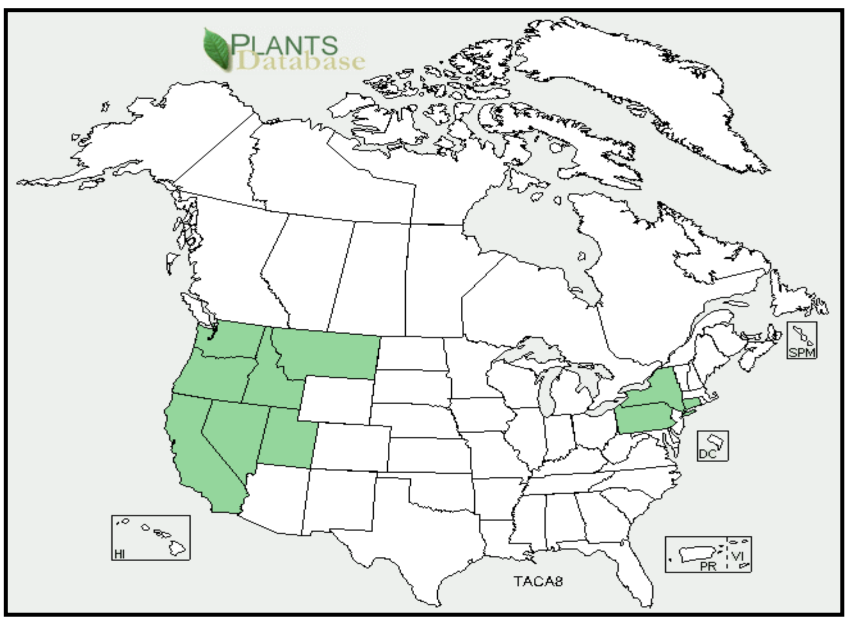

Figure 2.1: Distribution of Taeniatherum caput-medusae (L.) Nevski, in USA (CA, CT, ID, MT, NV, NY, OR, PA, UT, WA).

Source: Plants Database, United States Department of Agriculture.

Germination, Establishment and Growth Characteristics

Medusahead grows in areas that have relatively mild to cold temperatures in winter, with hot summers (Maurer *et al*., 1988). It is generally found in areas that receive fall, winter, and spring moisture followed by dry summers (Amy, 2001), with annual precipitation of 10 to 40 inches (250-1,000 mm), and an upper precipitation limit of approximately 50 inches (1,270 mm) (Dahl and Tisdale, 1975; Maurer *et al*., 1988; Amy, 2001). Infestations primarily occur in former sagebrush-grass or bunchgrass communities that receive 10 to 20 inches (250-500 mm) of annual precipitation (Dahl and Tisdale, 1975; Maurer *et al*., 1988; Amy, 2001). Areas above 4,500 feet (1,370 m) elevation with well-drained coarse soils may be less susceptible to invasion (Dahl and Tisdale, 1975; Lusk *et al*., 1961).

Medusahead germination is typically rapid and occurs under a broad temperature range (optimal 10-15^{o} C) (Amy, 2001; Bovey *et al*., 1961; Davies, 2008; Major *et al*., 1960). Most seeds germinate in the fall after the first rain, usually in October, and continue to grow through the winter in mesic climates (Goebel *et al.* 1988; Davies and Svejcar, 2008; Major *et al*., 1960; Murphy and Turner, 1959). During the winter months, growth is slowed markedly by low temperatures. Leaves, stems and roots increase in number through the winter and roots can reach a 40-inch (100 cm) depth by early February (Smith *et al*., 1999; Amy, 2001; Murphy and Turner, 1959). Roots grow in winter and early spring (Lusk *et al*., 1961), and reach deep into the soil allowing medusahead to effectively outcompete desirable native vegetation for soil nutrients and water (Dahl and Tisdale, 1975; Davies, 2008). As a result, medusahead often dominates disturbed areas in soils with high moisture-holding capacities and slow percolation rates (Sharp *et al*., 1957; Maurer *et al*., 1988; Lusk *et al*., 1961). Growth accelerates in the spring with increasing temperatures and, by late May or early June, seeds are in the milk or early dough stage and are generally mature by late June to early July, a few weeks later than most annual grasses (Davies and Svejcar, 2008; Maurer *et al*., 1988). Seeds remain in spikes until dispersal in late summer or early fall (Maurer *et al*., 1988; Sharp *et al*., 1957). Seedlings emerge from soil depths of up to 8 cm (3-4 in) (Maurer *et al*., 1988; Amy, 2001) growing in stands that vary in density from several hundred to 2,000 plants per square foot (Maurer *et al*., 1988). This variance is directly related to annual precipitation, soil type, and other vegetation in the area. Medusahead flowers in early spring, and by June or July its seeds (Figures 2.2a and 2.2b), covered with tiny barbs, are mature (Zimmerman, 2002).

The barbs help the seeds attach to livestock, humans or vehicles as they pass (Davies and Svejcar, 2008; Zimmerman, 2002; Miller *et al*., 1999). Plant height ranges from 8 to 20 inches (20-50 cm), depending on the site, and produce tillers, but very few leaves (Amy, 2001; Murphy and Turner, 1959). Medusahead has a distinctive flower head, the blades are more or less involutes, narrow, 1-2.5 mm broad, short, 3-6 cm long, glabrous to puberulent, with the margins sometimes ciliate, and the auricles very short and inconspicuous (Maurer *et al*., 1988; Amy, 2001).

Medusahead's late maturity and the availability of soil moisture late in the growing season allow it to produce large amounts of seeds, enhancing site occupation in subsequent generations (Smith *et al*., 1999; Maurer *et al*., 1988). The seeds can also germinate and produce a dense litter under low moisture conditions without directly contacting a moist substrate (Furbush, 1953; Davies, 2008). Nitrogen, possibly provided by fertilizers, can stimulate some dormant seeds to germinate (Maurer *et al*., 1988; Dahl and Tisdale, 1975;

Amy, 2001; Murphy and Turner, 1959).

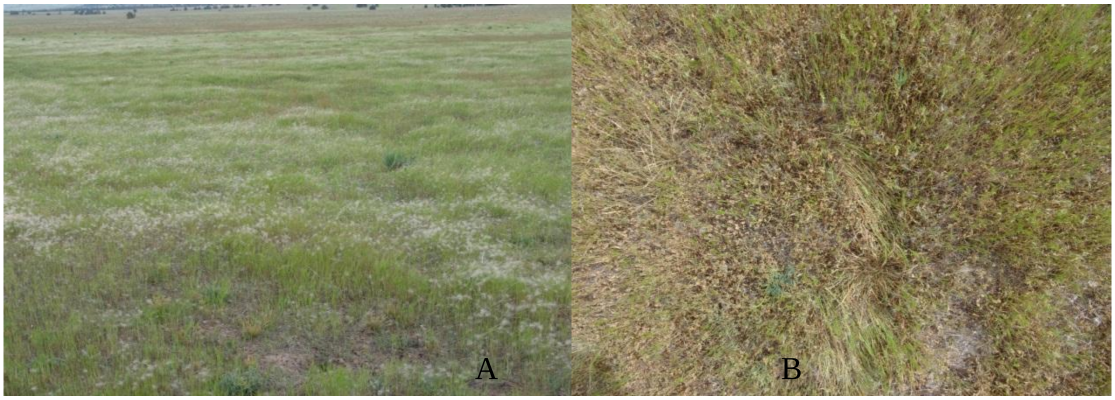

Figure 2.2: Heavy medusahead infestation by early spring (A) and by June or July (B) in the Burns, Oregon area.

The inflorescence contains 2 to 3 spikelets per node, and each spikelet contains 1 seed and produces an average of 7.1 seeds per spike (Maurer *et al*., 1988; Lusk *et al*., 1961). Spikelet heads are spike-like, about 1.5-5 cm long excluding awns, while the main axis does not break apart in fruit (Maurer *et al*., 1988). The Florets are two per spikelet, with the upper much reduced and sterile (Amy, 2001; Maurer *et al*., 1988). Medusahead has two types of flat awns. The longer of the two contains barbs that point upward (Maurer *et al*., 1988). Plants in dense stands usually produce one spike. In open areas, the number of spikes per plant typically increases to 3 to 5 (Maurer *et al*., 1988). Awns and glumes are flattened and stiff, with minute upward pointing barbs lining margins (Maurer *et al*., 1988). Lemmas are narrow-lanceolate, (5) 6-8 mm long, very scabrous throughout, prolonged into a long, flattened and divergent awn (2) 3-7 cm long (Maurer *et al*., 1988). The lodicules are about 0.8 mm long, oblanceolate, and ciliat, and the anthers are 0.6-1 mm long (Maurer et al., 1988). Spikelets are separated from the head above glumes (Amy, 2001; Maurer *et al*., 1988). Glumes are awn-like, ascending and about 1-4 cm long, straight to slightly curved, and fused at the base (Amy, 2001; Lusk *et al*., 1961; Maurer *et al*., 1988).

Medusahead-dominated stands usually have more than 100 plants per square foot; however, densities of 1,500 to 2,000 plants per square foot have been found in a valley in southern Idaho (Amy, 2001; Maurer *et al*., 1988). Fertile lemma are narrowly lanceolate, roughly 5-8 mm long, 3-veined, and tapered into a straight to curved awn about 3-7 cm long (Amy, 2001; Maurer *et al*., 1988). The blades are usually 1-3 mm wide, flat along the margins, with typically 2-4 per stem. The sheaths are slightly inflated and glabrous, and the ligules are short, usually 0.2-0.5 mm long (Lusk *et al*., 1961; Maurer *et al*., 1988). The collar region is usually covered with sparse long hairs, with the auricles glabrous, up to ~ 0.5 mm long (Nelson and Wilson, 1969; Amy, 2001). Mature foliage surfaces often appear glassy under magnification (Figure 2.3). The awns are straight and compressed when green, becoming twisted and erratically spread upon drying: thus, its appearance resembles the Greek demigod medusa's head of snakes, giving rise to the plant's common name (Nelson and Wilson, 1969; Maurer *et al*., 1988; Murphy and Turner, 1959).

Medusahead is principally self-pollinated (Murphy and Turner, 1959; Amy, 2001; Maurer *et al*., 1988), and occurs in seral and late-successional plant communities, becoming a seral invader after disturbance (Amy, 2001). Medusahead often grows in dense stands on disturbed sites where climax perennial grasses have been removed, often to the exclusion of other species (Amy, 2001). The growth habits, life cycles, and ecological adaptations of medusahead and cheatgrass are similar, and the annuals typically grow in association until medusahead becomes dominant and eventually exclusive (Davies *et al*., 2008). Medusahead invades vast areas formerly dominated by annual grasses such as cheatgrass (Davies, 2008; Zimmerman, 2002).

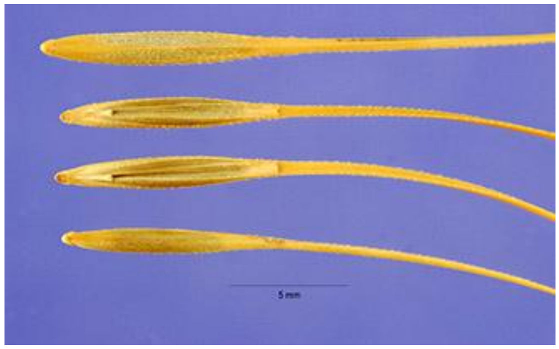

Figure 2.3: Mature foliage surface of Medusahead under magnification.

Source: United States Department of Agriculture

Medusahead is entirely dependent on seed production for regeneration (Sharp *et al*., 1957). It is an extremely capable seeder with a large annual production of up to 6,000 seeds per ft^2 of soil. Viability in litter and soil last for at least one year, rendering the plant capable of producing dense stands in succeeding years (Sharp *et al*., 1957; Dahl and Tisdale, 1975; Amy, 2001; Murphy and Turner, 1959). Newly matured seeds require a cool after-ripening period of ~ 3-4 months and contain a germination inhibitor in the awns that must degrade before germination can occur (Maurer *et al*., 1988).

Medusahead often turns bright green when the other annuals are brown, making identification easier (Figure 2b). As it matures, it turns shades of purple and eventually tan. Mature seeds remain attached to the long-awned florets (Nelson and Wilson, 1969; Maurer *et al*., 1988). Vegetative characteristics of the seeds are similar to those of mature plants, except that the blades are ~ 0.5 mm wide (Murphy and Turner, 1959). Seedlings can survive desiccation of the primary root and develop adventitious roots when moisture becomes available (Murphy and Turner, 1959; Maurer *et al*., 1988). Seeds are dispersed for relatively short distances and dispersal decreases as the distance from the plant increases (Amy, 2001; Davies, 2008; Murphy and Turner, 1959; Maurer *et al*., 1988). Dispersal is locally affected by wind and water, and to greater distances by soil movement, human activities, and clinging to the feet and fur of animals (Zimmerman *et al*., 2002). The relatively long period of medusahead seed dispersal, from July to October, may be an adaptation to increase the likelihood of its long barbed awns dispersing aided by vehicles and animals, as decreasing animal and vehicle contact with medusahead when its seeds and can be dispersed would limit its spread (Davies, 2008).

As medusahead grows, it increases in silica content, making it unpalatable to livestock and limiting any consumption by herbivores early in its life cycle (Bovey *et al*., 1961; Fosberg, 1965; Swenson *et al*., 1964; Davies, 2008; Young *et al*., 1999). The stiff awns and hard florets also injure the eyes and mouths of grazing animals (Davies, 2008). Seed-eating birds usually avoid feeding on the seeds (Murphy and Turner, 1959; Davies, 2008). Its dense layer of litter, because of the silica content, decomposes slower than that of other plants (Bovey *et al*., 1961; Fosberg, 1965; Goebel *et al*., 1988). This litter suppresses native plant growth while encouraging the germination of its own seed, and creates an enormous load of fuel that can lead to devastating wildfires (Zimmerman et al., 2002; Blank *et al*., 1996; Davies and Svejcar, 2008; Miller *et al*., 1999; Sharp *et al*., 1957; Murphy and Turner, 1959; Davies, 2008). Medusahead also depletes upper soil moisture early in the growing season and accesses deep soil moisture late in the growing season (Davies and Svejcar, 2008; Maurer *et al*., 1988; Swenson *et al*., 1964).

Managing rangelands to promote and maintain large perennial bunchgrasses is critical for plant community resistance to medusahead invasion (Davies *et al*., 2008; Davies and Svejcar, 2008). Plant communities that are resistant to medusahead invasion have higher densities of large perennial bunchgrasses than communities that are less resistant (Davies *et al*., 2008). Preventing the spread of medusahead and increasing desirable plant community resistance to invasion will reduce the establishment of new infestations; however, successful medusahead management will also require searching for and eradicating new infestations (Davies *et al*., 2008). Maintaining good stands of perennial vegetation helps to prevent medusahead invasion, but restoration of native vegetation without first removing this weed has not been successful (Maurer *et al*., 1988; Amy, 2001; Davies and Svejcar, 2008).

History of medusahead establishment in conterminous United States

Medusahead is an annual grass native to Eurasia (Davies and Svejcar, 2008; Miller *et al*., 1999; Sharp *et al*., 1957; Murphy and Turner, 1959; Davies, 2008) (Figure 5). In Asia, medusahead is widespread, occurring in Turkmenistan, Iran, Syria, and in the northern portion of Israel in low mountain and plateau areas. Carbonized seeds of this weed have been found in early agricultural archaeological sites in Iran (Maurer et al., 1988). Medusahead has been a part of agriculture since the beginning of livestock domestication. In the United States, it has been described as an aggressive winter annual weed that is changing the ecology of western rangelands (Maurer *et al*., 1988; Miller *et al*., 1999; Sharp *et al*., 1957; Murphy and Turner, 1959).

First introduced into the U.S. in the early 1880s, it was discovered growing in Oregon in 1887 by Thomas Howell *(*Maurer *et al*., 1988; Amy, 2001; Young and Evans, 1970*)*.

Nevski recommended, in 1934, that the Russian types of medusahead should be classified in a separate genus, *Taeniatherum* (Maurer *et al*., 1988*)*. In the 1960s, Jack Major, of the University of California, suggested that there are three geographic and morphologically distinct taxa: *T. caput-medusae*, *T. asperum*, and *T. crinitum*. After traveling in Russia, Major thought the proper classification for the plant introduced to North America was *Taeniatherum asperum* (Maurer *et al*., 1988*)*.

The Danish scientist Signe Frederiksen revised the genus in 1986 by separating the previously mentioned distinct taxas into subspecies of *Taeniatherum caput-medusae* (Maurer *et al*., 1988). The currently accepted scientific name of medusahead is *Taeniatherum caput-medusae* (L.) Nevski. There are three subspecies found in Europe: *Taeniatherum caput-medusae* ssp. *caput-medusae*, *Taeniatherum caput-medusae* ssp. *cinitum* (Schreb.) Meldris, and *Taeniatherum caput-medusae* ssp. *asperum* (Simk.) Meldris. The subspecies *caput-medusae* is mostly restricted to Spain, Portugal, southern France, Algeria, and Morocco (Figure, 2.4). Subspecies *crinitum* is found in Greece and the Balkans and east into Asia. The range of subspecies asperum completely overlaps the other two subspecies (Maurer *et al*., 1988).

By the early 1990s, 14 million acres of public lands in the Intermountain West were infested with medusahead, cheatgrass (*Bromus tectorum L*.), or both; however, the area at risk of invasion by these two grasses is at least 60 million acres. Unfortunately, medusahead is continuing to spread rapidly. Its extent increased from 18 to 31 of Oregon’s 36 counties between 1962 and 2004. In Idaho, rangelands infested by medusahead more than doubled between 1957 and 1992 (Davies, 2008). It has invaded fields, dry roadsides, and disturbed sagebrush slopes in British Columbia, Washington, Idaho, Oregon, and California. Since its discovery in Oregon, medusahead has invaded millions of acres in the Pacific Northwest, California, Utah, Montana, Pennsylvania, New York and Nevada (Figure, 1).

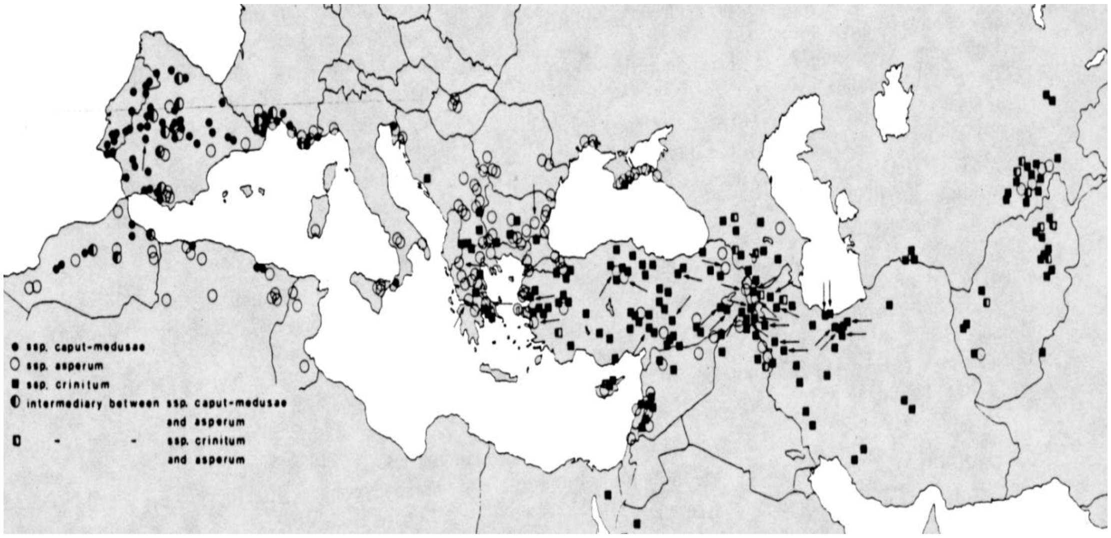

Figure 2.4: The grass origins in areas bordering the Mediterranean Sea, extending eastward to central Asia. The centre of origin is Southwest Asia.

The rapid spread of medusahead is a serious management concern, because it reduces grazing capacity by up to 80%, degrades wildlife habitat, decreases biodiversity, and potentially alters ecosystem functions (Davies, 2008). An alarming but rarely mentioned impact of medusahead invasion is that it may exacerbate the decline of sagebrush-obligate wildlife species, like the sage grouse as it replaces plant communities provide the critical habitat (Davies and Svejcar, 2008).

LITERATURE CITED

Amy, J. 2001. Taeniatherum caput-medusae. In: Fire Effects Information System. U.S. Department of Agriculture, Forest Service, Rocky Mountain Research Station, Fire Sciences Laboratory (Producer). http://www.fs.fed.us/database/feis/

Blank, R. R., F. L. Allen and J. A. Young. 1996. Influence of simulated burning of soil-litter from low sagebrush, squirreltail, cheatgrass, and medusahead on water-soluble anions and cations. International Journal of Wildland Fire. 6(3):137-143.

Bovey, R. W., D. LeTourneau, and L. C. Erickson. 1961. The chemical composition of medusahead and downy brome. Weeds 9:307-311.

Dahl, B. E. and E. W. Tisdale. 1975. Environmental factors related to medusahead distribution. Journal of Range Management 28:463-468.

Davies, K. W. 2008. Medusahead dispersal and establishment in sagebrush steppe plant communities. Rangeland Ecology & Management 61:110-115.

Davies, W. K., and T. J. Svejcar. 2008. Comparison of Medusahead-Invaded and Non-invaded Wyoming Big Sagebrush Steppe in Southeastern Oregon. Rangeland Ecology & Management 61(6):623-629.

Fosberg, M. A. 1965. Relationship of cheatgrass and medusahead to soils in the Colombia River Basin. Proceedings of the Cheatgrass Symposium Vale, OR. U.S. Dept. of the Interior, Bureau of Land Management, Washington, D.C.

Furbush, P. 1953. Control of medusa-head on California ranges. Journal of Forestry. 51:118-121.

Goebel, C. J., M. Tazi, and G. A. Harris. 1988. Secar bluebunch wheatgrass as a competitor to medusahead. Journal of Range Management 41:88-89.

Lusk, W.C., M.B. Jones, D.T. Torell, and C.M. McKell. 1961. Medusahead palatability.

Journal of Range Management 14:248-251.

Major, J., C. M. McKell, and L. J. Berry. 1960. Improvement of medusahead-infested rangeland. Leaflet 123. Davis, CA: University of California, California Agricultural Experiment Station. 6 p

Maurer, T., J. R. Mary and G. Audrey. 1988.*Taeniatherum caput-medusae* Medusahead. *Global Invasive Species Team. The Nature Conservancy* *http://wiki.bugwood.org/Taeniatherum_caput-medusae*

McKell, C.M., A.M. Wilson, and B.L. Kay. 1962. Effective burning of rangelands infested with medusahead. Weeds 10:125-131.

Miller, H. C., D. Clausnitzer, and M. M. Borman. 1999. Medusahead. *In:* R.L. Sheley and J.K. Petroff . Biology and management of noxious rangeland weeds. Corvallis, OR: Oregon State University Press. pp. 271-281.

Murphy, A. H. and D. Turner. 1959. A study on the germination of Medusa-head seed. Bulletin. 48: 6-10.

Nelson, J. R. and A. M. Wilson. 1969. Influence of age and awn removal on dormancy of medusahead seeds. Journal of Range Management 22: 289-298.

Sharp, L.A., M. Hironaka, and E.W. Tisdale. 1957. Viability of medusahead seed collected in Idaho. Journal of Range Management 10:123-126.

Smith, H. A., W. S. Johnson, J. S. Shonkwiler, and S. R. Swanson. 1999. The implications of variable or constant expansion rates in invasive weed infestations. Weed Science 47:62-66.

Swenson, C.F., L. Duane, E.C. Lambert. 1964. Silica in medusahead. Weeds. 12: 16-18

Torell, P. J. 1967. Dowpon-an aid to reseeding medusahead-infested rangeland. Down to Earth 23: 6-8.

Torell, P. J., E. C. Lambert., H. H. Robert. 1961. The medusahead problem in Idaho. Weeds.9:124-131.

Young, J. A. and R. A. Evans. 1970. Invasion of medusahead into the Great Basin. Weed Science 18:89-97.

Young, J. A. and R. A. Evans. 1971. Medusahead invasion as influenced by herbicide and grazing on low sagebrush sites. Journal of Range Management 24:451- 454.

Young, J. A., C. D. Clements, and G. Nader. 1999. Medusahead and clay: the rarity of perennial seedling establishment. Rangeland 6:19-23.

Zimmerman, J.R., Johnson, W.S., Eiswerth, M.E. Medusahead: Economic Impact and Control in Nevada. University of Nevada-Reno Fact Sheet FS-02-37.

CHAPTER 3: AERIAL IMAGE POSITIONING TOOL 2.1: AN AUTOMATED PROCESS FOR RAPID COARSE GEO-REFERENCING OF AERIAL PHOTOGRAPHY

S. K. Ndzeidze, K. E. Johnson, M. Louhaichi, and D. E. Johnson

Key Words: Digital Aerial Photography, Image Registration, Georectification, Global Positioning System

ABSTRACT

With recent advances in digital camera technology, computer hardware, and software, aerial photographs are easier to collect, store, and transfer than ever before. The challenge in using this technology is the considerable time spent determining photo locations and subsequent geo-referencing so that images can be used for spatial analysis. We coupled low-cost GPS loggers to track aircraft/camera position, altitude, and bearing with high spatial/temporal accuracy, and developed computer software to automatically rough geo-position images. A Canon XSi digital camera, (synchronized to GPS time on Universal Time using the US Naval Observatory's Master Clock) is mounted in the belly of an aircraft positioned to acquire vertical images. This camera can be set to take frequent images and store them on a laptop computer. The camera records the time the image was taken and writes it in the header file of the image. The GPS records the position and elevation of the aircraft. By adjusting camera time to GPS time, software can rotate the image to account for aircraft direction and automatically position the images based on the lens characteristics and height above the ground. The Aerial Image Positioning Tool software then rotates, scales and creates the geographic position of image. This position in incorporated in (Keyhole Markup Language (KML) referencing. A world file, which provides coordinate and scale information, and a projection file is also created for those images that were taken on true north/south flightlines. The program also specifies the geographic projection and datum used. Our algorithm can be used to batch process files, leading to extremely fast coarse geo-referencing of aerial photos that are generally accurate to within 100 meters. For higher accuracy, control points can be chosen from the rough corrected images and overlaid on a United States Department of

Agriculture (USDA) National Agriculture Imagery Program (NAIP) base map for further correction of the image distortion caused by aircraft orientation or terrain. The ease and speed of the course recording and image positioning using the Aerial Image Positioning Tool makes large-scale landscape monitoring much more cost effective and efficient.

INTRODUCTION

The primary objective of this study is to create a program to tag aerial photos with GPS coordinates using trigonometric functions to calculate ground coverage and pixel size while correcting for error generated by altitude and direction. The Aerial Image Positioning Tool is a computer program developed to reduce the difficulties encountered when transferring aerial photographic imagery to planimetric base maps. We focused on developing a process by which we could take and store sequential digital images, automatically locate the camera position, rotate images to account for aircraft direction, and rough position the images so they could be used in conjunction with other GIS and image analysis programs. Knowing the camera's focal length and sensor size enables the calculation of the camera's angle of view, and consequently the scale of the image as a function of the altitude of the aircraft above the ground. Using these values and assuming the latitude and longitude values were at the center of the image, an estimate of the location for each corner of the image, as well as the pixel size, can be calculated.

The Aerial Image Positioning Tool corrects for camera time offset from GPS time, finds the position of the camera for all images, reads the bearing from the GPS log file, rotates the image to correct for aircraft direction, scales the image, then rough positions the image and creates KML files. KML files allowed us to display images rotated at any angle, not just rectangular facing north or south, in Google Earth. Our software also creates World Files for images taken on flightlines that are true north and south. Once these rough-corrected images have been produced, a georeferenced base map such as NAIP, orthophotographic or Digital Orthophotographic Quadrangle (DOQ) GIS data can be underlain or overlain on aerial photographs to further correct images.

PREVIOUS WORK

Previous studies document the difficulty and frustration encountered in producing fast, less time consuming, and accurate image rectification. Xin (2006) used an accurate geo-referencing model for each image and a Digital Elevation Model for the working area in order to generate orthorectified images. Although his procedure is highly automatic, some options and interaction are still required to guarantee product quality. Kawai and Saji (2007) attempted automatic registration of aerial oblique images and a digital map. However, their method did not improve the computation time, extraction of intersections from digital maps, and the accuracy of the local registration angles and heights when aerial oblique images were taken. Rau and Chen (2004) examined geometrical model building and its application to orthorectification for aerial images. Mosaicing has remained the most reliable and immediate solution to aerial image correction. Photographic image mosaicing algorithms often address two different problems-smoothing geometric and radiometric discontinuities in adjacent images, and choosing the best image source at each point. The latter problem may be due to different cloud coverage in each of the images (Afek and Brand, 1998). Afek and Brand (1998), in that article "mosaicing of orthorectified aerial images", address the problem of smoothing geometric and radiometric discontinuities in adjacent images. The paper, however, disregards many important aspects usually considered by a human operator. This selection of rectification might also fail to understand the respective location of the mosaiced images when these intersect in a non-regular way.

One type of algorithm assumes that no geometric or radiometric corrections are needed. These algorithms merely select a seam line that yields the best results for the rigid transformation mosaicing procedure (Hummer-Miller, 1989; Shiren *et al*., 1989). Zobrist *et al*. (1983) performed geometric and radiometric corrections along seam lines selected by the operator after automatic correlation enhanced the detection of tie points along the line. This algorithm was used for composite orthophoto production (Hood *et al*., 1989). Another algorithm (Albertz *et al*., 1992) added contrast correction to the traditional intensity correction. Ladd *et al*. (2006), listed several possible sequences of georeferencing or rectifying, and mosaicing multiple images together to generate a large georeferenced image. A basic choice is to start by mosaicing all the images. The resulting composite image would have the possibility of more control points. Another option would be to georeference one image and then mosaic others to that one image. Yet another option is to georeference each individual image and then mosaic all the images together based upon their coordinates. This is the ideal solution since it is easier to track errors, allowing for very high resolution, precision, and accuracy throughout the mosaic (JI and Jensen, 2000; Jensen, 2009). Kim *et al*. (2010) present a georeferencing method that automates the approximate georeferencing of vertical analog aerial photo exposures in areas of low relief to digital orthophoto quads. However, there are numerous limitations: The extent and resolution of the photos must be similar, and there must be an adequate number of common, persistently identifiable, features in both images. The software needs to have access to an ArcGIS license (proprietary, expensive) and the photos most be near vertical, with terrain relief a small fraction of the flying height.

Theoretical Framework of World Files and Georeferencing

A world file is a plain text computer data file used by geographic information systems to geo-reference raster map images. Small-scale rectangular raster image maps can have an associated world file for GIS map software which describes the location, scale and rotation of the map. Tiff world files (.tfw) are six-line files with decimal numbers on each line (Figure 3.1). Using the world file, image files can be imported into ARC/INFO or ArcView and co-ordinates can be input from the world file to maintain geographic integrity.

```
0.333558637640449 (size of pixel in x direction)
0.000000000000 (rotation term for row)
0.000000000000 (rotation term for column)
-0.333558637640449 (size of pixel in y direction)
384419.046678781 (x coordinate of centre of upper left pixel in map units)
4850556.47315363 (y coordinate of centre of upper left pixel in map units)
```

Figure 3.1: A .tfw world file for image 0002 taken during an August 16, 2009 flight.

Geo-referencing centers on aligning spatial data (layers that are shape files: polygons, points, etc.) to an image file such as a historical map, satellite image, or aerial photograph. To georeference is to align something to an earth-centered coordinate system such as longitude and latitude (Ladd *et al*., 2006). The alignment process is a simple rotation and translation of the rectified image based upon Ground Control Points (GCPs) visible in the image (Ladd *et al*., 2006). When an image is georeferenced to the earth's surface, the user can overlay additional geospatial datasets. Aerial photos, as a source of landscape imagery, need to be georectified to accurately register imagery to ground coordinates and geometrically correct them to remove distortions introduced during image capture. Many programs incorporate rectification and georeferencing into one command, allowing the user to both rectify and georeference an image based upon one set of GCPs (Hunt *et al*., 2003; Jensen, 2009). One popular way to georeference an image is to use an orthographic base image; an image that has already been rectified and georeferenced to a known precision (Ladd *et al*., 2006). Air photos need to be on projection before being transferred for use in GIS and image processing software because of geometric differences between photo and map. Although it requires immense amounts of manual correction, aerial imagery is increasingly used to provide a rich source of geographic information.

METHODS AND MATERIALS

DATA COLLECTION

The first image on the camera is of the US Naval Observatory Master Clock (if the Web site can be accessed) (Figure 3.2) or of a handheld GPS display showing the GPS date and time taken just prior to the flight. The GPS image shows the true GPS time. This image is used to determine the difference between the camera's time (imprinted in the photo metadata) and the GPS or Naval Observatory time. With the time difference known for each image, we were able to extract the latitude, longitude, bearing, altitude, and airspeed of the aircraft/camera for each photo taken.

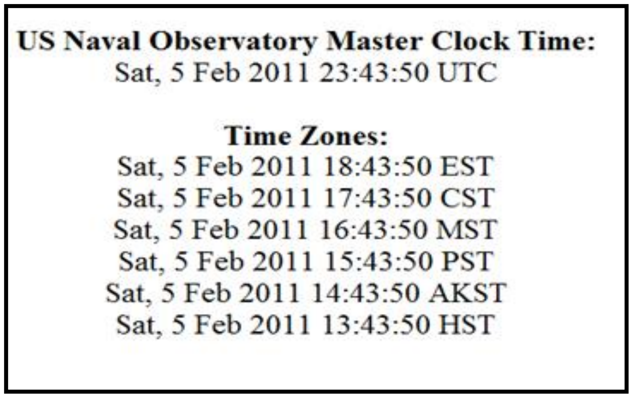
US Naval Observatory Master Clock Time:
Sat, 5 Feb 2011 23:43:50 UTC

Time Zones:
Sat, 5 Feb 2011 18:43:50 EST
Sat, 5 Feb 2011 17:43:50 CST
Sat, 5 Feb 2011 16:43:50 MST
Sat, 5 Feb 2011 15:43:50 PST
Sat, 5 Feb 2011 14:43:50 AKST
Sat, 5 Feb 2011 13:43:50 HST

Figure 3.2: Screen Image of the USNO Master Clock taken just prior to a flight.

After taking the first image, the camera was oriented so that it pointed straight down with the top of the camera towards the front of the aircraft. Accuracy is compromised when the camera is tilted: and keeping the aircraft as level as possible during camera installation and image acquisition is critical.

Aerial photography and GPS data collection

Aerial photographs were collected using a 12.40 megapixel Canon EOS Rebel XSi camera fitted with a 28mm lens. This camera was connected to a laptop computer which controlled the camera and received images as they were taken. Each image header file recorded date and time the images were taken as well as the camera settings. The equipment was mounted in the belly of a Cessna 182 fixed-wing aircraft (Figure 3.3 and 3.4). The aircraft, through an inverter, provided 110 volt power to the equipment. Photographs were taken at 5-second intervals while the aircraft flew a grid over the study area (Figure 3.5). The position of the aircraft was recorded at 1-second intervals by two GPS units, one for redundancy. In our study flight lines formed a grid with 1000m spacing. To keep the aircraft on track the pilot used an additional GPS system.

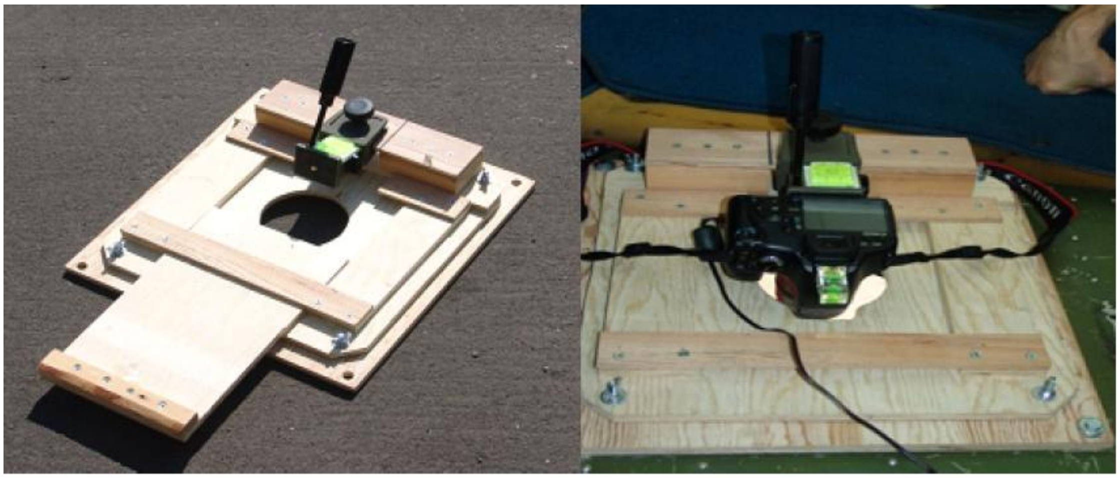

Figure 3.3: Wood board apparatus (Left) and mounted digital camera, compass, and bubble level inside the belly of a Cessna 182 (Right).

The aircraft was tracked with a continuously recording WAAS enabled GPS that saved National Marine Electronics Association (NMEA) data strings in an ASCII text format. It is crucial that the GPS has a position fix before beginning data collection. Our GPS logger records the NMEA $GPRMC, $GPGGA, and $GPGSA data strings of the NMEA GPS Sequence (Figure 3.5) at 1 second intervals on Secure Digital (SD) storage media. A typical track log consists of data points that are tagged with the latitude, longitude, altitude, time, date, velocity, and quality of the GPS location (Figure 3.7).

Figure 3.4: Location of the camera lens on a Cessna 182 equipped for aerial photography.

The time is based on Satellite Time, which is synchronized by the US Naval Observatory. It is the Official Source of Time for the Department of Defense (DoD) and the Global Positioning System (GPS), as well as a Standard of Time for the United States. Because time is measured so accurately, we can use it to synchronize data collected by other devices and in other formats as long as the clocks are synchronized to US standard time (Johnson *et al*., 2008).

Figure 3.5: A laptop computer is mounted in the Cessna 182 aircraft and connected to the 12.40 megapixel Canon EOS Rebel XSi and GPS to collect aerial images every 5 seconds, storing the data in a 1.5 terabyte external hard drive.

Two independent GPS units (for redundancy) recorded the aircraft position at 1-second intervals. Both GPS units continuously logged their position in a SFE data logger with a US Globalsat EM-406 GPS module using a SiRF Star III chipset and an embedded antenna. This provides a continuous breadcrumb log of positions for approximately eight hours when powered by four AA batteries. We evaluated the GPS accuracy using a fixed position test over 10.72 hours with a unit placed 2m above level ground with open sky conditions (38,600 positions). The mean error was 1.76m (std. dev. = 1.08m) and 25.86% of points were within 1 m, 67.42% within 2m, 86.73% within 3 m and 98.90% within 5m. Only 14 points had errors greater than 10m (0.36%). Data were gathered in a text format that could be read in MS Excel, MS Notepad, or Word and Global Geomatic Solution's (GGS) Logger Converter Tool was then used to convert the GPS logged points to Comma Separated Values (CSV) files for each points location (Figure 3.8).

Figure 3.6: The self-contained WAAS GPS device used on our study. Approximately 98.90% positions of a sample of 38,600 positions taken during a static test (open sky, 2m above level ground) were within 5 m of the true location. Mean error was 1.76m (Std. Dev. 1.08m) and the maximum error was 12.2m over 38,600 continuously logged points (10.72 hours).

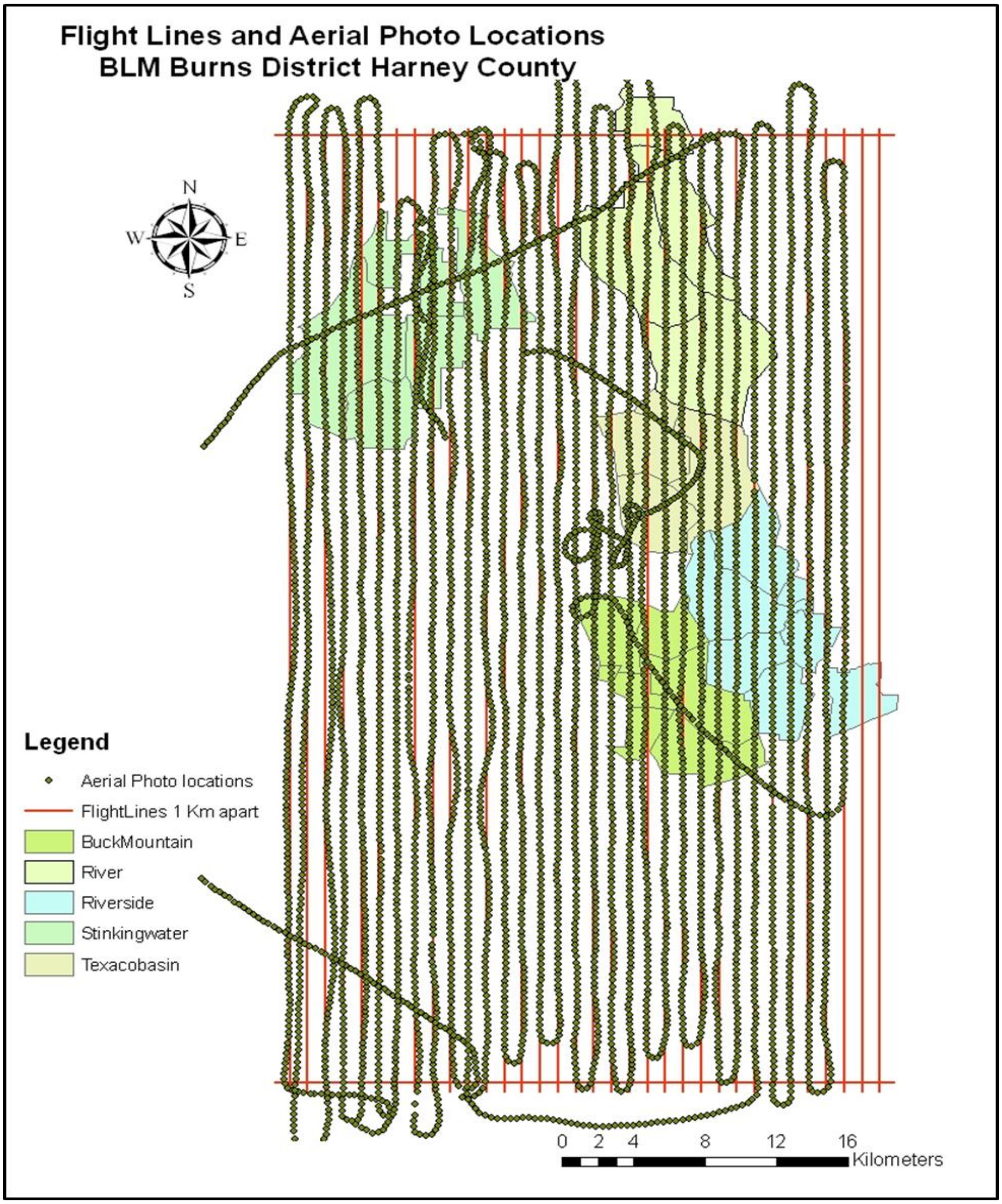

Figure 3.7: GPS recorded flight lines of the aircraft used to map our study area in Harney County, Oregon.

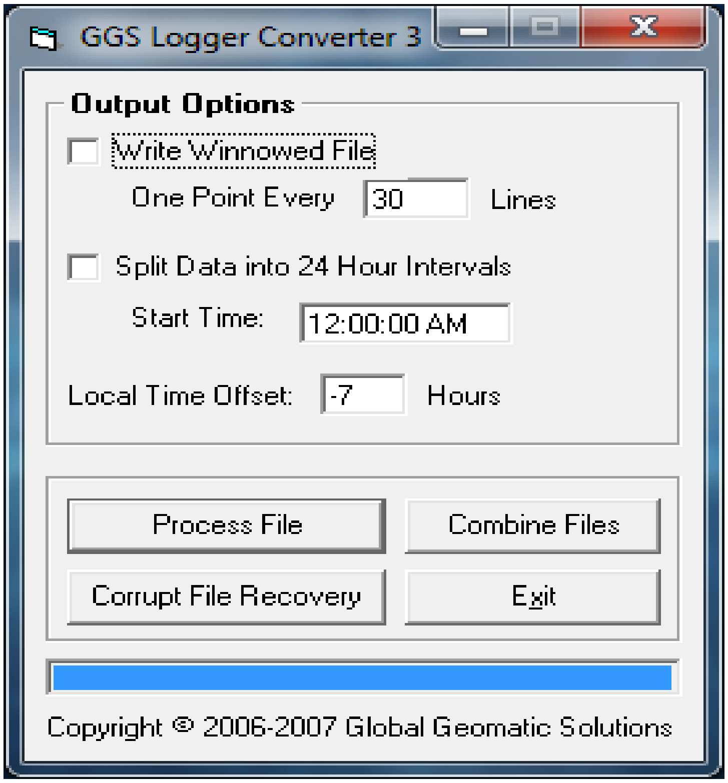

Figure 3.8: GGS Logger Converter software display. This program was used to convert NMEA sentences to CSV file format that was compatible with Aerial Photograph Positioning Tool and GIS software.

RESULTS AND DISCUSSION

Aerial Image Positioning Tool and Image Rectification Computation

We designed the Aerial Image Positioning Tool software to automate the correction process. The opening window (Figure 3.9) has text boxes to input the variables needed for geo-referencing and image projection. It consists of input areas for the image date and time, and the GPS time (hour, minute, second, day, month and year). The GPS and image date/time variables are used to calculate the time offset between camera time and the GPS time which is more accurate. Once the offset is known, the position of the aircraft can be determined for each aerial image. This position is assumed to be directly over the principal point of the image. Height above ground level is calculated by subtracting the ground elevation from the GPS recorded altitude at that point. Camera properties such as the focal length, sensor size (horizontal and vertical), and pixels numbers both horizontal and vertical are read from the image header file. The GPS projection used is latitude longitude and the datum is obtained from the GPS unit used for data collection (Figure 3.9).

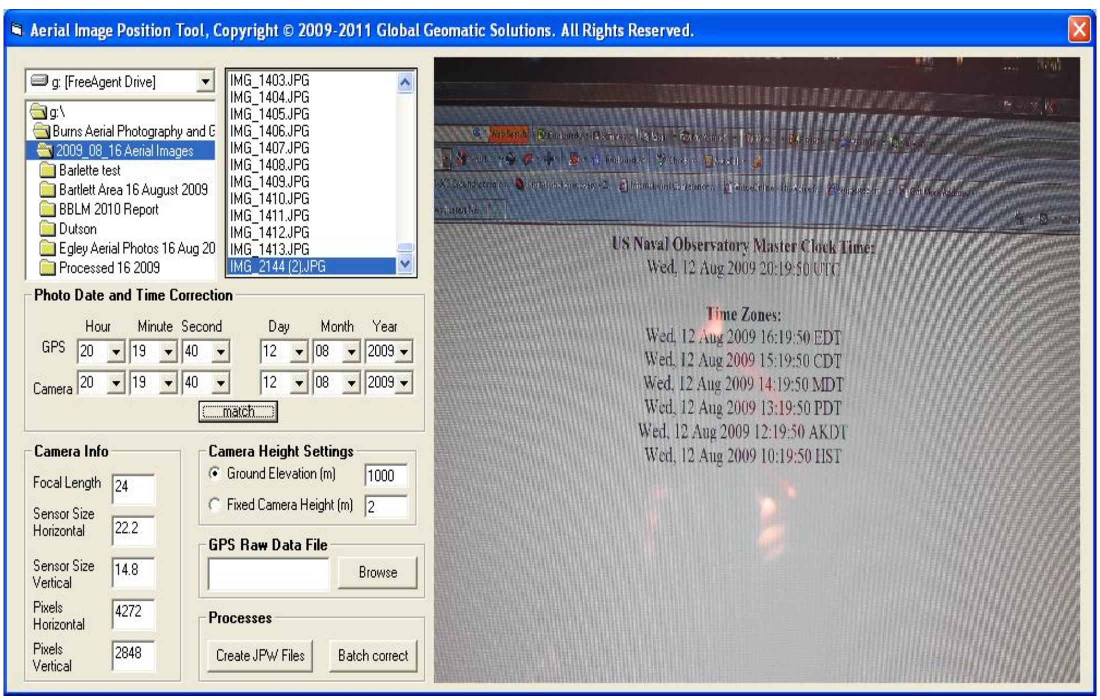

Figure 3.9: Aerial Image Positioning Tool opening window with text boxes for relevant variables used in digital aerial photograph geo-rectification and projection.

We uploaded all images, the image of the GPS time or US Naval Observatory time, as well as all aerial images in JPEG format, and the aircraft tracklogs in CSV format to the same folder. The average ground elevation was obtained from the National Elevation Dataset (NED), maintained be the USGS. We did this in Global Mapper by moving the mouse over a loaded DEM to read the surface elevation values. This altitude affects the accuracy of the projection scale. Errors can occur if the area being photographed varies widely in elevation.

The camera information was loaded automatically from the image header files; however, it should be verified via the camera manual or by looking under the advanced properties for one of the jpeg files (Figure 3.10). Lastly, the GPS tracklog file in CSV format, which contains the aircraft track, was used to compute the positions.

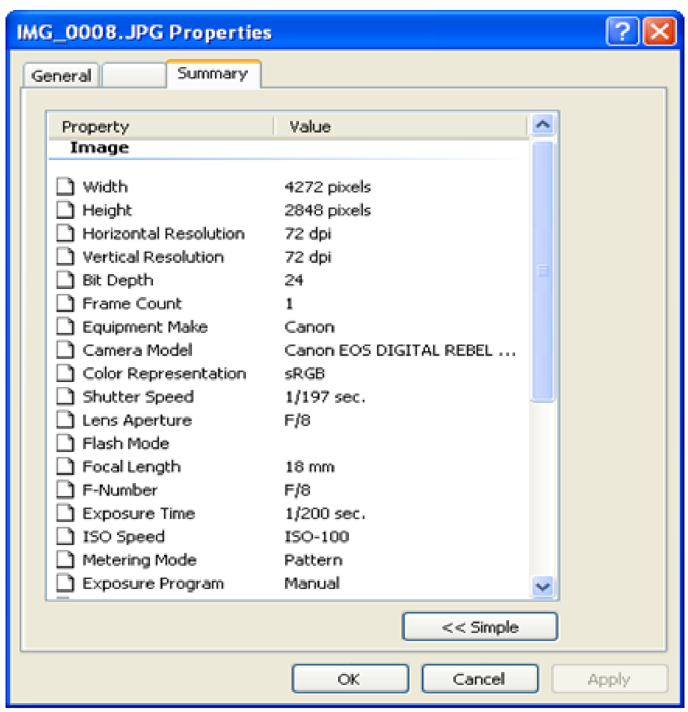

Figure 3.10: Camera values found in the camera manual under the advanced properties of one of the jpeg image files.

These files and associated information were then used in the Aerial Image Positioning Tool to create KML and projection files that register the images when viewed with appropriate software. The process is rapid whereby each image is coarse rectified in less than a second. Our aerial images (4272 pixels by 2848 pixels) had a ground resolution of 0.42 m and 100 images were geo-referenced every 60 seconds. Because images have projection information associated with them they can be opened for spatial analysis in GIS software such as Global Mapper and ArcGIS and digital processing software's such as VegMeasure 2, ENVI, Erdas Imagine and Auto Vista or some other suitable program for mosaicing (Figure 3.11). We typically display images in Google Earth by selecting the KML file with the corresponding name (Figure 3.12 and 3.13).

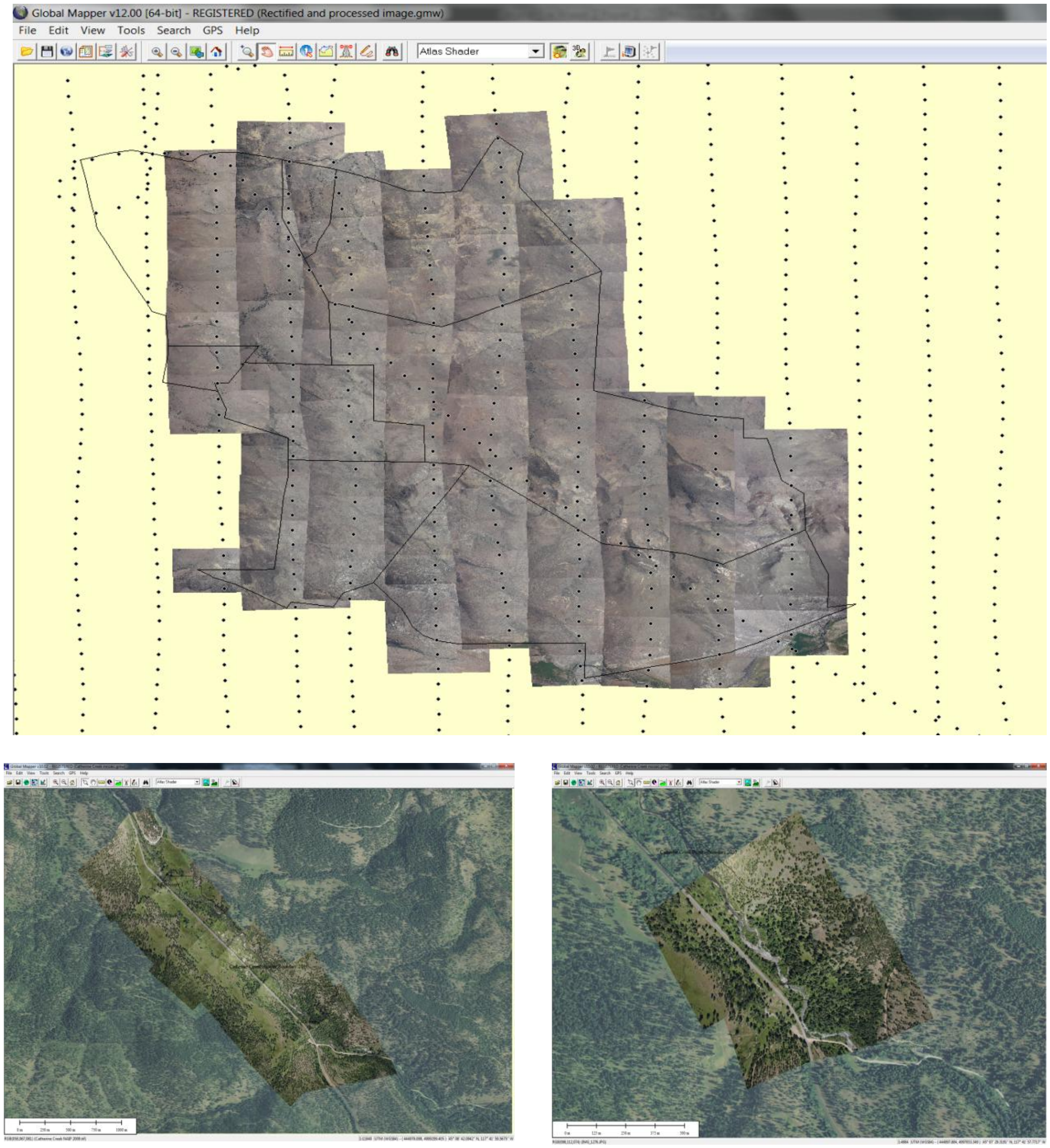

Figure 3.11: Coarse geo-referencing of aerial photography across the Buck Mountain BLM allotment (top) and two passes over Catherine Creek in Wallowa County, Oregon. Images were taken at five second intervals.

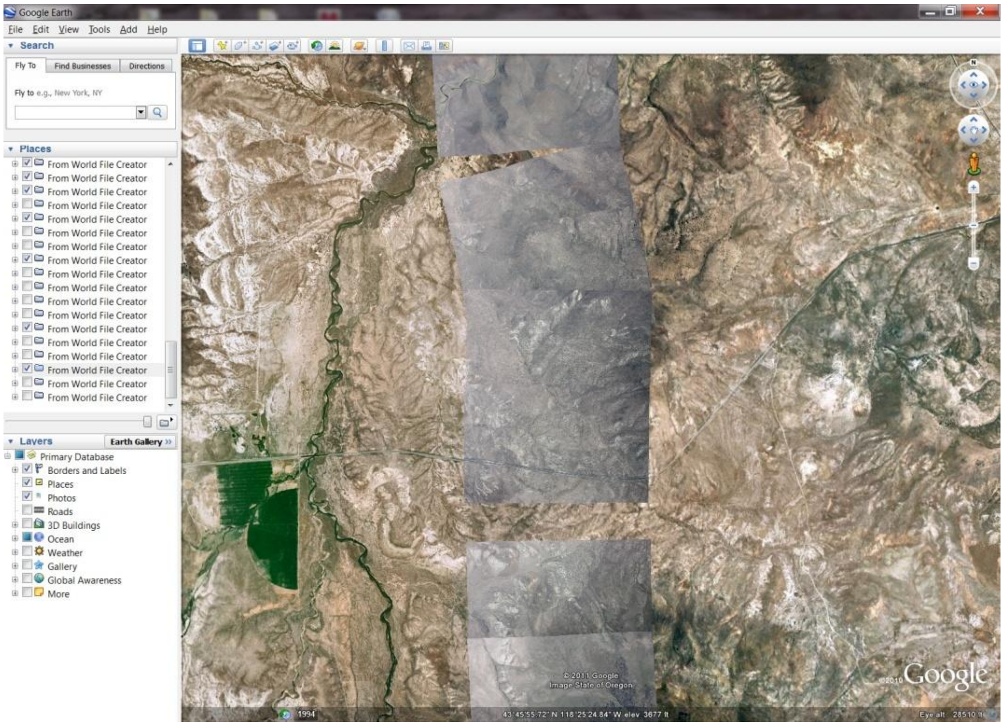

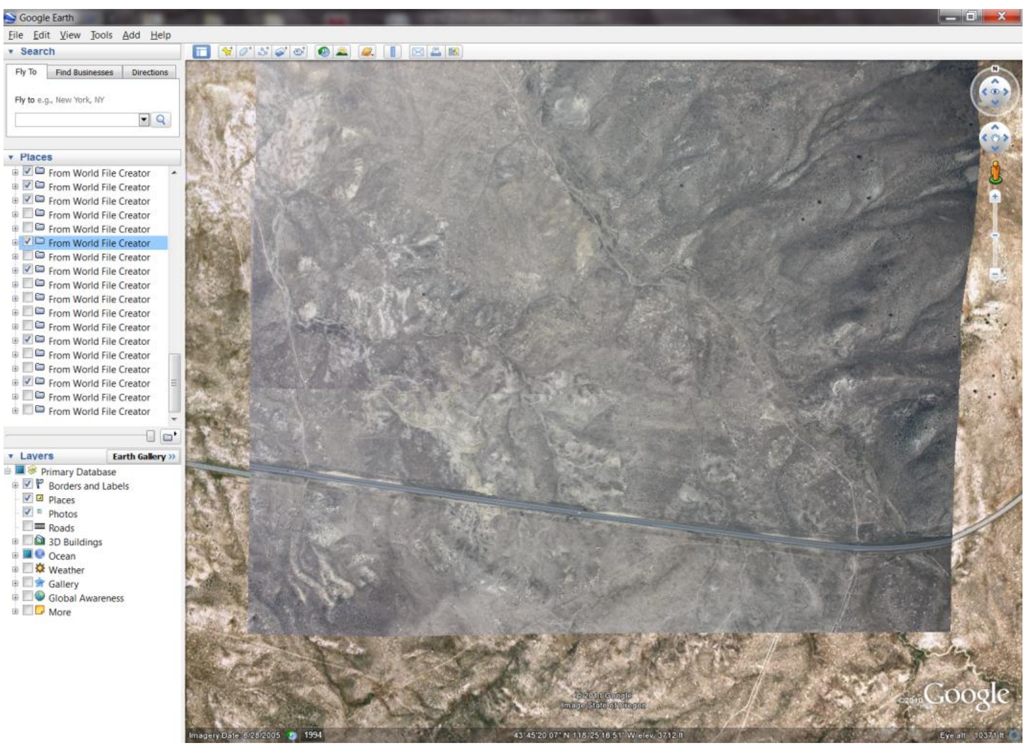

Figure 3.12: KML geo-referenced aerial image files opened in Google Earth.

The Aerial Image Positioning Tool can efficiently handle several thousand images and quickly coarse rectify them. By processing small batches, the rectification can proceed faster. For example, 3,700 images were collected during a June, 2010 flight and processed in batches of 300 images. The batches with 300 images correct at about an image every second and require seven minutes of processing time.

Error analysis

Error with this method comes from the pitch, roll, and yaw of the aircraft as it moves across the area of interest, which directly affects how the camera is tilted in relation to the ground below. These geometric errors can be large when working with slow moving, light-weight aerial platforms such as ultralight or microlight aircraft. There are also errors, resulting from the lag time between image acquisition and writing of the file. As aircraft speed increases these lags increase the error in position. Camera lenses also have distortion, which can be pronounced in wider-angle lenses. Commercial software is available to remove some of this distortion and should be applied if possible.

We evaluated the geometric error in our automatically corrected images by comparing the rough-corrected images with the same images that had been manually rectified using NAIP 2009 images as the base reference. NAIP orthorectification processing removes feature displacements and scale variations caused by terrain relief and sensor geometry. The 2009 NAIP imagery with 1 meter Ground Sample Distance (GSD) is orthorectified to within +/- 6 meters of true ground position and meets national mapping standards. Table 3.1 (Appendix 1) shows the detailed analysis of the aircraft direction, image error and offsets, and the time displacement of selected images. The Principal Point Error (PPE) significantly varied with respect to north bound and south bound due to the rectification method. The process of subtracting the angles of rotation from the image to align the image with the image orthogonal axis gave the southbound image a larger PPE (Table 3.2). This is the simplest method of rectification because of the two dimensional projective transformation used. 2D projective entails rotates on transformations which are always with respect to the origin. To rotate about a particular fixed point we must first translate the object so that the fixed point is at the origin. We then perform the rotation and then the inverse of the original translation to move the fixed point back to its original position. The projective transformation uses linear functions to map the image coordinates into ground coordinates. In Equation 1, Xw and Yw are the world coordinates, while x and y are the coordinates for the same location in the image, and c, d, and e are constants. Using the GlobalMapper11, we manually rectified images (Figure 3.13) and compared the error difference with the Aerial Image positioning tool rough geo-rectification error (Figure 3.14). Ten images were selected in this process. The error was determined by overlaying the images, rotating them southbound, and then measuring the NW, NE, SE and SW corners of the images.

$$X_w = \frac{d_1 x + e_1 y + c_1}{d_3 x + e_3 y + 1}$$

$$Y_w = \frac{d_2 x + e_2 y + c_2}{d_3 x + e_3 y + 1}$$

Equation 3.1: Xw and Yw world coordinates image location.

These measurements gave us an average Principal Point Error of 101.18m. Because the southbound was rotated, its principal error was negative. The average pixel size measured was 0.42m for the left angle pixels and 0.41 for the right angle pixel sizes. The average long axis measured 1823.18 m and the short axis measured 1191.09 meters, giving the image a very high resolution.

Table 3.2: Principal Point Error for aerial image positioning tool error and manual image rectification.

Image	Easting Aircraft	Northing Aircraft	N or S bound	Ground Elevation (m)	Aircraft Elevation (m)	Height Above Ground (m)	Theoretical Pixel Size (m)	PP Error (m)	Long Axis (m)	Short Axis (m)	Pixel Size LA	Pixel Size SA	Mean Pixel Size (m)
136	383849.181	4840582.808	N	1118.4	3127.4	2009	0.418220123	109	1827	1179	0.427668539	0.413974719	0.420821629
234	382135.881	4832449.369	S	1289.8	3088.2	1798.4	0.418220123	-106	1706	1092	0.399344569	0.383426966	0.391385768
121	383782.574	4835297.05	N	1157.1	3143.7	1986.6	0.418220123	95	1785	1217	0.417837079	0.427317416	0.422577247
457	387194.828	4839333.04	N	1256.9	3159.4	1902.5	0.418220123	97	1779	1212	0.416432584	0.425561798	0.420997191
304	379984.032	4842929.62	N	1149	3141.6	1992.6	0.418220123	64	1824	1183	0.426966292	0.415379213	0.421172753
291	379949.88	4838376.07	N	1282	3155.3	1873.3	0.418220123	44	1703	1122	0.398642322	0.393960674	0.396301498
228	382143.616	4834454.349	S	1273	3092.6	1819.6	0.418220123	-99	1747	1131	0.408941948	0.397120787	0.403031367
218	382096.933	4837868.275	S	1159.7	3101.9	1942.2	0.418220123	-104	2177	1192	0.509597378	0.418539326	0.464068352
65	385602.166	4837350.765	S	1129.9	3111.3	1981.4	0.418220123	-174	1839	1267	0.430477528	0.444873596	0.437675562
62	385587.63	4838346.618	S	1129.2	3116.8	1987.6	0.418220123	-107	1849	1246	0.432818352	0.4375	0.435159176
69	385666.316	4835962.455	S	1138.2	3118.1	1979.9	0.418220123	-114	1819	1261	0.42579588	0.442766854	0.434281367
Mean								101.18	1823.18	1191.09	0.42	0.41	

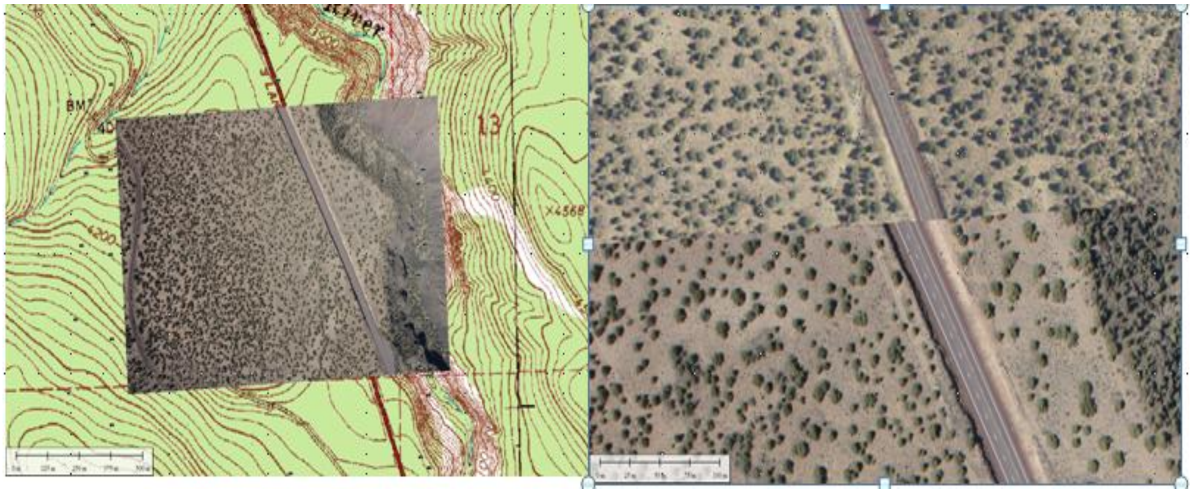

Figure 3.13: Displacement error when using aerial Image Positioning Tool because of image rotation and/or crabbing of the Aircraft.

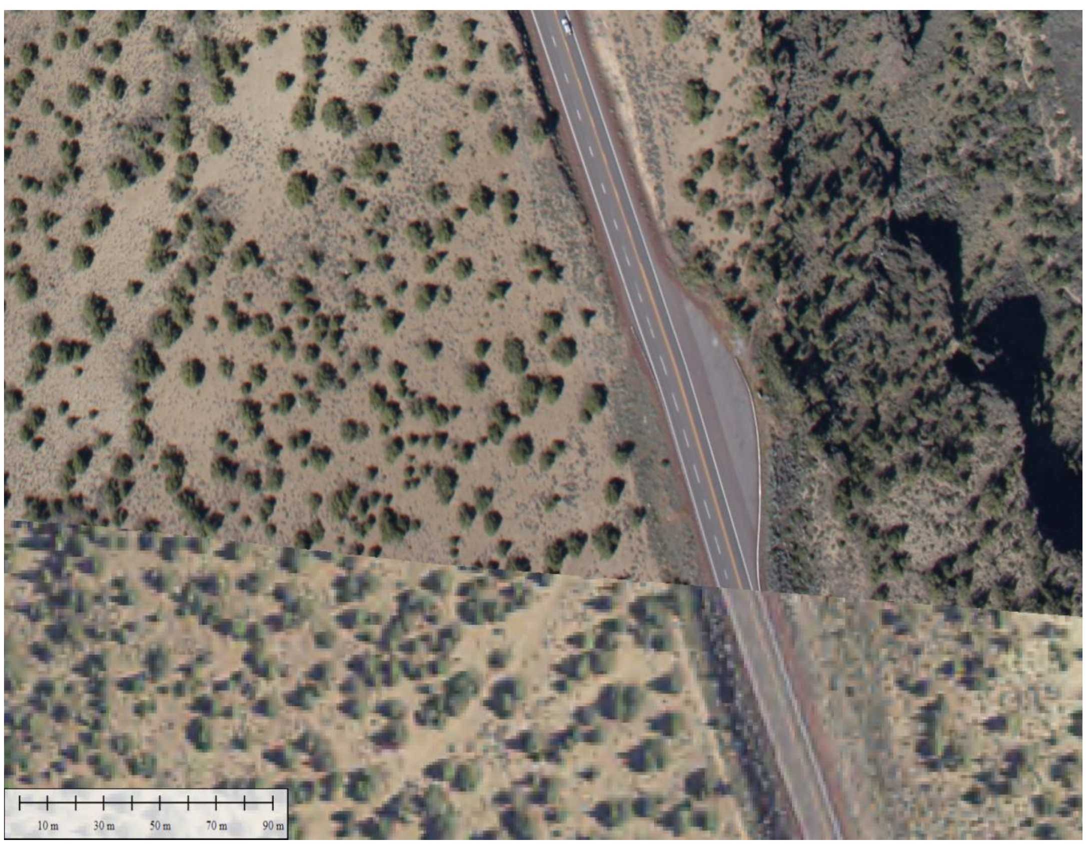

Figure 3.14: Manually re-rectified image adjusted to conform to a NAIP 2009 image.

Cost efficiency and aerial image collection

Our protocol allowed us to survey extensive areas via high-resolution photographic sampling in a format that is inexpensive and easily stored, shared, and interpreted. The cost of our aerial surveys, because images were digital, was low on a per hectare basis. In this study, we had a total over-target flight time of 18 hours 58 minutes and collected 10,362 aerial images (Table 3.3).

Aircraft and pilot costs totaled $250/hour (in the air), thus total cost of the 10,360 photographs for the three flights was $4758 (Table 3.3). Since we could shoot 720 images/hr with a GSD of 0.42m, our cost was $0.46 per image with 60% overlap. In our study each image covered 215 ha with 60% overlap or approximately $0.535/km^2.

Table 3.3: Total cost of flight and image collection.

Date of Survey	Duration of flight during time of image collection	Average altitude	Total time (hours)	Total time		Average Velocity from GPS during image collection		Total flight distance covered (m/s)	Total Average flight distance covered (km/min)	Cost per ($)		Total number of images	Total cost (cost/min /total time/ min)/ flight ($)	Total cost per image photographed (total images /total cost) ($)
				min	Sec.	m/s	Km/ hrs			hour	min			
May 28 2009	10:33:24 to 14:29:18	2643	3 hrs 55min 54 sec.	236	14160	54.80	197.28	775968	12.93	250	4.17	2,788	984,12	0.35
15 August 2009	8:44:10 to 16:52:36	2823	8hrs 08min 26sec.	489	29340	54.01	194.44	1584653.4	26.41	250	4.17	4,781	2039.13	0.43
16 August 2009	9:12:54 to 16:08:52	2870	6hrs 56min 02sec	416	24960	66.35	238.86	1656096	27.60	250	4.17	2,893	1734.72	0.60
		2778.7	18hrs 58min 22sec.	1141	68460	Av. 58.39	Av. 210.20	4016717.4 (4016.717 4 Km)	Av. 22.31	250	4.17	10,362	4757.97 (Av. =1586)	Av. $0.46/image

CONCLUSIONS

We developed the Aerial Image Positioning Tool for the rough positioning of digital images acquired from aircraft so they could be used in conjunction with GIS and image analysis programs. Our process resulted in extremely fast rough geo-referencing of aerial photographs, generally accurate within 100 meters, which is close enough to make targeting specific areas for routine observation possible. Our program reduces the cost of rangeland and ecosystem monitoring from aircraft.

Once rough corrected images are available in a GIS program, it is possible to choose sites for closer monitoring or select areas of interest for quick aerial observation. We have used this method for monitoring rangeland weeds, land use changes, and to assess rangeland recovery after fires. If higher geospatial accuracy is needed, it is possible to select ground control points from USDA National Agriculture Imagery Program (NAIP) imagery and re-rectify the rough corrected images. The ease and speed of the initial image positioning makes large-scale monitoring much more cost effective and efficient.

LITERATURE CITED

ESRI. 2010. ArcGIS User's Manual. Environmental Systems Research Institute, Inc. Redlands, CA.

Global Mapper LLC. 2010. GlobalMapper User's Guide. Global Mapper Software LLC. Parker, CO.

Hood, J., L. Ladner, and R. Champion, 1989. Image Processing Techniques for Orthophotoquad Production. Photogrametric Engineering and Remote Sensing 55:1323-1329.

Hummer-Miller, S. 1989. A Digital Mosaicking Algorithm Allowing for an Irregular join 'Line'. Photogrammetric Engineering & Remote Sensing 55:43-47.

Hunt E. R. Jr., J. H. Everitt, J. C. Ritchie, M. S. Moran, T. D. Booth, G. L. Anderson, P. E. Clark, and M. S. Seyfried. 2003. Applications and research using remote sensing for rangeland management. Photogrammetric Engineering and Remote Sensing 69:675-693.

Jiann-Yeou, R. and Liang-Chien, C. 2004. Geometrical Building Modeling and Its Application to the Ortho-Rectification for Aerial Images. Journal of Photogrammetry and Remote Sensing 9(1):53-76.

Kang, Z, Zhang L, Zlatanova, S, and Li, J. 2009. An automatic mosaicking method for building facade texture mapping using a monocular close-range image sequence. *ISPRS* Journal of Photogrammetry and Remote Sensing, doi:10.1016/j.isprsjprs.2009.11.003 (Elsevier: SCI).

Kawai, S. and Saji, H. Automatic Registration of Aerial Oblique Images and a Digital Map. SICE Annual Conference 2007. Sept. 17-20, 2007, Kagawa University, Japan.

Kim, J. S., M. Christopher and B. James. (2010). Automated Georeferencing of Historic Aerial Photography. The Journal of Terrestrial Observation, Vol. 2, No. 1:

pp 57-65.

Ladd, G. B., A. Nagchaudhuri, T. J. Earl, M. Mitra, G.L. Bland. 2006. Rectification, georeferencing and mosaicking of images acquired with remotely operated aerial platforms. ASPRS 2006 Annual Conference Reno, Nevada, May 1-5, 2006.

Lamb, D.W., M.M. Weedon and L.J. Rew. 1999. Evaluating the accuracy of mapping weeds in seedling crops using airborne digital imaging. Avena spp. in seedling triticale (X. Triticosecale).Weed Research 39:481-492.

Minhe, J.I., and J. R. Jensen. 2000. Continuous Piecewise Geometric Rectification for Airborne Multispectral Scanner Imagery. Photogrammetric Engineering & Remote Sensing 66(2):163-171.

Motrena, P. and J.M. Rebordao.1998. Invariant models for ground control points in high resolution images. International Journal of Remote Sensing 19(7):1359-1375.

Shih, F. Y. and O. R. Mitchell, 1992. A Mathematical Morphology Approach to Euclidean Distance Transformation. IEEE Transactions on Image Processing, 1(2):197-204.

Strunz, G., W. Knpfle, and A. Roth. 1994. Automation of Tie Pointing Procedure for the Geocoding of Satellite Images. International Archives of Photogrammetry and Remote Sensing, 30(3):

Murino, V. U., Castellani, A. Etrari and A. Fusiello. 2002. Registration of very time-distant aerial images. Proceedings of the IEEE International Conference on Image Processing, 3:989-992.

Wendy, W. 2006. Automated Georeferencing for Rapid Data Production. Photogrammetric Engineering & Remote Sensing, April 2006. pp 336-338

Xin, Y., J. Li, and Q. Cheng. 2007. Automatic generation of remote sensing image mosaicks for mapping large natural hazards areas. In Li, J., S. Zlatanova and A. Fabbri, (eds.) Geomatics Solutions for Disaster Management, Lecture Notes in

Geoinformation and Cartography, Vol.18, Springer Verlag, Berlin, ISBN 978-540-72106-2, pp.61-73.

Xin, Y. 2006. Image Correction for Digital Mapping. Proceedings of the ASPRS Annual Conference, Reno, NV., USA .

Xin, Y. and D. Parent. 2004. Automated Procedure of a Prototype Mapping System. Proceedings of the ACRS Annual Conference, Chiang Mai, Thailand.

Yehuda, A. and A. Brand. 1998. Mosaicking of Orthorectified Aerial Images Photogrammetric. Engineering and Remote Sensing 64(2) 115-125.

Yingen, X. and F. Quek. 2006. Automatic Aerial Image Registration Without Correspondence. ICVS ’06: Proceedings of the Fourth IEEE International Conference on Computer Vision Systems, pp. 25-33.

Yubin, X. Image correction for digital mapping. PCI Geomatics Inc. 50 West Wilmot St., Richmond Hill, Ontario L4B 1M5, Canada.

Zobrist, A.L., N.A. Bryant and R.G. Mclead, 1983. Technology for Large Digital Mosaics of Landsat Data. Photogrammetric Engineering and Remote Sensing 49:1325-335

CHAPTER 4: MOBILE MAPPING OF MEDUSAHEAD (*TAENIATHERUM CAPUT-MEDUSAE* (L.) NEVSKI) INFESTATIONS

S.K. Ndzeidze, K.E. Johnson, M. Louhaichi, P.E. Clark, and D.E. Johnson

Key Words: GIS, GPS, Laptop Computer, Digitization, External hard drive, Cross-sectional survey, 4-wheel drive pick-ups, Mobile Mapping Systems.

ABSTRACT

Medusahead (*Taeniatherum caput-medusae (L.)* Nevski) poses a serious challenge as it expands across arid and semi-arid rangelands. Traditional field mapping of noxious weed infestations is done by technicians who must find infestations, locate themselves on the map, and draw in the infestation boundaries. Although this is effective, the transfer of data to a format usable in GIS applications is time-consuming, inefficient, repetitive, and prone to error. This study developed a mobile mapping survey protocol for mapping invasive weeds using a GPS-enabled laptop computer in the field. This process increased the accuracy of data collection, and facilitated storage and subsequent management of spatial data. We tested protocols for medusahead detection and monitoring from fixed-wing aircraft, helicopters, and 4-wheel drive pick-ups. The hardware/software system employed a computer that was equipped with a WAAS-enabled GPS antenna running Global Mapper software to map infestations as points, lines and areas. Digitization was done on-screen using underlying base maps. The base maps were of three types: 1) USGS National Elevation Dataset (NED) Digital Elevation Models, 2) USGS 7.5-minute Digital Raster Graphics, and 3) USDA National Agriculture Imagery Program (NAIP) 1m resolution digital ortho quarter quad tiles (DOQQs). Our field position within 10m was indicated on the GIS base maps as we surveyed. This eliminated technician errors resulting from misreading paper maps. Both the NAIP and DRG maps were useful for digitizing infestation polygons and defining their extent. We conducted five road/trail survey routes across the study area covering a total of 269 kilometers. On average we mapped 1.5 medusahead infestation polygons per kilometer and traveled at an average speed of 438 m/min. Approximately

11.1 infestations were mapped every hour during our surveys. Overall, a total of 410 infestation polygons were mapped during 2,008 minutes (33 hours 47 minutes) of survey. Mobile mapping on road survey routes was effective but limited to areas with established roads and trails. Mapping from fixed-wing aircraft was not limited by the road/trail network. On average, an infestation polygon was mapped every 6.8 km of flight line. Since the observation distance was much greater (≈ 2,000m above ground), only large and dense medusahead infestations were mapped. There was also a tendency for technicians digitizing infestation to become airsick. Helicopter survey was much closer to the ground and infestations were easier to find but this type of survey was much more expensive. Mobile field mapping accurately located infestations so that control actions could be planned and efficiently implemented. Combining field data collection and GIS mapping capabilities in a mobile computer system is an innovative and progressive step forward for invasive weed management.

INTRODUCTION

Mobile Mapping Systems (MMS) combine personal computers equipped with a GPS antenna, loaded with GIS software, and databases to facilitate mapping and field-data collection of spatial data. Mobile mapping systems have been developed to map features on landscapes and are very useful in remote areas with expansive, homogeneous landscapes. These systems permit GIS mapping in the field with much of the convenience of a laboratory or office-based system. We employed a computer equipped with Global Mapper software, powered by an AC power inverter connected to the vehicle's electrical system, and connected to a GPS antenna. This system permitted, "on the spot" visual judgment, GPS capture and digitization to map the extent of weed infestations on the Burns District of the USDI Bureau of Land Management. Updating existing databases with new information and the synchronization of changes between the project site and laboratory are one of the major advantages. MMS has been suggested as a means of generating accurate and lower cost solutions for field survey and GIS data collection.

Previously, field mapping and the location of a phenomenon were very cumbersome and a huge amount of spatial information had to be taken to the field as paper maps, often in the form of map books. Most of this Information had to be sketched, as notes on paper maps were entered into a GIS-compatible database when the field worker returned to the laboratory. Data collected in the field were often recorded on forms that were taken to the field, filled out on a clipboard, and entered into a database upon returning to the office, an inefficient, repetitive, process prone to error (ESRI, 2009).

The basic requirements for mobile mapping include a georeferenced field map, such as high resolution NAIP data or DOQ base maps, a good GPS and a computer to store the acquired data. Natural resource mapping often requires a field survey for a better understanding of spatial extent. During our mobile mapping, study transects of high resolution images were taken as ground truth support for the location and level of infestation within some of the digitized area features. Critical to mobile mapping is the field data collection of the most updated geospatial information with a streamlined cross-sectional drive across the target landscape. The GPS device enabled the integration of locations and positioning systems of new data.

STUDY OBJECTIVE

The principal objective of this study was determine the extent to which mobile mapping can be used as a preliminary study measure for determining the extent and proliferation rate of infestations. We also determined the accuracy and reliability of the data collection and storage systems. This study focused on developing a rapid data collection system using hand held computers, Global Positioning System (GPS) receivers, mobile geographic information systems (GIS), and computing software.

MATERIALS AND METHODS

Study Area

Our study area included five Burns District BLM allotments: Stinking Water, Texaco Basin, Riverside, Buck Mountain, and Warm Springs and surrounding areas in Harney County, Oregon (Figure 4.1). This area is characterized by many large and small basins separated by north-south trending mountains. The climate is dry and relatively cold. Basins are vegetated with drought-tolerant upland species such as big sagebrush, rabbitbrush, needlegrass, ricegrass, and squirreltail. The rolling to steep hills and mountains contain scattered stands of western juniper. Stream and riparian areas consist of grassy meadows with scattered willows. Medusahead (*Taeniatherum caput-medusae (L.)* Nevski) is expanding into and dominating large areas of the sagebrush grassland and poses a serious ecological threat. This area is a mixture of public and private lands with large distances between roads and trails.

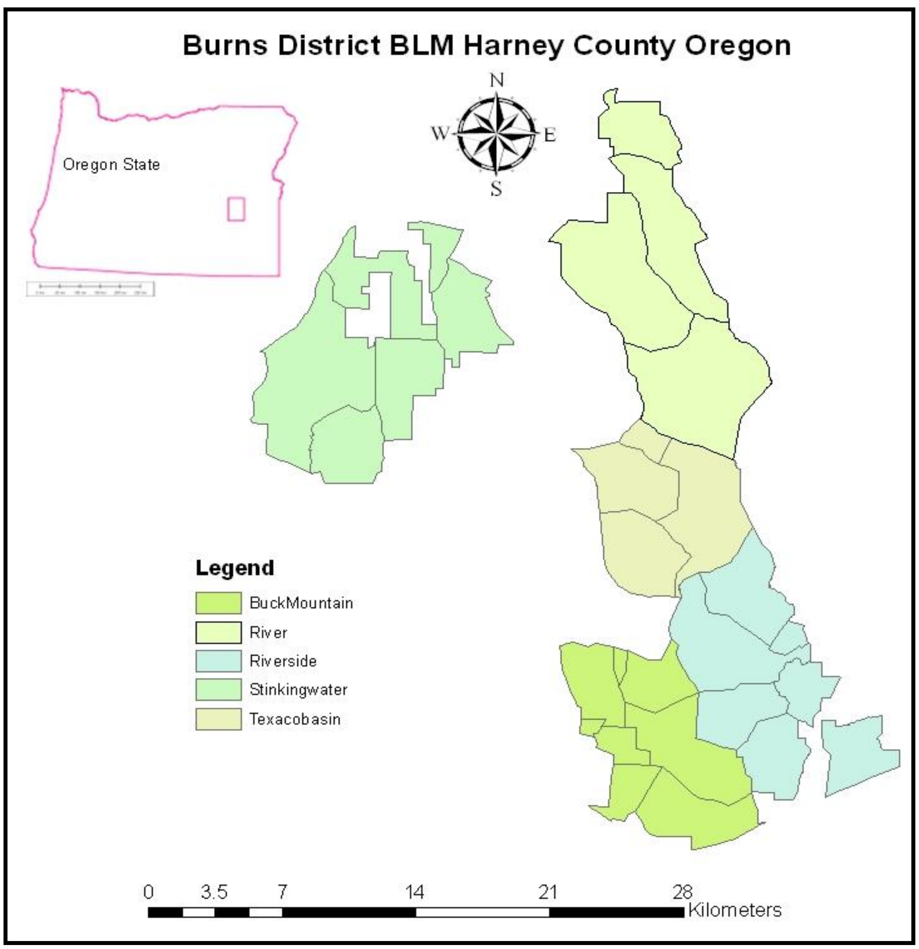

Figure 4.1: Study area in Burns district BLM allotments Oregon.

Mobile Mapping System

Mapping was done with a Panasonic Toughbook® laptop computer connected via a USB cable to an external Pharos® iGPS-500 GPS receiver with a waterproof remote magnetic mount antenna (Figure 4.2). The laptop was also equipped with a cooling pad to avoid overheating and unexpected shut down. Power was supplied to the units using a 12 volt DC to 115 volt AC inverter. The laptop used the Microsoft® Windows XP® operating system and was loaded with Global Mapper® 11 software. Also loaded on the laptop were 1:24,000 USGS Topographic Digital Raster Graphics (DRG) and 2005 and 2009 National Agriculture Imagery Program (NAIP) color aerial imagery with a ground resolution of 1 m. NAIP imagery was correct to a horizontal accuracy within 6 meters of photo-identifiable ground control points. In addition, two continuously recording GPS receiver were also placed in the vehicle to log the survey route at 1-second intervals. A four-wheel drive pickup was used to carry the equipment across the study area (Figure 4.2 and 4.3).

The external GPS antenna allowed GlobalMapper® GIS software to track the vehicle on-screen with geographically registered aerial photography (NAIP 2009) or 7.5 minute topographic DRG maps as base layers (Figure 4.3). The position provided by the GPS was shown on-screen in real time on either a topographic or an aerial photographic background, which could be zoomed in or out depending on the size of the infestation. We digitized boundaries of medusahead infestation as we progressed across the landscape, adding notes if desired.

Figure 4.2: Four-wheel drive pickup equipped with roof mounted GPS antenna used to map invasive weed infestations in Harney County, Oregon.

The GPS data from the WAAS-enabled GPS device memory was downloaded and processed using GGS Logger Conversion software, converting the logged points to shape files (Johnson, 2009) (Figure 3.8). Using the data converted to points, and the time and speed between each point, it was possible to calculate the distance travelled between any two points on the map.

Figure 4.3: Medusahead infestation along a rural road and field collection of data using off-road all-terrain vehicles (ATV) in Harney County, Oregon.

Data Collection

Five trips to the study area were made (Figure 4.4). The first mobile ground-truth survey and data collection for digitization of infested areas was on June 6, 2009, the second on July 7, 2009 and the third was on August 13 and 14, 2009. The last survey was from August 18 to19, 2010 (Table 4.1 and Figure 4.4). As we encountered medusahead infestations during the traverses, they were digitized on-screen and entered into a database.

Our ability to see infestations along the road was influenced by the topography of the location. At some locations where the road was elevated we could see medusahead at considerable distance. Other areas were obstructed by hills. Visible distance therefore depended on the viewshed across the landscape. We conducted viewshed analyses using Global Mapper 11.1. This analysis allowed us to use elevation grid data with a user-specified observer location, height, and radius to determine all areas within the selected radius with a clear line of sight. We used viewshed analysis the Buck Mountain and Riverside allotments to determine the number of infestation polygons mapped per visible area.

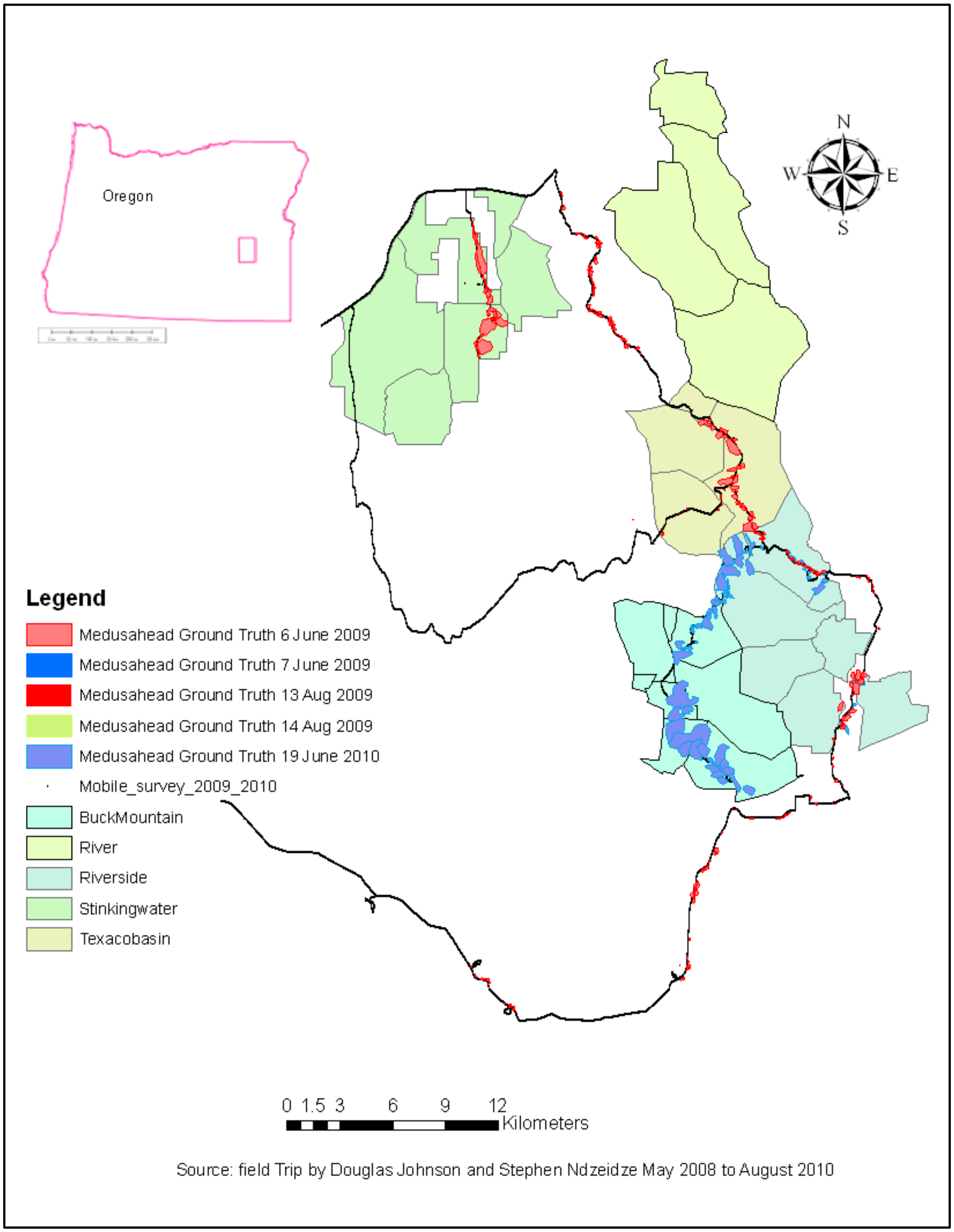

Figure 4.4: Burns District BLM road transects and off- road infestations mapped using transects perpendicular to the road.

Aerial Reconnaissance

Aerial reconnaissance (28 May 2009) using a Cessna 182 aircraft was conducted after the first mobile cross sectional survey on the ground was completed. The same mobile mapping system used for ground mapping was used in the aircraft. Known and mapped medusahead infestations were used as “training sites” so that other infestations could be visually identified from the air. After examination of these training sites, we flew gridded flight lines approximately 1,000 m apart at an altitude of 2,000m above the ground to survey for medusahead (Figure 3.7). As we flew across the landscape we digitized infestations, as was done during the road survey.

RESULTS AND DISCUSSION

Mobile mapping of infestations

We mapped 410 medusahead infestations during our 270 km traverse across the research site (Table 4.1). Infestations were scattered throughout the survey areas as shown in Figure 4.4. Our survey required 23 hours of field mapping time on the site (Table 4.1). Infestations near roads were easily detected and mapped while those at greater distances were more difficult to see. The farthest infestation mapped was 1.3km from the vehicle. As would be expected, only large, dense infestations were visible at distances greater than several hundred meters. Doubtful observations were confirmed by stopping and walking to the location, since medusahead and cheatgrass often look alike from a distance.

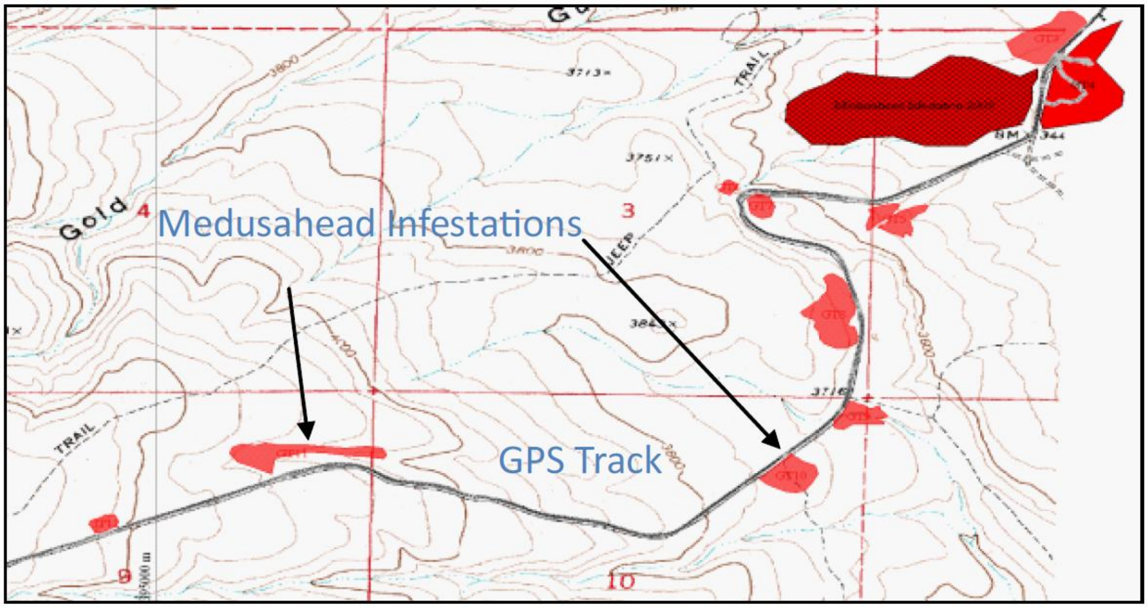

Figure 4.5: GPS track on a road transit and digitized infestations on a USGS 7.5 minute topographic quadrangle base map.

While digitizing infestations, we found the NAIP data most useful for positioning infestations but the 7.5 minute DRG maps were also very helpful. In addition, we used the distances measuring tool in Global Mapper 11.1 to verify our position of the mapped polygons. Medusahead infestations often have indistinct boundaries and grade into surrounding vegetation. Scattered plants can be found at considerable distances from core infestations and are very difficult to map. Thus, our maps should be considered as representing heavy and continuous stands. Accurate mapping of core infestations is possible, especially with stop-and-go travel. We drive slowly until an infestation is found, then stop and digitize its extent. Because of the frequent stops we suggest that a team of two people, a driver and observer, be used and that the vehicle be equipped with a warning light bar for safety. Frequent stops and transects on foot perpendicular to the road add to accuracy in mapping and enable off road infestations to be found or verified (Figure 4.5).

Environmental and technological variables affected the efficiency of mobile mapping of medusahead. The vehicle's speed, condition of the road, time of day, topography/viewshed, associated shrubby or tall vegetation, and weather all affected detection. Our study area was topographically rough with elevations ranging from 1,000m to 2,000m (Figure 4.6). This resulted in considerable variation in the search area along the survey route.

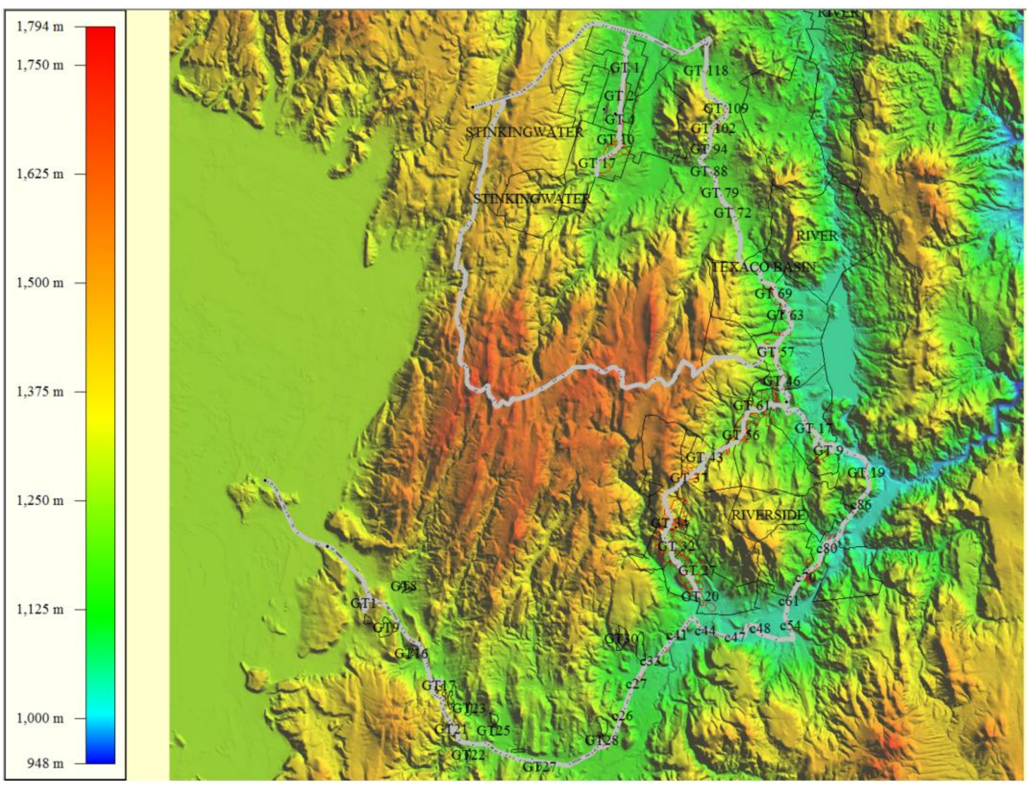

Figure 4.6: Topographic map of study area (the Burns BLM District) showing the track log and medusahead infestations along the drive through route.

Approximately 270 km of road were sampled during the two-year study and we estimate that approximate 27km^2 of rangeland was actually sampled. Infestation polygons occurred on average every 1.5 per kilometer (Table 4.1) and on average, 11.1 infestations were mapped every hour.

Table 4.1: Mobile cross sectional drive through mapping of medusahead infested areas within the Burns BLM District allotments

Date of Survey	Allotments	Total number of digitized infested areas	Mapping Time	Mapping Minutes	Distance covered and velocity			Average Mapped infestation / Distance (Km)	Average mapped infestation / Time	
					Total Surveyed distance	Average (Velocity km/hrs) base on GPS logging				
					Km	Per second	Per hour	Infestation /Km	Per Min	Per hour
6-Jun-09	Stinking water, Texaco Basin, Riverside	200	10:39:00 to 18:27:00	478 (7hrs 58min)	58.693	5.7	20.52	3.41	0.58	35.08
7-Jun-09	Riverside	78	9:04:34 to 16:04:33	420 (6Hrs 59min)	58.281	8	28.8	1.34	0.16	9.75
18-Jun-10	Riverside	20	13:46:06 to 16:15:43	149 (2Hrs 29min)	20.696	2.2	7.92	0.96	0.15	9.09
19-Jun-10	Buck Mountain,	50	10:07:03 to 18:53:15	526 (8hrs 46min)	23.578	0.8	2.88	2.12	1.04	62.5
13-Aug-09	Stinking water, Texaco Basin	30	10:46:33 to 15:57:00	310 (5hrs 10min)	46.136	1.6	5.76	0.65	0.31	18.75
14-Aug-09	Warm Spring	32	13:21:02 to 18:46:28	325 (5hrs 25min)	62.06	5.1	18.36	0.51	0.10	6.27
Total/ Average	Field Work[1]	410		2208 (36hrs 08min)	269.444	3.9	14.04	1.49	0.39	23.57

The Buck Mountain Allotment was heavily infested and sampling was slower. We averaged only 2.8 km/hr during the road survey with 2.1 infestations per km of survey. This survey was complicated by rough terrain and a poor road. The Stinking Water, River, Riverside, Texaco Basin areas sampled on June 6, 2009 were also heavily infested although data collection took a proportionally shorter time, averaging 29 km/hr and 27.3 plots mapped per hour because the road was good.

The autonomous GPS units recorded the location, velocity, date, and time every 1 second during the survey. Using these GPS data we examined the relationship between the number of infestations mapped per km and the average velocity of the survey. A poor correlation ($R^2 = 0.2355$) exists between the rate infestations are mapped and the velocity of survey (Figure 4.7). The pattern in Figures 4.8 to 4.13 of vehicle movement reveals that relationship between velocity and infestations mapped typically had a stop and go.

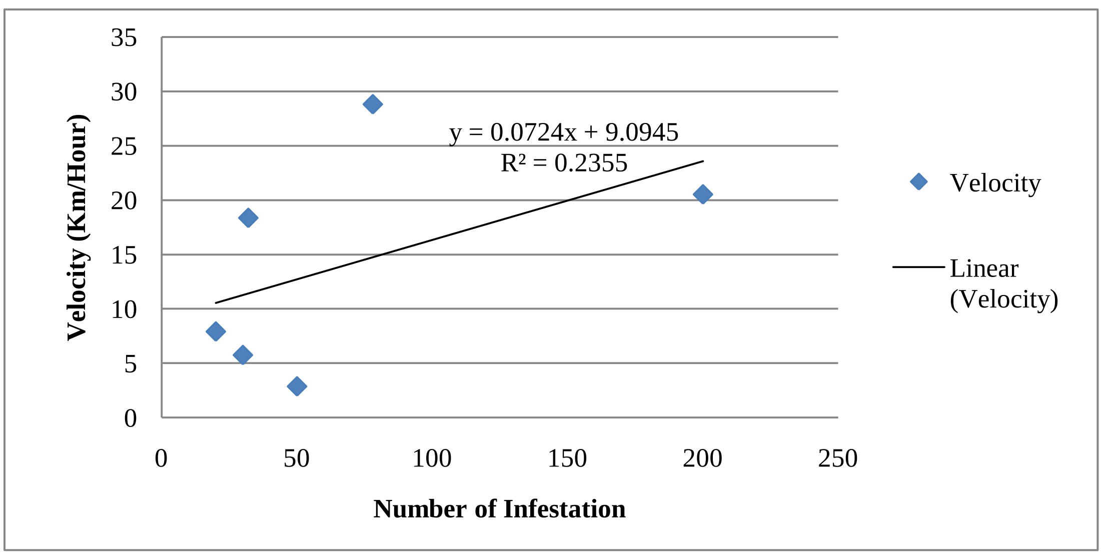

Figure 4.7: A low positive correlation exists between the mapped infestation plots and velocity of mobile mapping.

Figure 4.8 shows the velocity of the mobile drive through conducted during June 6, 2009 traverse across the Stinking Water, Texaco Basin and Riverside allotments. This traverse covered a distance of 58.7 km at an average velocity of 5.7 m/s, mapping a total of 200 plots in 478 minutes (7hrs 58min), averaging 3.4 plots per kilometer and 35 plots mapped every hour during the 7 hours 58 minute drive through (Table 4.1 and Figure 4.8). Based on the total distance, time covered, and velocity and plots mapped across this transect, we concluded that there was a heavy infestation of medusahead in all three allotments. Figure 4.8 shows a higher infestation during the June 6, 2009 mapping than June 7, 2009, given that the two expeditions cover almost the same distance (59 km and 58 km respectively) and wide varying average plots mapped per hour (35.08 plots/hour and 9.75 plots/hour respectively).

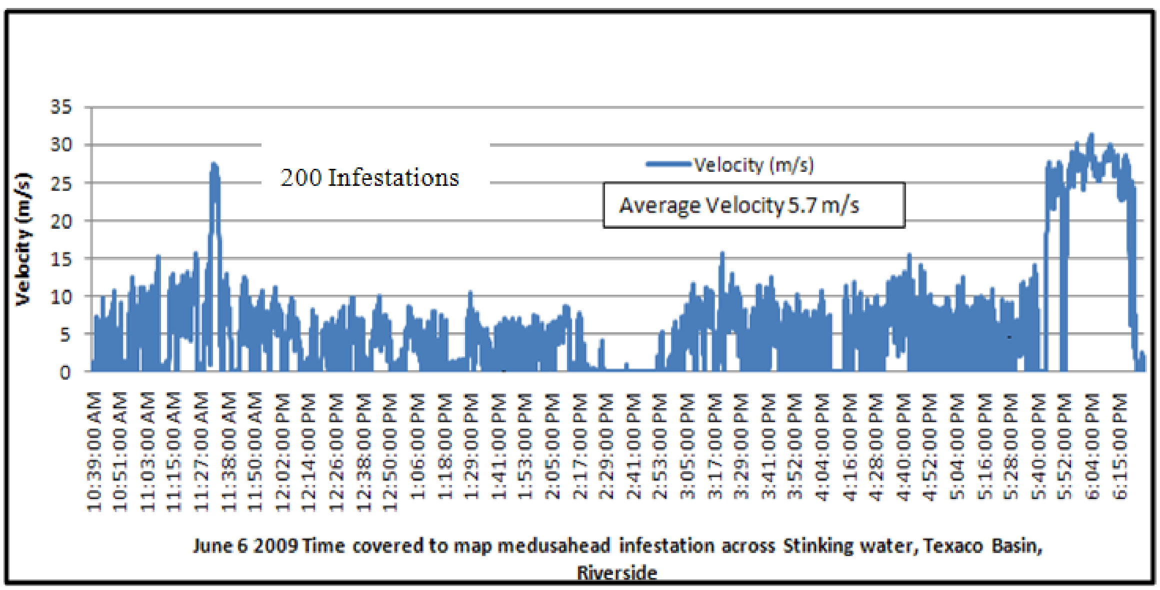

Figure 4.8: The velocity plot of the mobile mapping of medusahead conducted on June 6 2009. 200 infestations were mapped over the 7 hour 58min survey. This shows the stop-and-go nature of the road survey. Note that some travel can be quite rapid.

A different pattern of GPS-logged velocity was seen in another traverse (Figure 4.9). This expedition covered the Riverside and Warm Spring allotments, mapping a total 78 plots during the seven hours drive through. Less infestation was observed during the June 7, 2009 mobile mapping drive through. At an average velocity of 8 m/s, a total distance of 581 km was covered in 420 minutes (6hrs 59minutes). Here an average of 1.3 plots was mapped every kilometer, with an average of 9.1 plots being mapped per hour. A great contrast exists between the velocity in infested and non-infested areas (Figure 4.9). The high velocity indicates less infestation relative to the June 6, 2009 drive through that covered almost similar distance and time (Table 4.1).

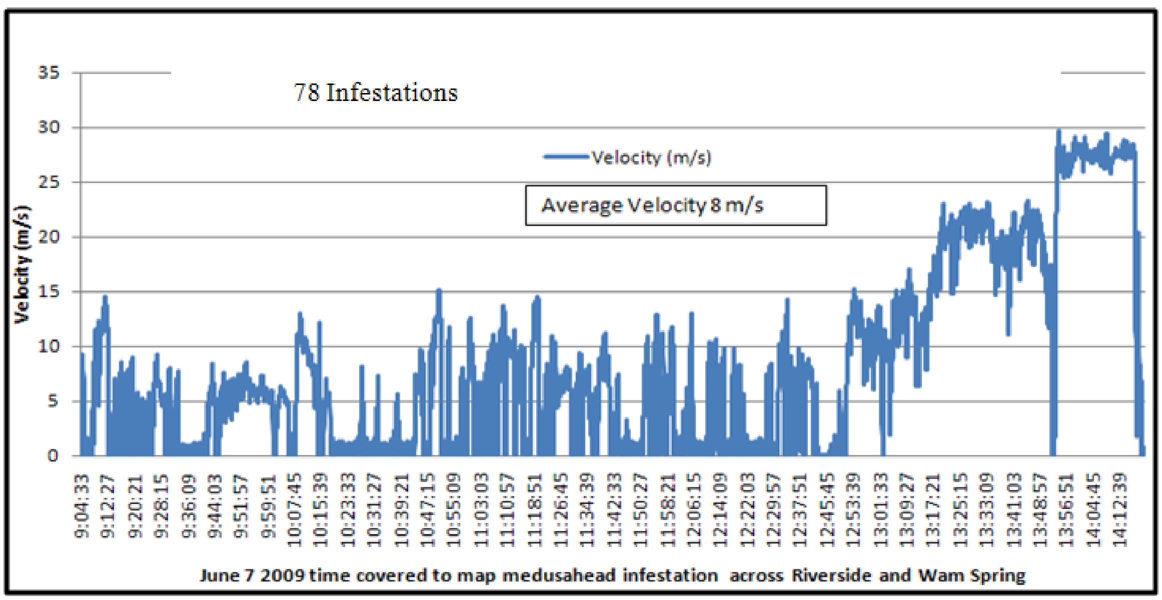

Figure 4.9: June 7, 2009 velocity (m/s) and time covered for mobile drive-through mapping of medusahead infestation.

For the mobile drive through of August 13, 2009 across the Stinking Water and Texaco Basin allotments, the total distance surveyed was 46 km in 5 hours and 10 minutes, mapping a total 30 plots (Figure 4.10). This region of Stinking Water and Texaco Basin was less infested, compared to the June 6, 2009 survey results. A different pattern was observed in figures 4.11, 4.12 and 4.13.

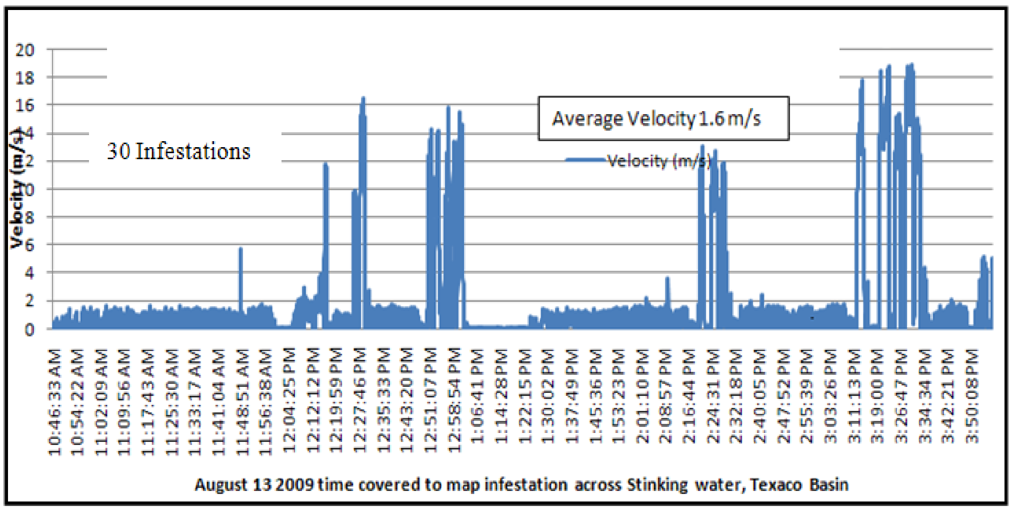

Figure 4.10: August 13, 2009 velocity (m/s) and time covered for mobile drive-through mapping of medusahead infestation.

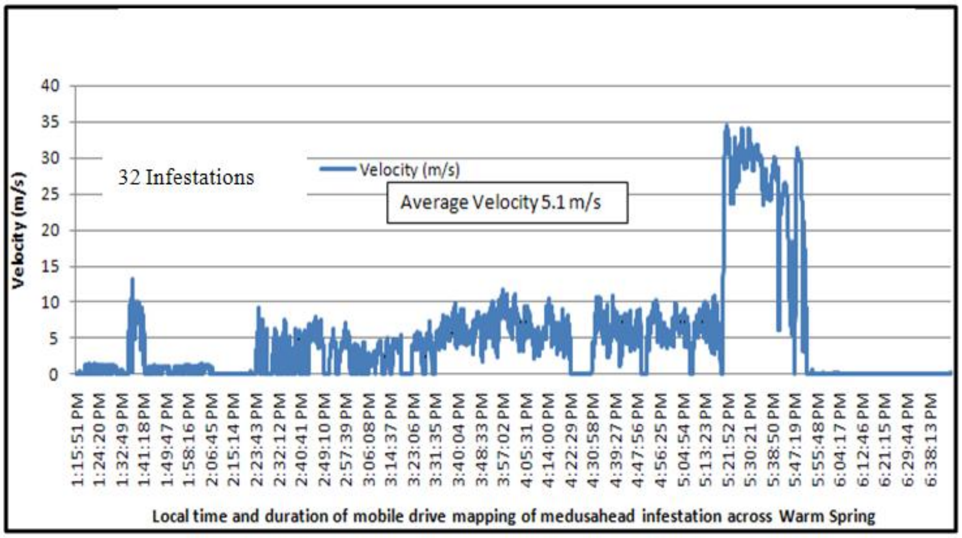

Figure 4.11: August 13, 2009 velocity (m/s) and time covered for mobile drive-through mapping of medusahead infestation.

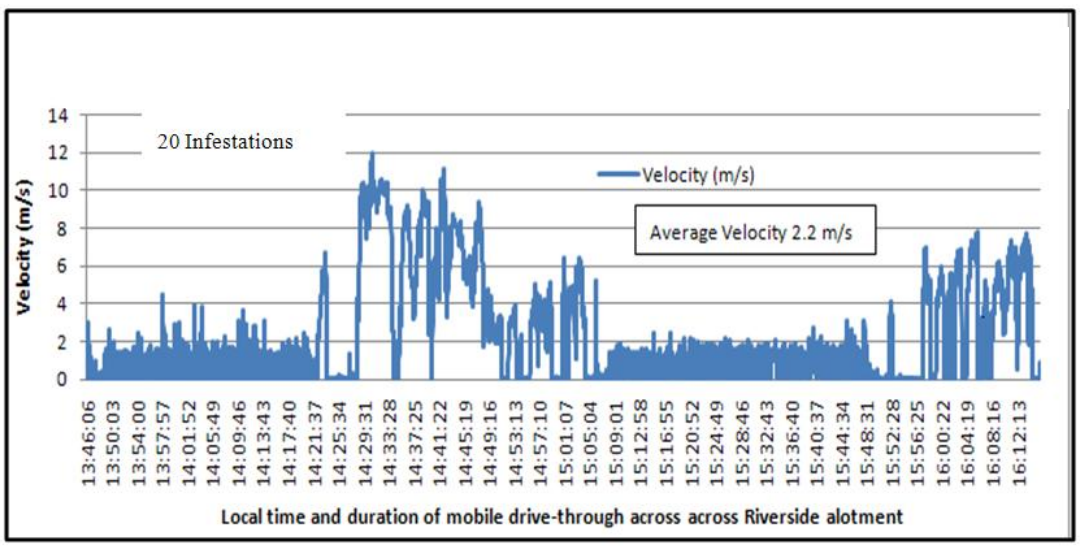

Figure 4.12: June 18, 2010 velocity (m/s) and time covered for mobile drive-through mapping of medusahead infestation.

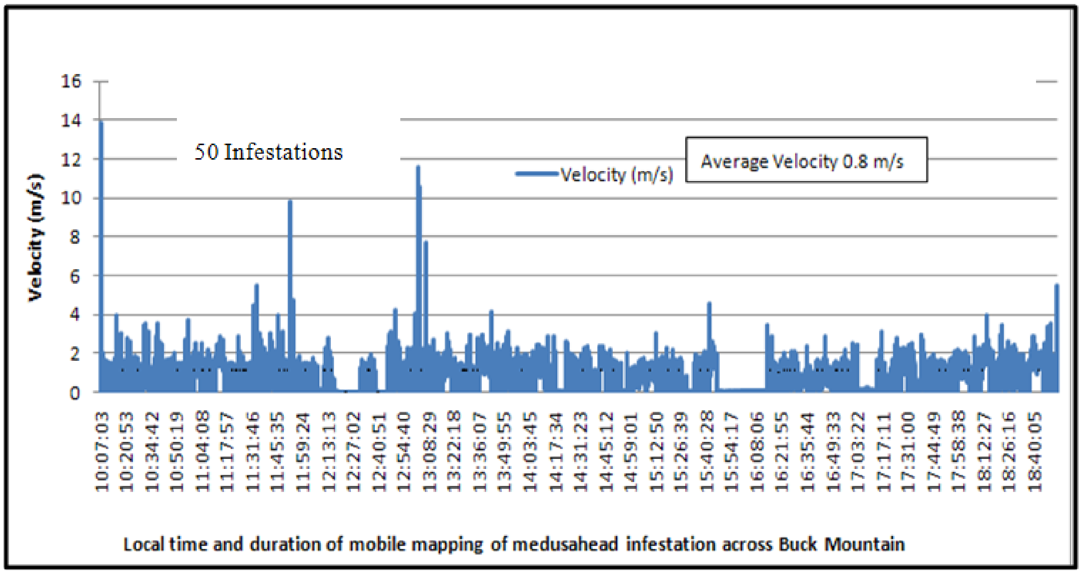

Figure 4.13: June 19, 2010 velocity (m/s) and time covered for mobile drive-through mapping of medusahead infestation.

The overall mobile cross sectional drive-through mapping of medusahead infestation covered a total distance of 270 km at an average velocity of 3.9 m/s. An average of 1.5 plots was mapped every km and about 11.1 plots were mapped every hour during the mobile mapping.

Viewshed analysis of mobile mapping across the Buck Mountain and Riverside landscape

We performed a viewshed analysis with a maximum visible radius range of 2 km to get an idea of the area potentially visible from 11 sample locations on the survey in the Buck Mountain and Riverside allotments. We generated 11 viewsheds, identifying areas that are potentially visible from these points (Figure 4.14 and Table 4.2).

Viewshed coverage averaged 59.4% of the 2 km radius circles. There were on average 10 medusahead infestations mapped per sample viewshed. The number of infestations varied- viewshed 6 (46% visible) had 22 infestations while viewshed 8 (52% visible) had only 1 infestation (Table 4.2). We regressed the surface area visible against the number of infestations mapped and found a poor coefficient of determination (r^2= 0.0036). Even in areas without good topographic visibility over long distances, many infestation polygons can be mapped.

Table 4.2: Viewshed analysis of visible area covered and number of medusahead infestations mapped during road survey on Buck Mountain and Riverside allotments.

Description	Maximum distance radius (km)	Observer height above ground (m)	% of land surface visible	No of infestations mapped/ view shed
1	2	1.7	86.5	9
2	2	1.7	55.6	10
3	2	1.7	35.6	4
4	2	1.7	60.7	9
5	2	1.7	65.2	14
6	2	1.7	46.7	22
7	2	1.7	46.7	14
8	2	1.7	43.4	5
9	2	1.7	51.9	1
10	2	1.7	53.1	16
11	2	1.7	58.2	6
Average	2	1.7	54.9	10

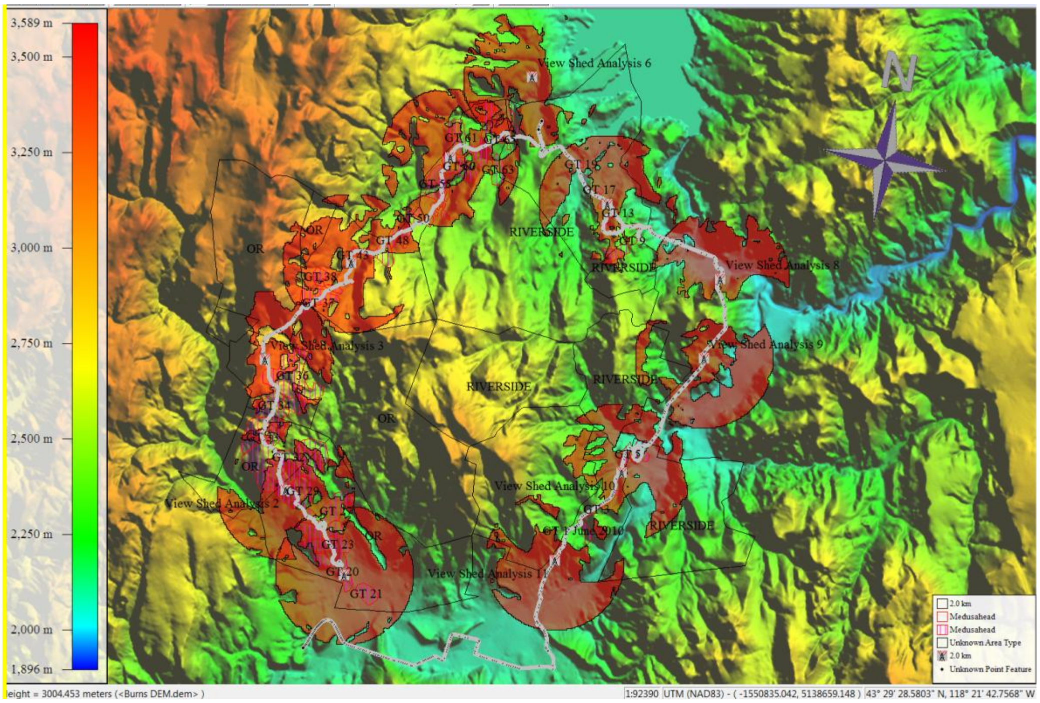

Figure 4.15: The view of DEM for viewshed across drive-through and 2 km radius view of mapped infested areas across Buck Mountain allotment.

At some times of the year medusahead can be distinguished by color, especially if the stand is dense; more than 1000 plants per m^2 (Amy, 2001; Maurer *et al.*, 1988). The ability to distinguish medusahead varies from year-to-year depending upon above ground production and plant size. In some years infestations show dramatic contrast with other vegetation, yet in other years medusahead is easily confused with other annual grasses such as cheatgrass. We have found, as have other authors, that it is easiest to identify when it turns bright green and contrasts with other annuals or when it turns shades of purple and tan as it drys (Nelson and Wilson 1969; Maurer *et al.*, 1988; Murphy and Turner, 1959).

Aerial Reconnaissance

Aerial reconnaissance (Figure 4.17) was conducted immediately after the first mobile cross sectional ground survey (May 28, 2009). We observed infestations from the air and digitized them similarly to what was done from the pickup. There is a tendency for the digitizing technician to become air sick which will limit this technique to technicians tolerant to motion while doing close work. Flying at approximately 67 m/s, the total distance covered was 180 km for duration of 44 minutes (Table 4.3). 26 infestation polygons were digitized with a total area of approximately 4.6 km^2 (Table 4.4). As seen in Figure 4.17, only relatively large infestations were observed (Table 4.4) and the smallest infestation mapped was 3ha. On average, an infestation polygon was mapped every 6.8 km or 1 polygon every 1.7 minutes (Table 4.3). Figure 4.17 shows the aerial reconnaissance of May 28, 2009 with flight lines and path of the aircraft logged by GPS over the Stinking Water Allotment. Aerial survey was hampered by longer observation distances than ground survey and only large, dense "core" infestations were detected. Because the entire site could be surveyed, aerial mapping was very valuable for areas between roadways. Flying lower would decrease observation distance but increase the difficulty of digitization because the aircraft would have to turn frequently to stay over the site and give the digitizing technician time to enter polygons. Lower, slower flight also increases risk to the aircraft and crew.

Table 4.3: Aerial reconnaissance of the Stinking Water area Allotment infestation

Date of Survey	Duration of reconnaissance	Total time	Total digitized area	Average Velocity from GPS (m/s)	Flight distance covered (m/s)	Average distance/ mapped infestation (km)	Average mapped infestations/ Minute	Average flight Altitude from GPS (m)
May 28 2009	10:31:20 to 11:15:16 AM	44 min 04 sec	26	67.01	177174.44 (177.17km)	6.81	0.59 infestations	3126.9

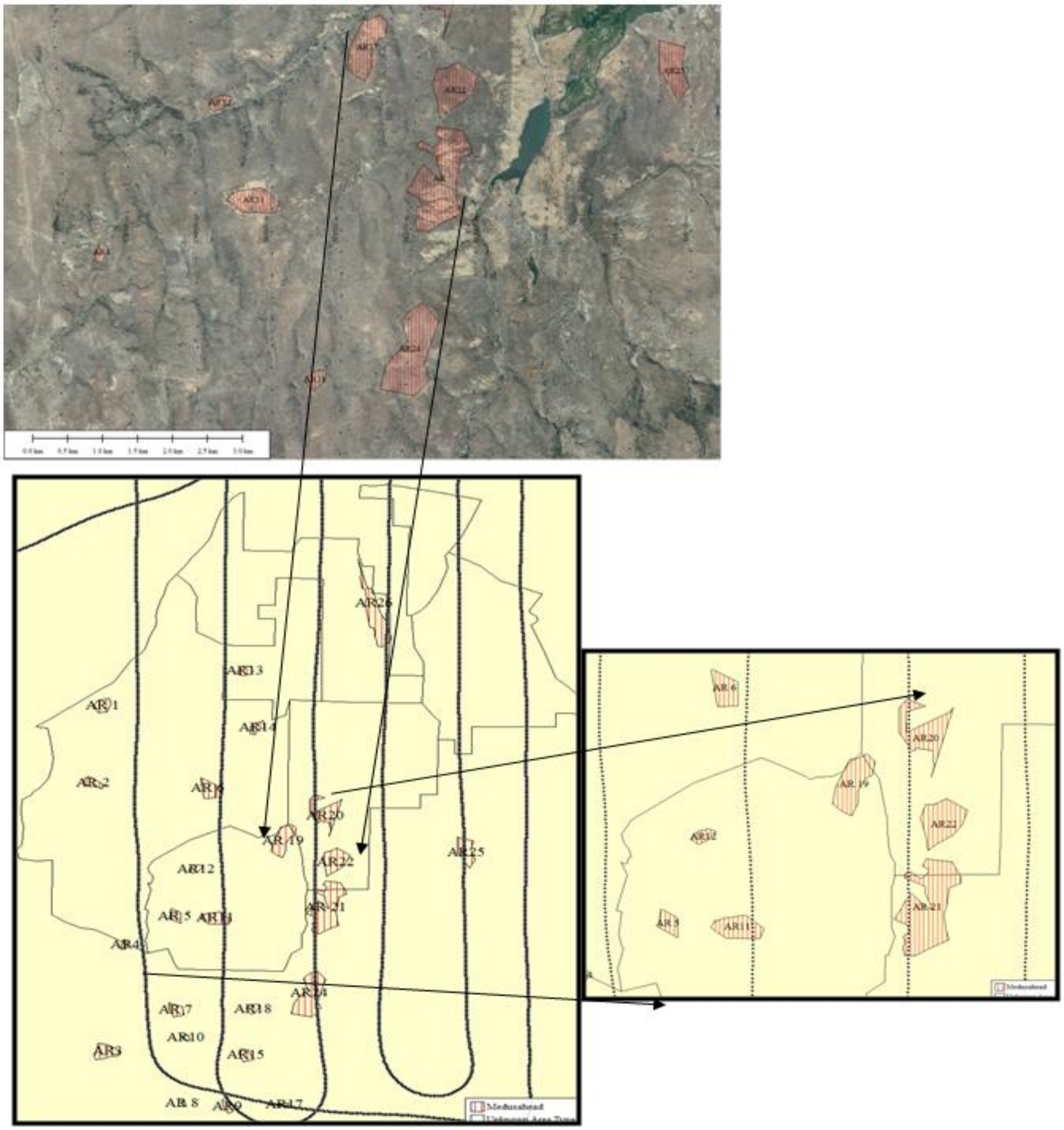

Figure 4.17: Aerial reconnaissance and aircraft flight lines logged by GPS over the Stinking Water Allotment on May 28, 2009. Flight lines are shown in black and medusahead infestations in red.

Table 4.4: Aerial Reconnaissance (AR) area covered and digitized infestations.

Area ID	Aerial Reconnaissance	Perimeter	Enclosed area (hectare)
AR 1	Medusahead Infestation 4	1.07 km	2.09
AR 10	Medusahead Infestation 24	670.92 m	2.62
AR 11	Medusahead Infestation 23	1.278 km	10.22
AR 12	Medusahead Infestation 22	1.705 km	16.16
AR 13	Medusahead Infestation 21	1.199 km	7.99
AR 14	Medusahead Infestation 3	791 m	3.68
AR 15	Medusahead Infestation 2	1.81 km	19.50
AR 16	Medusahead Infestation 25	2.52 km	31.19
AR 17	Medusahead Infestation 1	5.9 km	58.20
AR 18	Medusahead Infestation 18	2.29 km	24.66
AR 19	Medusahead Infestation 17	3.7 km	63.35
AR 2	Medusahead Infestation 15	2.34 km	33.15
AR 20	Medusahead Infestation 16	5.57 km	77.57
AR 21	Medusahead Infestation 13	4.546 km	33.17
AR 22	Medusahead Infestation 19	1.347 km	8.83
AR 23	Medusahead Infestation 26	5.57 km	77.57
AR 24	Medusahead Infestation 14	2.52 km	31.19
AR 25	Medusahead Infestation 12	958 m	5.91
AR 26	Medusahead Infestation 11	600 m	1.28
AR 3	Medusahead Infestation 10	1.19 km	8.98
AR 4	Medusahead Infestation 9	1.26 km	7.41
AR 5	Medusahead Infestation 8	1.07 km	7.39
AR 6	Medusahead Infestation 7	909 m	5.15
AR 7	Medusahead Infestation 6	1.89 km	20.31
AR 8	Medusahead Infestation 5	662 m	2.14
AR 9	Medusahead Infestation 20	1.333 km	12.18
Total	26	46.60 Km	466.60

Conclusions

Traditional weed mapping using paper maps is time consuming and therefore costly. Mobile mapping combines data collection and mapping into one operation that results in shorter time in the field. Mobile mapping and digitizing of medusahead infestations at close range from a 4-wheel drive vehicle with a GIS program on a laptop equipped with a GPS antenna yielded highly accurate maps and reduced field mapping time. These maps, when compared with future mapping efforts, should enhance our understanding of the mechanisms that medusahead employs as it spreads across the landscape. This information, coupled with knowledge of the biology and ecology of medusahead, should lead to more effective control programs.

To this end, mobile mapping provides a reliable mapping protocol to acquire and share spatial data. This study demonstrated the empirical relationship between advance geospatial tools such as GPS, GIS software, and laptop computers and suggests that a Mobile Mapping Systems significantly aid major mapping efforts. Our geospatial protocols for weed mapping facilitate collection of scientifically sound information that can help protect native ecosystems.

LITERATURE CITED

Alfred, J. W. and A.M. De Jeu. 2007. Sensible Field Computing: Evaluating the Use of Mobile GIS Methods in Scientific Fieldwork. Photogrammetric Engineering and Remote Sensing June 2007 pp 651-662

Ellum, C. and N. El-Sheimy. Land-Based mobile mapping systems Canada. Photogrammetric Engineering and Remote Sensing, January 2002, Pp. 13-18.

Grejner-Brzezinska, D. A. 2002. Direct Georeferencing at The Ohio State University: A Historical Perspective. Photogrammetric Engineering and Remote Sensing. Journal of the American society for Photogrammetry and remote Sensing 68(6):

ESRI 2010. ArcGIS User's Manual. Environmental Systems Research Institute, Inc. Redlands, CA.

Gao, J., 2002. Integration of GPS with remote sensing and GIS - Reality and prospect. Photogrammetric Engineering and Remote Sensing 68(5):447-453.

Global Mapper LLC. 2010. Global Mapper User's Guide. Global Mapper Software LLC. Parker, CO.

He, G.P., D. Cunningham, and J. Bossler. 1994. Spatial Data Collection with the GPSVan Mobile Mapping System. Proceedings, ISPRS Commission IV Symposium 30(4):107-113.

He, G.P., G. Dedes, G. Orvets, and J.D. Bossler. 1994. Generation of transportation GIS by Integrating GPS, INS and Computer Vision Technology. Proceedings, 3rd International Colloquium of LIESMARS, WTUSM, Wuhan, PR China, pp. 91-99.

Li, J and M.A. Chapman. 2008. Terrestrial mobile mapping systems towards real-time geospatial data collection Geospatial Information Technology for Emergency Response. ISPRS Book Series, Vol. 6, Taylor & Francis, London, pp. 103-119.

Montoya, L., 2003. Geo-data acquisition through mobile GIS and digital video - An urban disaster management perspective. Environmental Modelling and Software 18(10):869–876.

Novak, K. 1995. Mobile mapping Technology for GIS Data Collection. Photogrammetric Engineering and Remote Sensing. Journal of the American society for Photogrammetry and remote Sensing. 61(5):493-501.

Si, X. and Li, J. 2008. Integrating agent-based modeling and GIS for realistically simulation of traffic control plan for emergency evacuation. Joint ISCRAM-China and Gi4DM Conference, Harbin, China, August 4-6, 8pp.

Tao, C. V. and Li, J. 2007. Foreword: Advances in Mobile Mapping Technology. ISPRS Book Series, Vol. 4, Taylor & Francis, London, ISBN 978-0-415-42723-4, pp 11-14.

Tao, C.V. and Li, J. (eds.). 2007. Advances in Mobile Mapping Technology. ISPRS book Series, Vol. 4, Taylor &Frances, London, ISBN 978-0-415-42723-4, 176pp.

Tripcevich, N., 2004b. Mobile GIS in archaeological survey. The SAA Archeological Record, 4(3):17-22.

Tsou, M.H., 2004. Integrated mobile GIS and wireless internet map servers for environmental monitoring and management. Cartography and Geographic Information Science, 31(3):153-165.

CHAPTER 5: DETECTION OF MEDUSAHEAD (*TAENIATHERUM CAPUT-MEDUSAE* (L.) NEVSKI) USING HIGH FREQUENCY, SEQUENTIAL, GLOBALLY POSITIONED DIGITAL IMAGES.

S.K. Ndzeidze, M.D. Johnson, K.E. Johnson, and D.E. Johnson

Key Words: Digital Aerial Images, GPS, GIS, Remote Sensing, Digital Image Processing, High resolution, Low cost.

ABSTRACT

Medusahead (*Taeniatherum caput-medusae (L.) Nevski*) is invading and transforming vegetation communities throughout the Western United States, steadily becoming one of the most troublesome of the exotic annual grasses on rangelands. Medusahead invades sites by establishing small-localized infestations, which can rapidly spread and dominate a landscape following a disturbance such as fire. Medusahead replaces native vegetation and shrubs, creating near monocultures and negatively impacting wildlife and domestic livestock. Sequential high frequency aerial mapping of invasive weed cover at seasonal or yearly intervals can indicate the proliferation rates and areas of infestation, the rate of spread. Our research evaluated the use of sequential, GPS positioned, digital color aerial photography collected within a strict protocol and analyzed with reliable software as a means of mapping medusahead. Aerial photographs were collected with a 12.40 megapixel Canon EOS Rebel XSi camera fitted with a 28mm lens mounted in the belly of a Cessna 182. Images had a ground pixel resolution of 0.42 m. The camera was controlled with a laptop computer, which also received and stored the acquired images. Photographs were taken at 5-second intervals while the aircraft flew a grid over the study area approximately 1500m above ground level. The position of the aircraft was recorded at 1- second intervals via GPS units. Simultaneously, medusahead infestations were mapped and photographed on the ground. These infestations were used as calibration sites to assign spectral values (red, green and blue) for use in image classification. We developed software for photographic image positioning for geospatial and landscape analysis.

INTRODUCTION

Medusahead is an exotic, noxious winter annual grass that typically invades sagebrush steppe rangeland communities of many western states, as well as several in the northeast part of the country and in Canada (Figure 5.1) (Amay, 2001; Davies, 2008). This pattern indicates that the plant can expand to a much larger area because the environmental conditions that it grows under are quite diverse. This aggressive winter annual weed, introduced into the U.S. in the 1880s (Young and Evans, 1970), was first discovered growing in Oregon in 1887 by Thomas Howell (1903) as *Elymus caput-medusae* (Maurer et al. 1988; Amy, 2001). By the early 1990s, 14 million acres of public lands in the Intermountain West were infested with medusahead, cheatgrass (*Bromus tectorum L*.), or both. However, the area at risk for invasion by these two grasses is at least 60 million acres. Unfortunately, medusahead is already spreading rapidly, having infested 18 Oregon counties in 1962 and 36 in 2004.

In Idaho, rangelands infested by medusahead have more than doubled between 1957 and 1992 (Davies, 2008). The rapid spread of medusahead is a serious management issue, reducing grazing capacity by up to 80%, degrading wildlife habitat, decreasing biodiversity and potentially altering ecosystem functions (Davis, 2008). An alarming but rarely mentioned impact of medusahead invasion is that it may exacerbate the decline of sagebrush-obligate wildlife species, like sage-grouse, as it replaces native plant communities providing critical habitat (Davies and Svejcar, 2008).

Medusahead infestations commonly begin discretely among similar looking species, such as cheatgrass and bunchgrasses, before abruptly overwhelming and displacing competitor species. This similarity makes mapping medusahead distribution a difficult task and contributes to the costly measures needed to control and restore the ecosystem once medusahead establishes dominance.

Remote sensing for medusahead detection and distribution mapping has been limited, because this requires very high-resolution images. New airborne and satellite sensors promise to improve our ability to spectrally distinguish medusahead from other species, but the techniques remain inadequate and are not yet economically practical. Evangelista *et al*. (2009) noted that the detection of invasive plants using remote sensing may be improved if the target species has phenological attributes that are distinctive from native vegetation. For example, leafy spurge (*Euphorbia esula L.*) has yellow-green inflorescences that are spectrally unique when compared to associated flora (Evangelista *et a*l., 2009). Similarly, yellow starthistle (*Centaurea solstitialis*), tamarisk (*Tamarix spp*.), yellow hawkweed (*Hieracium pratense*), oxeye daisy (*Chrysanthemum leucanthemum*), and Chinese tallow (*Sapium sebiferum*) also have distinctive colorations that can facilitate remote sensing (Booth *et al*., 2005). Other species have been detected by their extended growing periods. Broom snakeweed (*Gutierrezia sarothrae*), a perennial sub-shrub, has been remotely sensed during its early-season greening (Evangelista *et al*., 2009). Cheatgrass (*Bromus tectorum*), an invasive annual grass, has also been successfully detected because it germinates in winter months prior to most native grasses (Booth *et al*., 2005, Evangelista *et al*., 2009). The distinctiveness of any phonological attribute can vary widely with regional climate, latitudinal gradients, and species richness within an ecosystem. As a result, the timing of acquiring remotely sensed data is critical and can be difficult to predict (Evangelista *et al*., 2009). The objective of this study was to determine if we could accurately map medusahead using sequential, GPS positioned, digital color aerial photographs collected with a strict protocol.

MATERIALS AND METHODS

Study Area

The BLM Burns district in Harney County falls within the High Desert Ecological province in south central Oregon (Figure 4.1). The study area consists of 2,000 km^2 (750 $mile^2$) in northeastern Harney County, on land managed by private ranches and the USDI (United States Department of Interior) Bureau of Land Management. This area has abundant medusahead infestations both along rural roads and highways and in remote areas. The region is characterized by large and small closed basins surrounded by extensive terraces, basaltic ridges, hilly uplands, isolated buttes, and mountains (Anderson *et al*., 1998). Figure 5.1 shows the color change of medusahead by early spring (May to June) and summer (August). This largely influences the spectral signature and classification due to reflectance at different wavelengths. The spectral signature varies greatly between the seasons, prompting separate classification specifications for the same area with respect to seasons. The growth habits, life cycles, and ecological adaptations of medusahead and cheatgrass are similar, and the annuals typically grow in association until medusahead becomes dominant and eventually exclusive (Davies *et al*., 2008).

Figure 5.1a: A heavy medusahead infestation in Burns, Oregon in early spring.[1]

Figure 5.1b: Medusahead in early June in Burns, Oregon.

[1] August field trip 2009 by Douglas Johnson and Stephen Ndzeidze. Oregon State University

Aerial Imagery

Aerial Photography was collected with a 12.40 megapixel Canon EOS Rebel XSi camera (Figure 3.3) fitted with a 28mm lens mounted in the belly of a Cessna 182 (Figure 3.4). The camera was controlled with a laptop computer, which also received and stored the acquired images (Figure 3.5). Photographs were taken at 5-second intervals while the aircraft flew a grid over the study area approximately 2,780 m above ground level. Flight lines were followed grid lines at intervals of 1,000 m (Figure 3.7) overlaid on NAIP imagery to closely monitor the flight over the mapped area. The pilot also used a GPS to remain on track. Photographs were stamped with the date/time recorded to the nearest second. Position of the aircraft was monitored at 1-second intervals using two recording GPS units accurate within 2m. GGS logger converter software was used to convert GPS logged points to comma separated values files that can be opened in any GIS software (Figure 3.8) and aerial photographs were rough positioned using the Aerial Photograph Positioning Tool.

The aircraft flew at an average speed of 58 m/s at an average altitude of 2,800m. A total of 2,788 images (28 May 2009), 4,781 images (15 August 2009), and 2,893 images (16 August 2009) were collected during the three flights. A total of 10,362 images were photographed (Table 5.1). Each image measured 4,272 by 2,848 pixels with a ground resolution of 0.42m (Figure 5.3). Each image was stored in the RGB format (Johnson *et al*., 2009). Images covered all study allotments.

VegMeasure2 Software

Images were processed using VegMeasure 2, a software package that allows classification of multiple images based on user-controlled classification of the Red, Green, and Blue (RGB) digital numbers of features in the digital image. This program allows the user to design a detection protocol based upon the color characteristics of the feature of interest.

We employed a RGB Spherical Extraction and calibrated the computer by selecting a minimum of 25 locations (pixels) known to have severe medusahead infestations and extracted the RGB pixel values. Tolerance around these pixels was set at a Euclidian distance of 20. Each pixel in an image with a distance (*d*) in the color cube less than 20 units from the RGB value of a known medusahead value was classed as medusahead. Euclidian distance values were calculated using the formula:

$$d = \sqrt{(R-r)^2 + (B-b)^2 + (G-g)^2})$$

Where:

d = Euclidian distance value from medusahead DN

R = Pixel value of medusahead red

r = Pixel value of image red

B = Pixel value of medusahead blue

b = Pixel value of image blue

G = Pixel value of medusahead green

g = Pixel value of image green

We classified a series of random images (usually 5) with known infestations (calibration sites) taken on the same day, under similar light conditions and recorded the range of RGB values that represented infestations. These images provided the spectral signatures (RGB digital numbers) that identified medusahead across the study area. As points were added a viewing image on the screen was automatically pre-classified so that we could identify regions on the image with known infestations that were not being identified (Figure 5.2). As this training process continued and locations (pixel values) were added, we reached a point where the image stabilized and new areas were not being added on the windowed image. At this point, the training data set was saved so it could be retrieved in the future to process all images collected under similar light conditions. A series of test images were then classified using the RGB pixel settings to determine if the classification was acceptable. If acceptable, the rest of the images in the set were classified with the saved settings and new classified images were saved as classified ASCII raster maps. In addition, a summary table was written listing each image and the relative proportion classified as infested with medusahead.

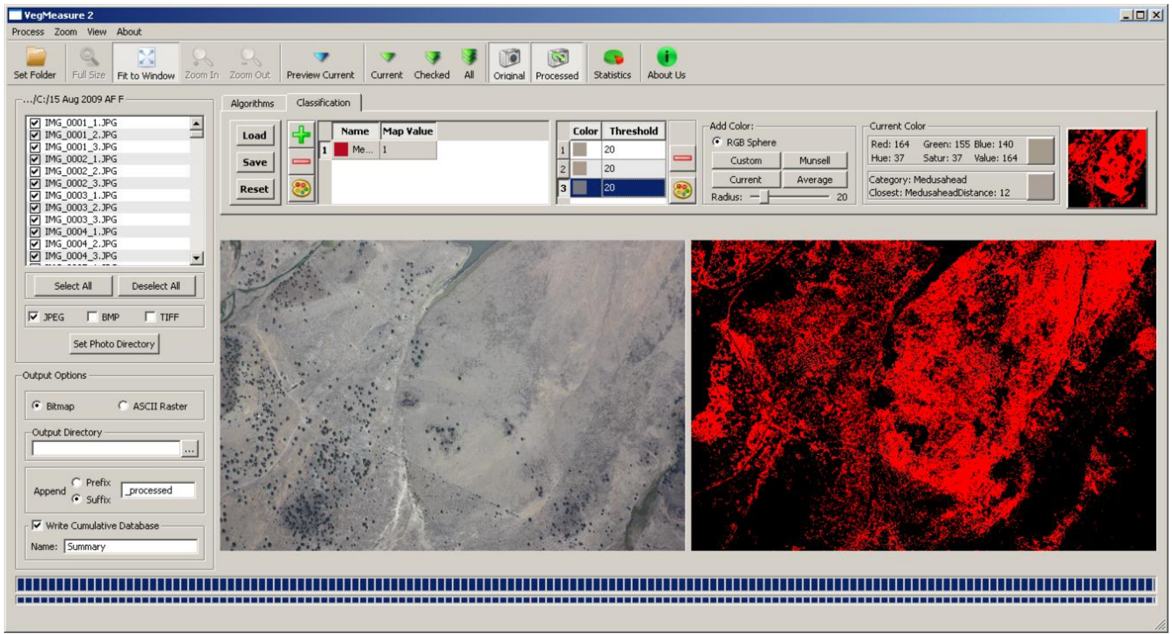

Figure 5.2: Screen capture of the VegMeasure 2 software classification page with a classified aerial image collected over the Burns District of the BLM in Harney County, Oregon.

RESULTS AND DISCUSSION

When viewed from the ground, the greatest visible contrast between medusahead and other vegetation was during the late spring and early summer. At these times large, dense infestations could be seen at distances up to 2 km away. When viewed vertically downward, however, soil color made detection somewhat more difficult because of the upright stature of medusahead reduced the amount of leaf visible (Figure 5.1a and 5.1b). In spring medusahead had a yellow-green hue while in summer it was pale yellow. We also noted that medusahead infestations are not readily distinguishable in some years, especially with poor growing conditions, so that medusahead may not be apparent in aerial photographs.

We were able to detect medusahead in digital aerial photographs taken in both spring and summer 2009. Because the summer 2009 coverage was more complete, we focused our analysis on these images.

Detection and Classification with VegMeasure2 Software

A total of 7,674 images (4,781 images on 15 Aug 2009 and 2,893 images on 16 August 2009) were collected during the two summer flights (Table 5.1) (Figure 5.3). These images were processed using the VegMeasure 2 classification algorithm based on the color of known infestations. Images were digitally processed by carefully identifying RGB pixel values for the known medusahead infestations that corresponded to the observed digital numbers from the conventional color digital photograph.

Table 5.1: Summary of the aerial images collected during the three flights and the average infestation rate for medusahead on the Harney County study area.

Date	Allotment	Number of Images	Average Flight altitude	Average Image Resolution	Percentage of Infestation		Average Digital Numbers of Medusahead Infestations (Spectral Signature)		
					Present	Absent	Red	Green	Blue
15 August 2009	Buck Mt., Stinking Water & Texaco Basin	4,781	2823	0.42m	34.9%	65.1%	168	158	144
16 August 2009	Warm Springs & River	2,893	2870	0.42m	20.6%	79.4%	164	154	140
Total		7,674				Mean	166	156	142

Figure 5.3: Aerial photo (4,272 by 2,848 pixels) with a ground resolution of 0.42m used for the detection of medusahead. Each image was rough corrected by determining the camera position when the image was taken, the bearing of the aircraft, the altitude above the ground and the focal length of the lens. Positions in the images were usually accurate to within 100m.

VegMeasure 2 produced a report indicating the percentage of each class in each image, as well as for all of the images collectively (Figure 5.7). VegMeasure 2 also output ASCII raster maps of areas classified and medusahead infested. Each image represents a sample and provided an estimate of infestation percentage for the approximately 214 ha covered by the image. Because the ground area represented in each image is overlapping, percent infestation values are not exclusive.

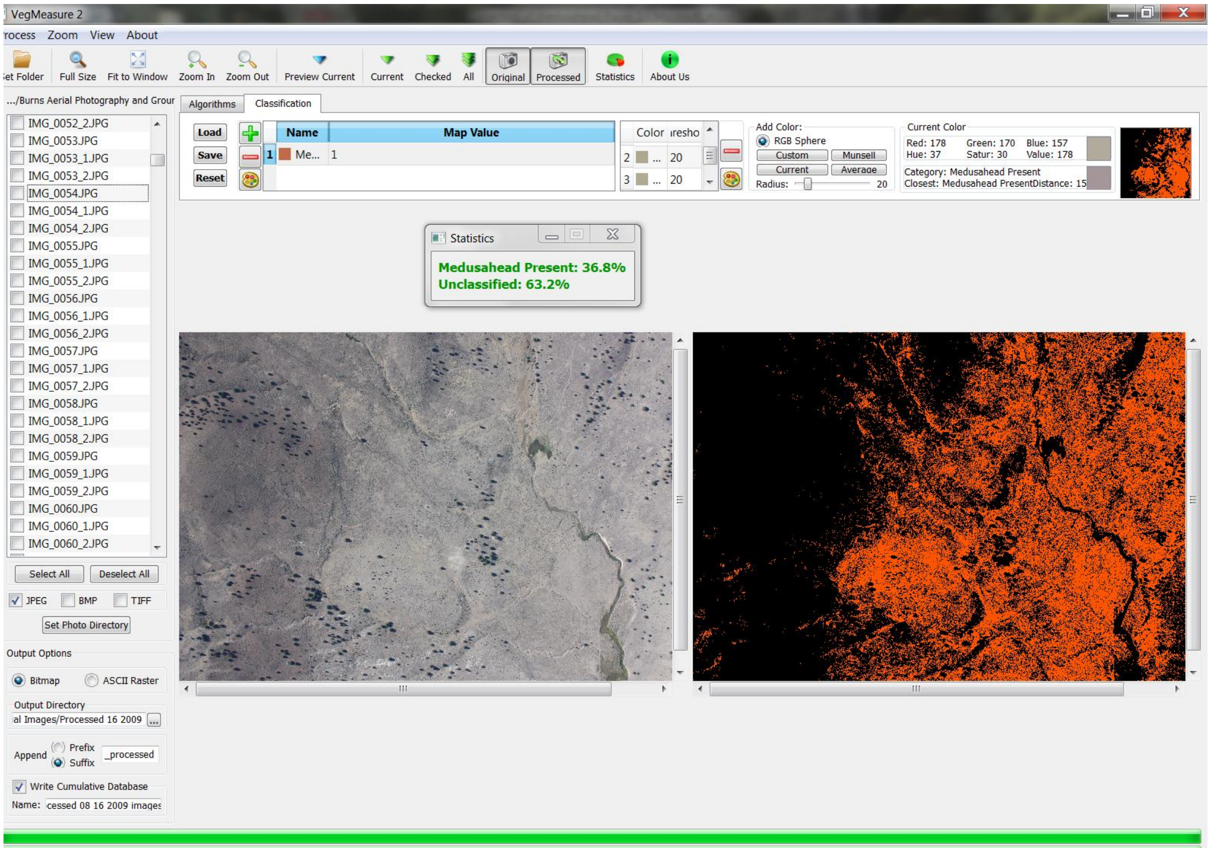

Figure 5.7: VegMeasure2 window with a color aerial image (left) and a classified image of medusahead infestations (right) based on spectral analysis. The right image shows the extent of medusahead infestation.

Table 5.2: Classified aerial images from the Buck Mountain allotment

Sample	Image	Present	Absent
1	IMG_1340	46.8	53.2
2	IMG_1344	25	75
3	IMG_1348	30.9	69.1
4	IMG_1352	20.4	79.6
5	IMG_1365	35.3	64.7
6	IMG_1498	35.1	64.9
7	IMG_1503	48.1	51.9
8	IMG_1730	34.6	65.4
9	IMG_1734	38.1	61.9
10	IMG_1737	31	69
11	IMG_1753	20.1	79.9
12	IMG_1868	43.6	56.4
13	IMG_1876	39.5	60.5
14	IMG_1880	33.7	66.3
15	IMG_1884	30.1	69.9
16	IMG_2081	39.3	60.7
17	IMG_2085	44	56
18	IMG_2089	40.9	59.1
19	IMG_2107	49.4	50.6
20	IMG_2214	38.9	61.1
21	IMG_2224	49.7	50.3
22	IMG_2228	38.7	61.3
23	IMG_2440	5.7	94.3
24	IMG_2442	30.7	69.3
25	IMG_2444	35.1	64.9
26	IMG_2561	21.4	78.6
27	IMG_2564	32	68
28	IMG_2575	12.8	87.2
29	IMG_0279	3.3	96.7
30	IMG_0284	20.5	79.5
31	IMG_0287	9.2	90.8
Average		**31.7**	**68.3**

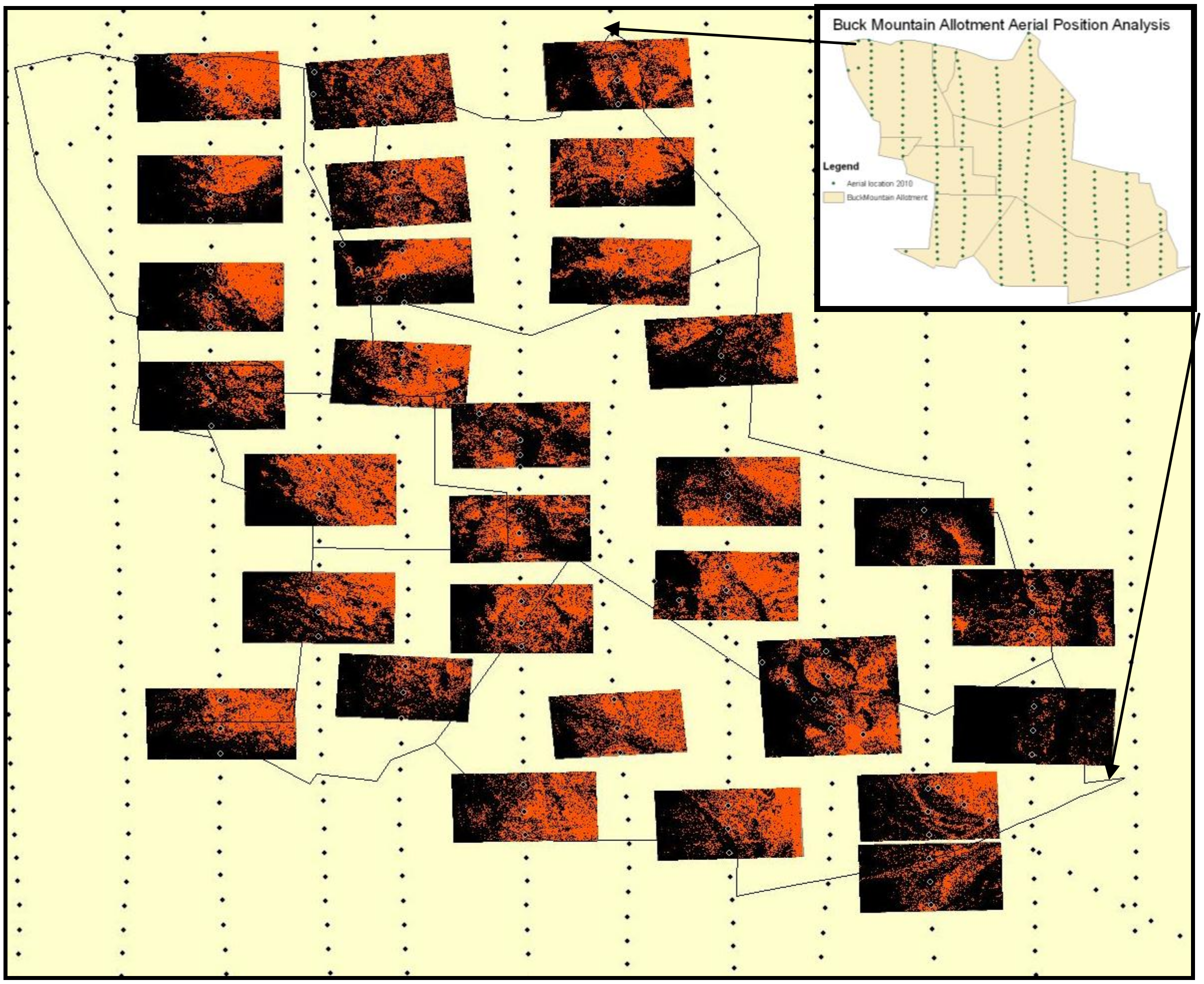

Figure 5.8: Geo-referenced and selected classified aerial images for medusahead infestation (red) across the Buck Mountain allotment.

Classification Error Matrix for Medusahead Detection

Classification accuracy was tested over the five BLM allotments (Table 5.1). For example, a total of 116 images (Appendix 1) cover the Buck Mountain allotment and we selected 31 for closer analysis of infestation (Table 5.2, Figure 5.8). The images were re-rectified to USDA NAIP 2009 base imagery and compared to data collected during ground surveys done simultaneously with the aerial flight. Figure 5.2 shows images used in the accuracy evaluation for the Buck Mountain allotment. Medusahead infestations are shown in red. The VegMeasure 2 classified images suggested that approximately 32% of the Buck Mountain allotment has medusahead infestation (Table 5.2 and Figure 5.8).

The error matrix for classification accuracy was tested using the ground reference data and the corresponding re-registered classified images. To ensure that areas were accurately surveyed on the ground and that small infestations were not missed in the ground survey, a 40m buffer was created on the transit survey routes and only these areas were considered. Four hundred random points were generated within this buffered area and used to determine overall, producer's, and user's accuracy. The overall accuracy of classification was 84% (Table 5.3).

Table 5.4: Error matrix resulting from comparison of 400 random ground locations surveyed in the study area compared with the classification of images using VegMeasure 2 software. Random locations were confined to a 40 buffer along ground survey routes to ensure that small infestations were not overlooked.

Medusahead Stands			Ground Truth		
			Y (yes)	N (no)	**Total**
	Classification	Y (yes)	310	26	**336**
		N (no)	36	28	**64**
		Total	**346**	**54**	**400**
	Producer's Accuracy Y= 310/346 = 89.59 % N=(28/54)*100= 51.85%			User's Accuracy Y=(310/336)*100= 92.26% N=(28/44)*100 = 63.63%	
Overall Accuracy = ((310+28)/400)*100 = 84.5%					

CONCLUSIONS

Our method of medusahead survey using high frequency, sequential globally positioned digital images allows the rapid survey of large areas for medusahead. Thousands of images can be rough corrected and automatically processed to indicate areas with medusahead using our protocol. Because we timed our aerial survey to times when the color of medusahead was distinct to observers on the ground both from oblique and vertical perspects, medusahead was also relatively distinct in digital aerial photographs. Our classification had an overall accuracy of 84%, which is good enough to be beneficial to land managers working on weed control projects. We suggest that the VegMeasure 2 software package and classification algorithms can be a very helpful when using the “present or absent” classification method of mapping, not only for medusahead but other weed infestations on rangelands.

LITERATURE CITED

Amy, J. 2001. Taeniatherum caput-medusae. In: Fire Effects Information System. U.S. Department of Agriculture, Forest Service, Rocky Mountain Research Station, Fire Sciences Laboratory (Producer). http://www.fs.fed.us/database/feis/

Anderson, G.L., J.H. Everitt, A.J. Richardon, D.E. Escobar. 1993. Using satellite data to map false broomweed (Ericameria austrotexana) infestations on south Texas rangelands. Weed Technology 7:865-871.

Asner, G.P. M.O. Jones, R.E. Martin, D.E. Knapp and R.F Hughes. 2008. Remote sensing of native and invasive species in Hawaiian forests. Remote Sensing of the Environment 112:1912-1926.

Blank, R. R., F. L. Allen and J. A. Young. 1996. Influence of simulated burning of soil-litter from low sagebrush, squirreltail, cheatgrass, and medusahead on water-soluble anions and cations. International Journal of Wildland Fire. 6(3):137-143.

Booth, D.Terrance, Samuel E. Cox, and Douglas E. Johnson. 2005. Detection-Threshold Calibration and Other Factors Influencing Digital Measurements of Ground Cover. Rangeland Ecology and Management 58:598-604.

Booth, D.T, S.E. Cox, M. Louhaichi and D.E. Johnson. 2004. Light weight camera frame for close-to-earth remote sensing. Journal of Range Management 57:675–678.

Bovey, R. W., D. LeTourneau, and L. C. Erickson. 1961. The chemical composition of medusahead and downy brome. Weeds 9:307-311.

Dahl, B. E. and E. W. Tisdale. 1975. Environmental factors related to medusahead distribution. Journal of Range Management 28:463-468.

Davies, K. W. 2008. Medusahead dispersal and establishment in sagebrush steppe plant communities. Rangeland Ecology and Management 61:110-115.

Davies, W. K., and T. J. Svejcar. 2008. Comparison of Medusahead-Invaded and Non-invaded Wyoming Big Sagebrush Steppe in Southeastern Oregon. Rangeland Ecology and Management 61: 6:623-629.

Evangelista, P. H., T.J. Stohlgren, J. T. Morisette and S. Kumar. 2009. Mapping Invasive Tamarisk (Tamarix): A Comparison of Single-Scene and Time-Series Analyses of Remotely Sensed Data. Remote Sensing 1:519-533.

Everitt, J.H. G.L. Anderson, D.E. Escobar, M.R. Davis, N.R. Spencer, R.J. Andrascik. 1995. Use of remote sensing for detecting and mapping leafy spurge (*Euphorbia esula*). Weed Technology 9:599-609.

Fosberg, M. A. 1965. Relationship of cheatgrass and medusahead to soils in the Colombia River Basin. Proceedings of the Cheatgrass Symposium Vale, OR. U.S. Dept. of the Interior, Bureau of Land Management, Washington, D.C.

Furbush, P. 1953. Control of medusa-head on California ranges. Journal of Forestry. 51:118-121.

Goebel, C. J., M. Tazi, and G. A. Harris. 1988. Secar bluebunch wheatgrass as a competitor to medusahead. Journal of Range Management 41:88-89.

Hamada, Y., D.A. Stow, L.L. Coulter, J.C. Jafolla, L.W. Hendricks. 2007. Detecting Tamarisk species (*Tamarix* spp.) in riparian habitats of Southern California using high spatial resolution hyperspectral imagery. Remote Sensing of the Environment 109:237-248.

Hirano, A., M. Madden, R. Welch. 2003. Hypersptectral image data for mapping wetland vegetation. Wetlands 23:436-448.

Hunt, E.R., Jr. J.H. Everitt, J.C. Ritchie, M.S. Moran, D.T. Booth, G.L. Anderson, P.E. Clard, M.S. Seyfried. 2003. Applications and research using remote sensing for rangeland management. Photogrammetry Engineering and Remote Sensing 69: 675-693.

Johnson K.D., S.K. Ndzeidze, M.D. Johnson, A.L. Wörz, M. Louhaichi and D.E Johnson. 2010. World File Maker User’s Guide. Global Geomatic Solutions. Oviedo, FL. 15p.

Johnson K.D., M.D. Johnson, and M. Louhaichi. 2007. GeoAlbum user’s guide. Global Geomatic Solutions. Corvallis, OR. 55p.

Johnson, M.D. Johnson, M. Louhaichi, P.E. Clark, A.L. Wörz, S.K. Ndzeidze, and D.E. Johnson. 2009. VegMeasure 2 user's guide. Department of Rangeland Ecology and Management, Oregon State University, Corvallis, OR. 25p.

Lass, L.W., H.W. Carson, R.W. Callihan. 1996. Detection of yellow starthistle (*Centaurea solstitialis*) and common St. Johnswort (*Hypericum perforatum*) with multispectral digital imagery. Weed Technology 10:466-474.

Lass, L.W., D.C. Thill, B. Shafii, T.S Prather. 2002. Detecting spotted knapweed (Centaurea maculosa) with hyperspectral remote sensing technology. Weed Technology 16:535-545.

Lass, W.L., T.S. Prather, N.F. Glenn, K.T. Weber, J.T. Mundt, J. Pettingill. 2005. A review of remote sensing of invasive weeds and example of the early detection of spotted knapweed (Centaurea maculosa) and babysbreath (Gypsophila paniculata) with a hyperspectral sensor. Weed Science 53:242-251.

Lusk, W.C., M.B. Jones, D.T. Torell, and C.M. McKell. 1961. Medusahead palatability. Journal of Range Management 14:248-251.

Major, J., C. M. McKell, and L. J. Berry. 1960. Improvement of medusahead-infested rangeland. Leaflet 123. Davis, CA: University of California, California Agricultural Experiment Station. 6 p

Maurer, T., J. R. Mary and G. Audrey. 1988.*Taeniatherum caput-medusae* Medusahead. *Global Invasive Species Team. The Nature Conservancy*

McKell, C.M., A.M. Wilson, and B.L. Kay. 1962. Effective burning of rangelands infested with medusahead. Weeds 10:125-131.

Medlin, C.R., D.R. Shaw, P.D. Gerard, F.E. LaMastus. 2000. Using remote sensing to detect weed infestations in Glycine max. Weed Science 48:393-398.

Miller, H. C., D. Clausnitzer, and M. M. Borman. 1999. Medusahead. *In:* R.L. Sheley and J.K. Petroff . Biology and management of noxious rangeland weeds. Corvallis, OR: Oregon State University Press pp. 271-281.

Murphy, A. H and D. Turner. 1959. A study on the germination of Medusa-head seed. Bulletin. 48: 6-10.

Nelson, J. R and A. M. Wilson. 1969. Influence of age and awn removal on dormancy of medusahead seeds. Journal of Range Management. 22: 289-298.

Rowlinson, L.C., M. Summerton and F. Ahmed. 1999. Comparison of remote sensing data sources andtechniques for identifying and classifying alien invasive vegetation in riparian zones. Water SA 25:497-500.

Sharp, L.A., M. Hironaka, and E.W. Tisdale. 1957. Viability of medusahead seed collected in Idaho. Journal of Range Management. 10:123-126.

Smith, H.A., W.S. Johnson, J.S. Shonkwiler, and S.R. Swanson. 1999. The implications of variable or constant expansion rates in invasive weed infestations. Weed Science 47:62-66.

Swenson, C.F., L. Duane and E.C. Lambert. 1964. Silica in medusahead. Weeds 12:16-18

Torell, P.J., E.C. Lambert and H.H. Robert. 1961. The medusahead problem in Idaho. Weeds 9:124-131.

Torell, P. J. 1967. Dowpon-an aid to reseeding medusahead-infested rangeland. Down to Earth 23:6-8.

Williams, A.P., E.R. Hunt Jr. 2002. Estimation of leafy spurge cover from hyperspectral imagery using mixture tuned matched filtering. Remote Sensing of the Environment 82:446-456.

Young, J. A. and R. A. Evans. 1970. Invasion of medusahead into the Great Basin. Weed Science. 18:89-97.

Young, J. A. and R. A. Evans. 1971. Medusahead invasion as influenced by herbicide and grazing on low sagebrush sites. Journal of Range Management 24:451- 454.

Young, J. A., C. D. Clements, and G. Nader. 1999. Medusahead and clay: the rarity of perennial seedling establishment. Rangeland 6:19-23.

Zimmerman, J.R., Johnson, W.S., Eiswerth, M.E. Medusahead: Economic Impact and Control in Nevada. University of Nevada-Reno Fact Sheet FS-02-37. http://www.unce.unr.edu/publications/files/nr/2002/FS0237.pdf

CHAPTER SIX: SUMMARY AND CONCLUSIONS

The rapid spread of medusahead in the conterminous United States has resulted in significant environmental damage, transforming and reducing significantly the health of rangeland ecosystems. Our study designed a protocol for the detection, mapping and image processing of medusahead (*Taeniatherum caput-medusae (L.) Nevski*) using high frequency, sequential, globally positioned digital images. The objectives of this project were to develop hardware, software, and sampling protocols for medusahead infestations, and to develop and improve the equipment and software components of the system. These objectives were to:

1. Refine Mobile Mapping techniques used to identify infestations on the ground;
2. Create a low-cost and efficient data collection system for high-resolution aerial imagery with auto-referencing (geographic registration) capability so that large numbers of images can be collected, easily processed and stored;
3. Update and improve VegMeasure 2 software (Johnson *et al*., 2009) with specific classification algorithms for medusahead;
4. Produce infestation maps for the study area in Harney County, Oregon Weed Management Area (approximately 667,077 ha or 2,575 mi^2 were photographed and classified);
5. Document operational protocols so they can be used countywide to detect, map, and monitor medusahead infestations.

While our project focused on the detection of medusahead, the technologies developed can be used for other weeds or vegetation types that are visually distinct.

Refine Mobile Mapping Techniques

The mobile mapping of invasive weeds employed a field hardened laptop computer equipped with a GPS antenna and underlying base maps including both topographic and orthophotographic imagery. This hardware combination facilitated accurate mapping of medusahead. Because field technicians always knew their position on the map and could zoom in and out on the topographic and orthographic maps, positions of infestations could be positioned very accurately. Direct digitization on the laptop in the field also reduced office time for data transfer and storage. We found that the mobile mapping system provided highly accurate and lower cost methods for field survey and GIS data collection.

We suggest six major components of a monitoring system for documenting rangeland invasive weeds 1) continuous recording GPS Tracking Unit, 2) four wheel drive vehicle or an all terrain vehicle (ATV), 3) field hardened laptop computer with a GPS antenna, 4) GIS Software such as ArcGIS 9.3, ERDAS, Global Mapper etc., 5) a 400-watt, 12 volt DC to AC power inverter, and 6) cooling pad for the laptop computer.

Auto-referencing Aerial Images

The combination of rapid GPS logging, synchronization of camera date/time with GPS date/time, automatic recording of camera parameters, and computer software enabled us to generate approximate x and y coordinates for the corners of every aerial image collected. Our Aerial Image Positioning Tool generated an image projection file and KML file that allows images to be opened in GIS programs. When opened they are positioned, rotated and scaled to their approximate position. These images were typically geographically correct to within 100m of true location. Our software allowed us to survey extensive areas via high-resolution aerial photographs, rough position them, and save them in a format that is cheaply and easily shared, stored and interpreted. For example, during two days in August 2009, we collected 7,674 images and rough positioned all of them in several hours of computer processing time. The aircraft and pilot costs totaled $250/hour or $4757.95 for the three flights. Since images were collected so rapidly and we could obtain up to 720 images/hr, our cost was $ 0.46 per image. In our study each image covered 215 ha (531 acres) with 60% overlap or approximately $ 0.535/km^2.

If greater positional accuracy is needed the images can be easily re-rectified to NAIP base imagery that meets national mapping standards. We suggest that as higher megapixel cameras, better camera mounting systems, and faster GPS logging devices become available, greater positional accuracies will be attained. In any case, our Aerial Image Positioning Tool renders digital mapping much less expensive that traditional film aerial photography.

Update and Improve VegMeasure 2 Software

VegMeasure 2 was used to batch classify aerial images using the spectral reflectance (digital numbers) in the red, green, and blue bands. We employed a RGB Spherical Extraction process and calibration by selecting a minimum of 25 locations (pixels) known to have severe medusahead infestations and extracted the RGB pixel values. Tolerance around these digital number values was set at a Euclidian distance of 20 to produce the infestation maps. This process produced a medusahead classification with an accuracy of 84.5%. We suggest that VegMeasure 2 should be improved by programming algorithms that automatically transfer projection, datum, rotation, and registration information to processed image files. We also think that an automatic splining algorithm based on the pattern of training points in the RGB color cube could improve accuracy.

Produce Infestation Maps of the Study Area

An infestation map of the study areas derived from our "medusahead present" classification was produced for weed specialists in Harney County, Oregon. Patterns of medusahead populations on this map should provide insight as to the dispersal mechanisms used by this weed and indicate areas that are at risk of invasion. A cursory examination suggests that the road and trail network is more heavily infested than areas far from roads. We have not statistically tested this observation but suggest that our data could be used to this purpose.

Detailed maps of specific sites within the study area could be used as reference for determining the rate of spread of medusahead or for judging the success of various control efforts. It seems reasonable that different weed control strategies should be evaluated using our monitoring technologies.

Document Operational Protocols

This thesis and subsequent publications document the procedures we used to map medusahead at fine scales. It is our hope that the work we did and the protocols we developed and evaluated can be used to preserve and protect native ecosystems in areas at risk of invasion by medusahead or other noxious weeds.

BIBLIOGRAPHY

Alfred, J. Wagtendonk and Richard A.M. De Jeu. 2007. Sensible Field Computing: Evaluating the Use of Mobile GIS Methods in Scientific Fieldwork. Photogrammetric Engineering and Remote Sensing June 2007 pp 651-662

Amy, J. 2001. Taeniatherum caput-medusae. In: Fire Effects Information System. U.S. Department of Agriculture, Forest Service, Rocky Mountain Research Station, Fire Sciences Laboratory (Producer). http://www.fs.fed.us/database/feis/

Anderson, G. L., J. H. Everitt, D. E. Escobar, N. R. Spencer, and R. J. Andrascik. 1996. Mapping leafy spurge (*Euphorbia esula*) infestations using aerial photography and geographic information systems. Geocarto International 11:81-89.

Anderson, G.L., C.W. Prosser, S. Haggar, and B. Foster, 1999. Change detection of leafy spurge infestations using aerial photography and geographic information systems, pp. 223-230, In: P. T. Tueller (ed.), Proceedings of the 17th Biennial Workshop Color Aerial Photography and Videography in Resource Assessment. American Society of Photogrammetry and Remote Sensing, Bethesda, MD.

Anderson, G.L., J.H. Everitt, A.J. Richardon, D.E. Escobar. 1993. Using satellite data to map false broomweed (Ericameria austrotexana) infestations on south Texas rangelands. Weed Technology 7:865-871.

Arnold, G. W., P. G. Ozanne, K. A. Galbraith, and F. Dandridge. 1985. The capeweed content of pastures in south-west Western Australia. Australian Journal of Experimental Agriculture 25:117-123.

Asner, G. P., M. O. Jones, R. E. Martin, D. E. Knapp and R. F. Hughes. 2008. Remote sensing of native and invasive species in Hawaiian forests. Remote Sensing of Environment 112:1912-1926.

Asner, G.P., C. A. Wessman, C. A. Bateson, and J. L. Privette. 2000. Impact of tissue, canopy and landscape factors on the hyperspectral reflectance variability of arid ecosystems. Remote Sensing of Environment 74:69-84.

Bethany, A. B. and J. F. Mustard. 2006. Characterizing the Landscape Dynamics of an Invasive Plant and Risk of Invasion Using Remote Sensing. Ecological Applications 16(3):1132-1147.

Blank, R. R., F. L. Allen and J. A. Young. 1996. Influence of simulated burning of soil-litter from low sagebrush, squirreltail, cheatgrass, and medusahead on water-soluble anions and cations. International Journal of Wildland Fire. 6(3):137-143.

Booth, D. T., S.E. Cox, and D.E. Johnson. 2004. Calibration of Threshold Levels in Vegetation-Cover Classification Software. 57th Annual Meeting for the Society for Range Management. 24th-30th January 2004 in Salt Lake City, USA.

Booth, D. T., S.E. Cox, M. Louhaichi, and D. E. Johnson. 2004. Technical Note: Lightweight Camera Stand for Close-to-Earth Remote Sensing. Journal of Range Management 57:675-678.

Booth, D.T., S. E. Cox, and D. E. Johnson. 2005. Detection-Threshold Calibration and Other Factors Influencing Digital Measurements of Ground Cover. Rangeland Ecology and Management 58:598-604.

Bovey, R. W., D. LeTourneau, and L. C. Erickson. 1961. The chemical composition of medusahead and downy brome. Weeds 9:307-311.

Byers, J.E., S. Reichard, J. Randall, I. Parker. 2002. Directing research to reduce the impacts of nonindigenous species. Conservation Biology 16(3): 630-640.

Carson, H.W., L.W. Lass, and R.H. Callihan.1995. Detection of yellow hawkweed with high-resolution multispectral digital imagery. Weed Technology 9:477-483.

Cochrane, M. A. 2000. Using vegetation reflectance variability for species level classification of hyperspectral data. International Journal of Remote Sensing 21:2075-2087.

Dahl, B.E. and E.W. Tisdale. 1975. Environmental factors related to medusahead distribution. Journal of Range Management 28:463-468.

Daniel, D., D. K. Giles, D. C Slaughter. 2003. Ground based vision identification for weed mapping using DGPS. American Society of Agricultural and Biological engineers. Paper No: 031005. ASAE Annual International Meeting. July 27- 30 Las Vegas, Nevada.

D'Antonio, C.M., N.E. Jackson, C.C. Horvitz, and R. Hedberg. 2004. Invasive plants in wildland ecosystems: merging the study of invasion processes with management needs. Frontiers in Ecology and the Environment 2: 513-521.

David, R. S. 2005. Remote sensing and site-specific weed management. Frontiers in Ecology and the Environment 3: 526-532.

Davies, K. W. 2008. Medusahead dispersal and establishment in sagebrush steppe plant communities. Rangeland Ecology & Management 61:110-115.

Davies, W. K., and T. J. Svejcar. 2008. Comparison of Medusahead-Invaded and Non-invaded Wyoming Big Sagebrush Steppe in Southeastern Oregon. Rangeland Ecology and Management 61: 6:623-629.

Dewey, S.A., K.P. Price, and D. Ramsey. 1991. Satellite remote sensing to predict potential distribution of Dyers woad (*Isatis tinctoria*). Weed Technology 5:479-484.

DiPietro, D. Y. 2002. Mapping the Invasive Plant *Arundo donax* and Associated Riparian Vegetation Using Hyperspectral Remote Sensing. M.A. thesis. Davis, CA: University of California, Davis, 49 p.

DiTomaso, J. M. 2000. Invasive weeds in rangelands: species, impacts, and management. Weed Science 48:255-265.

Ellum, C. and N. El-Sheimy. Land-Based mobile mapping systems Canada. Photogrammetric Engineering and Remote Sensing, January 2002, Pp. 13-18.

ESRI. 2010. ArcGIS User's Manual. Environmental Systems Research Institute, Inc. Redlands, CA.

Evangelista, P. H., T.J. Stohlgren, J. T. Morisette and S. Kumar. 2009. Mapping Invasive Tamarisk (Tamarix): A Comparison of Single-Scene and Time-Series Analyses of Remotely Sensed Data. Remote Sensing 1:519-533.

Everitt, B.J. 1998. Chronology of the spread of tamarisk in the Central Rio Grande. Wetlands 18:658-668.

Everitt, J. H., and D. E. Escobar. 1996. Use of spatial information technologies for noxious plant detection and distribution on rangelands. Geocarto International *11*:63-80.

Everitt, J. H., D. E. Escobar, and M. R. Davis. 2001. Reflectance and image characteristics of selected noxious rangeland species. Journal of Range Management 54:A106–A120.

Everitt, J. H., D. E. Escobar, M. A. Alaniz, and M. R. Davis. 1987. Using airborne middle-infrared (1.45–2.0 mm) video imagery for distinguishing plant species and soil conditions. Remote Sensing of Environment 22: 423-428.

Everitt, J. H., D. E. Escobar, M. A. Alaniz, and M. R. Davis. 1991. Light reflectance characteristics and video remote-sensing of prickly pear. Journal of Range Management 44:587-592.

Everitt, J. H., D. E. Escobar, M. A. Alaniz, M. R. Davis, and J. V. Richerson. 1996. Using spatial information technologies to map Chinese tamarisk (*Tamarix chinensis*) infestations. Weed Science 44:194-201.

Everitt, J. H., M. A. Alaniz, and D. E. Escobar. 1992. Using remote sensing to distinguish common goldenweed (*Isocoma coronopifolia*) and Drummon goldenweed (*Isocoma drummondii*). Weed Science 40:621-628.

Everitt, J.H. and C.J. Deloach. 1990. Remote sensing of Chinese Tamarisk (*Tamarix chinensis*) and associated vegetation. Weed Science 38:273-278.

Everitt, J.H. G.L. Anderson, D.E. Escobar, M.R. Davis, N.R. Spencer, R.J. Andrascik. 1995. Use of remote sensing for detecting and mapping leafy spurge (*Euphorbia esula*). Weed Technology 9:599-609.

Everitt, J.H., C. Yang, B.J. Racher, C.M. Britton and M.R. Davis. 2001. Remote sensing of redberry juniper in the Texas Rolling Plains. Journal of Range Management 54:254-259.

Everitt, J.H., C.Yang and H.B. Johnson. (2007). Canopy spectra and remote sensing of Ashe juniper and associated vegetation. Environmental Monitoring and Assessment 130:403-413.

Everitt, J.H., C.Yang, M.A. Alaniz, and M.R. Davis. 2006. Using spatial information technologies to detect and map invasive weeds in Texas riparian zones and waterways. MAPPS/ASPRS Fall Conference, November 6-10, 2006 San Antonio, Texas.

Everitt, J.H., C.Yang, M.A. Alaniz, M.R. Davis, F.L. Nibling, and C.J. Deloach. 2004. Canopy spectra and remote sensing of giant reed and associated vegetation. Journal of Range Management 57:561-569.

Everitt, J.H., G.L. Anderson, D.E. Escobar, M.R. Davis, N.R. Spencer and R.J. Andrascik.1995. Use of remote sensing for detecting and mapping leafy spurge (*Euphorbia esula*). Weed Technology 9:599-609.

Fosberg, M. A. 1965. Relationship of cheatgrass and medusahead to soils in the Colombia River Basin. Proceedings of the Cheatgrass Symposium Vale, OR. U.S. Dept. of the Interior, Bureau of Land Management, Washington, D.C.

Fuller, R.M. and L.A. Boorman.1977. The spread and development of *Rhododendron ponticum* L. on dunes at Winterton, Norfolk, in comparison with invasion by *Hippophaë rhamnoides* L. at Saltfleetby, Lincolnshire. Biological Conservation

12:83-94.

Furbush, P. 1953. Control of medusa-head on California ranges. Journal of Forestry. 51:118-121.

Gao, J., 2002. Integration of GPS with remote sensing and GIS - Reality and prospect. Photogrammetric Engineering and Remote Sensing 68(5):447-453.

Global Mapper LLC. 2010. Global Mapper User's Guide. Global Mapper Software LLC. Parker, CO.

Goebel, C. J., M. Tazi, and G. A. Harris. 1988. Secar bluebunch wheatgrass as a competitor to medusahead. Journal of Range Management 41:88-89.

Grejner-Brzezinska, D. 2001a. "Mobile Mapping Technology: Ten Years Later (Part One), Surveying and Land Information Systems, 61(2):75-91.

Grejner-Brzezinska, D. 2001b. "Direct Sensor Orientation in Airborne and Land-Based Mapping Applications", Report No. 461, Geodetic Geoinformation Science, The Ohio State University, 51p.

Grejner-Brzezinska, D. A. 2002. Direct Georeferencing at The Ohio State University: A Historical Perspective. Photogrammetric Engineering and Remote Sensing. Journal of the American society for Photogrammetry and remote Sensing 68(6):

Grejner-Brzezinska, D. A., R. Li, N. Haala, and C. Toth. 2004. From Mobile Mapping to Telegeoinformatics: Paradigm Shift in Geospatial Data Acquisition, Processing, and Management. Photogrammetric Engineering and Remote Sensing 70(2):197-210.

Haefner, S. 2004. Kite Aerial Photography. www.thehaefners.com/kap/?page5kites.

Hamada, Y., D.A. Stow, L.L. Coulter, J.C. Jafolla, L.W. Hendricks. 2007. Detecting Tamarisk species (*Tamarix* spp.) in riparian habitats of Southern California using high spatial resolution hyperspectral imagery. Remote Sensing of the Environment 109:237-248.

He, G.P., D. Cunningham, and J. Bossler. 1994. Spatial Data Collection with the GPSVan Mobile Mapping System. Proceedings, ISPRS Commission IV Symposium 30(4):107-113.

He, G.P., G. Dedes, G. Orvets, and J.D. Bossler. 1994. Generation of transportation GIS by Integrating GPS, INS and Computer Vision Technology. Proceedings, 3rd International Colloquium of LIESMARS, WTUSM, Wuhan, PR China, pp. 91-99.

Higgins, S.I. and D.M. Richardson.1996. A review of models of alien plant spread. Ecological Modeling 87:249-265.

Hirano, A., M. Madden, R. Welch. 2003. Hypersptectral image data for mapping wetland vegetation. Wetlands 23:436-448.

Hood, J., L. Ladner, and R. Champion, 1989. Image Processing Techniques for Orthophotoquad Production. Photogrametric Engineering and Remote Sensing 55:1323-1329.

Hughes, M.L., P.F. Mcdowell and W.A. Marcus. 2006. Accuracy assessment of georectified aerial photographs: Implications for measuring lateral channel movement in a GIS. Geomorphology 74:1-16.

Hummer-Miller, S. 1989. A Digital Mosaicking Algorithm Allowing for an Irregular join ‘Line’. Photogrammetric Engineering & Remote Sensing 55:43-47.

Hunt, E.R., Jr. J.H. Everitt, J.C. Ritchie, M.S. Moran, D.T. Booth, G.L. Anderson, P.E. Clard, M.S. Seyfried. 2003. Applications and research using remote sensing for rangeland management. Photogrammetry Engineering and Remote Sensing 69: 675-693.

Jiann-Yeou, R. and L. Chen. 2004. Geometrical Building Modeling and Its Application to the Ortho-Rectification for Aerial Images. Journal of Photogrammetry and Remote Sensing 9(1):53-76.

Johnson, K.D., M.D. Johnson, and M. Louhaichi. 2007. GeoAlbum user's guide. Global Geomatic Solutions. Corvallis, OR. 55p.

Johnson, K.D., S.K. Ndzeidze, M.D. Johnson, A.L. Wörz, M. Louhaichi and D.E Johnson. 2010. World File Maker User's Guide. Global Geomatic Solutions. Oviedo, FL. 15p.

Johnson, M.D. Johnson, M. Louhaichi, P.E. Clark, A.L. Wörz, S.K. Ndzeidze, and D.E. Johnson. 2009. VegMeasure 2 user's guide. Department of Rangeland Ecology and Management, Oregon State University, Corvallis, OR. 25p.

Joshi, C., J. de Leeuwand, I.C. Van Duren. 2004. Remote sensing and GIS applications for mapping and spatial modeling of invasive species. In: ISPRS 2004: Proceedings of the XXth ISPRS Congress: Geo-imagery bridging continents, 12-23 July 2004, Istanbul, Turkey. 7:669-677.

Kang, Z., L. Zhang, S. Zlatanova, and J. Li. 2009. An automatic mosaicking method for building facade texture mapping using a monocular close-range image sequence. *ISPRS* Journal of Photogrammetry and Remote Sensing, doi:10.1016/j.isprsjprs.2009.11.003 (Elsevier: SCI).

Kawai, S. and Saji H. Automatic Registration of Aerial Oblique Images and a Digital Map. SICE Annual Conference 2007. Sept. 17-20, 2007, Kagawa University, Japan.

Ladd, G. B., A. Nagchaudhuri, T. J. Earl, M. Mitra, G. L. Bland, G.M. Casady, R.S. Hanley, S.K. Seelan. 2005. Detection of Leafy Spurge (*Euphorbia esula*) Using Multidate High-Resolution Satellite Imagery. Weed Technology 19(2):462-467.

Ladd, G. B., A. Nagchaudhuri, T. J. Earl, M. Mitra, G.L. Bland. 2006. Rectification, georeferencing and mosaicking of images acquired with remotely operated aerial platforms. ASPRS 2006 Annual Conference Reno, Nevada, May 1-5, 2006.

Lamb, D.W., M.M. Weedon and L.J. Rew. 1999. Evaluating the accuracy of mapping weeds in seedling crops using airborne digital imaging. Avena spp. in seedling triticale (X. Triticosecale).Weed Research 39:481-492.

Lass, L. W., D. C. Thill, B. Shafii, and T. S. Prather. 2002. Detecting spotted knapweed (*Centaurea maculosa*) with hyperspectral remote sensing technology. Weed Technology 16:426-432.

Lass, L. W., H. W. Carson, and R. H. Callihan. 1996. Detection of yellow starthistle (*Centaurea solstitialis*) and common St. Johnswort (*Hypericum perforatum*) with multispectral digital imagery. Weed Technology 10:466-474.

Lass, L.W and R.H. Callihan. 1993. GPS and GIS for weed surveys and management. Weed Technology. 1993. 7:249-254.

Lass, L.W. and D.C. Thill. 2000. Detecting yellow starthistle (*Centaurea solstitialis*) with hyperspectral remote sensing technology. Proceedings of Western Society. Weed Science. 53:11.

Lass, L.W. and R.H. Callihan. 1997. The effect of phenological stage on detectability of yellow hawkweed (*Hieracium partense*) and oxeye daisy (*Chrysanthemum leucanthemum*) with remote multispectral digital imagery. Weed Technology. 11:248–256.

Lass, L.W. and T.S. Prather. 2004. Detecting the locations of Brazilian pepper trees in the Everglades with a hyperspectral sensor. Weed Technology. 18:437-442.

Lass, L.W., and R.H. Callihan (1997). The effect of phenological stage on detectibility of yellow hawkweed (*Hieracium pratense*) and oxeye daisy (*Chrysanthemum leucanthemum*) with remote multispectral digital imagery. Weed Technology 11:248-256.

Lass, L.W., B. Shafii, W.J. Price, and D.C. Thill. 2000. Assessing agreement in multispectral images of yellow starthistle (*Centaurea solstitialis*) with ground truth data using a Bayesian methodology. Weed Technology 14:539-544.

Lass, L.W., D.C. Thill, B. Shafii, T.S Prather. 2002. Detecting spotted knapweed (Centaurea maculosa) with hyperspectral remote sensing technology. Weed Technology 16:535-545.

Lass, L.W., H.W. Carson, R.W. Callihan. 1996. Detection of yellow starthistle (*Centaurea solstitialis*) and common St. Johnswort (*Hypericum perforatum*) with multispectral digital imagery. Weed Technology 10:466-474.

Lass, L.W., T.S. Prather and N.F. Glenn. 2005. A review of remote sensing of invasive weeds and example of the early detection of spotted knapweed (*Centaurea maculosa*) and babysbreath (*Gypsophila paniculata*) with a hyperspectral sensor. Weed Science 53:242–51.

Lass, L.W., Timothy S.P., Nancy F. G., Keith T. W., Jacob, T. M., and Jeffery, P. (2005). A review of remote sensing of invasive weeds and example of the early detection of spotted knapweed (*Centaurea maculosa*) and babysbreath (*Gypsophila paniculata*) with a hyperspectral sensor Weed Science 53(2):242-251.

Lass, W.L., T.S. Prather, N.F. Glenn, K.T. Weber, J.T. Mundt, J. Pettingill. 2005. A review of remote sensing of invasive weeds and example of the early detection of spotted knapweed (Centaurea maculosa) and babysbreath (Gypsophila paniculata) with a hyperspectral sensor. Weed Science 53:242-251.

Lestak, L.R., W.F. Manley, P.M. Sturtevant, J.A. Maslanik, C.E. Tweedie, and J. Brown. 2007. High-resolution rectified aerial photography for collaborative research of environmental change at Barrow, Alaska, USA. *Boulder*, Colorado USA: National Snow and Ice Data Center. DVD.

Li, J and M.A Chapman. 2008. Terrestrial mobile mapping systems towards real-time geospatial data collection Geospatial Information Technology for Emergency Response. ISPRS Book Series, Vol. 6, Taylor & Francis, London, pp. 103-119.

Lillesand, T. M., and R. W. Kiefer. 2000. Remote sensing and image interpretation. Fourth edition. John Wiley and Sons, Inc., New York, NY. 724 pp.

Lindholm, S. 2004. Aerial Digital Photography from a Balloon for Fifty Dollars. www.stanford.edu/;lindholm/chpropbal.html.

Lodge, D. 1993. Biological invasions: lessons from ecology. Trends in Ecology and Evolution 8:133-137.

Lusk, W.C., M.B. Jones, D.T. Torell, and C.M. McKell. 1961. Medusahead palatability. Journal of Range Management 14:248-251.

Mack, R.N., D. Simberloff, W. M. Lonsdale, H. Evans, M. Clout and F. A. Bazzaz. 2000. Biotic invasions: causes, epidemiology, global consequences, and control. Ecological Applications 10(3):689-710.

Major, J., C.M. McKell and L.J. Berry. 1960. Improvement of medusahead-infested rangeland. Leaflet 123. Davis, CA: University of California, California Agricultural Experiment Station. 6 p.

Mast, J.N., T.T. Veblen and M.E. Hodgson. 1997. Tree invasion within a pine/grassland ecotone: an approach with historic aerial photography and GIS modeling. Forest Ecology and Management 93:181-194.

Mathieu M.G. and S. de Blois. 2005. Mapping the invasive species *Phragmites australis* in linear wetland corridors. Aquatic Botany. Volume 83, Issue 4, Pp 310-320.

Maurer, T., J. R. Mary and G. Audrey. 1988.*Taeniatherum caput-medusae* Medusahead. *Global Invasive Species Team. The Nature Conservancy*.

McKell, C.M., A.M. Wilson, and B.L. Kay. 1962. Effective burning of rangelands infested with medusahead. Weeds 10:125-131.

McKell, C.M., A.M. Wilson, and B.L. Kay. 1962. Effective burning of rangelands infested with medusahead. Weeds 10:125-131.

Medlin, C.R., D.R. Shaw, P.D. Gerard, F.E. LaMastus. 2000. Using remote sensing to detect weed infestations in Glycine max. Weed Science 48:393-398.

Miller, H. C., D. Clausnitzer, and M. M. Borman. 1999. Medusahead. *In:* R.L. Sheley and J.K. Petroff . Biology and management of noxious rangeland weeds. Corvallis, OR: Oregon State University Press. pp. 271-281.

Minhe, J.I., and John R. Jensen. 2000. Continuous Piecewise Geometric Rectification for Airborne Multispectral Scanner Imagery. Photogrammetric Engineering & Remote Sensing 66(2):163-171.

Montoya, L., 2003. Geo-data acquisition through mobile GIS and digital video - An urban disaster management perspective. Environmental Modelling and Software 18(10):869–876.

Motrena, P. and J.M. Rebordao.1998. Invariant models for ground control points in high resolution images. International Journal of Remote Sensing 19(7):1359-1375.

MÜllerová, J., P. Pysek, V. Jarosík and J. Pergl. 2005. Aerial photographs as a tool for assessing the regional dynamics of the invasive plant species *Heracleum mantegazzianum.* Journal of Applied Ecology 42:1042-1053.

Murino, V.U., A.E. Castellani, and A. Fusiello. 2002. Registration of very time-distant aerial images. Proceedings of the IEEE International Conference on Image Processing, 3:989-992.

Murphy, A. H and D. Turner. 1959. A study on the germination of Medusa-head seed. Bulletin. 48: 6-10.

Mustafa, M., K. Steddom, G. J. Michels Jr. 2006. Estimating Biophysical Characteristics of Musk Thistle (*Carduus nutans*) With Three Remote Sensing

Instruments. Rangeland Ecology and Management 59(1):44-54.

Naylor, B. J., B. A. Endress, and C. G. Parks. 2005. Multiscale detection of sulfur cinquefoil using aerial photography. Rangeland Ecology and Management 58:447-451.

Nelson, J. R and A. M. Wilson. 1969. Influence of age and awn removal on dormancy of medusahead seeds. Journal of Range Management 22: 289-298.

Novak, K. 1995. Mobile mapping Technology for GIS Data Collection. Photogrammetric Engineering and Remote Sensing. Journal of the American society for Photogrammetry and remote Sensing. 61(5):493-501.

Okin, G. S., D. A. Roberts, B. Murray, and W. J. Okin. 2001. Practical limits on hyperspectral vegetation discrimination in arid and semiarid environments. Remote Sensing of Environment 77:212-225.

Pearlstine, L., S. Smith, E. Walsh, and J. Stenberg. 1998. Aerial Sampling for Brazilian Pepper on Canaveral National Seashore. Gainesville, FL: USGS Biological Resources Division, Florida Cooperative Fish and Wildlife Research Unit.

Perez, A.J., F. Lopez, J.V. Benlloch and S. Christensen. 2000. Colour and shape analysis techniques for weed detection in cereal fields. Computers and Electronics in Agriculture 25:197-212.

Peters, A.J., B.C. Reed, and M.D. Eve. 1992. Remote sensing of broom snakeweed (*Gutierrezia sarothrae*) with NOAA-10 spectral image processing. Weed Technology 6:1015-1020.

Peterson, E.B. 2005. Estimating cover of an invasive grass (*Bromus tectorum*) using tobit regression and phenology derived from two dates of Landsat ETM plus data. International Journal of Remote Sensing 26:2491-2507.

Ponzetti, J. M. 1997. Assessment of medusahead and cheatgrass control techniques at Lawrence Memorial Grassland Pre-serve. The Nature Conservancy of Oregon, Portland, Oregon, USA.

Rew, L.J. and R.D. Cousens. 2001. Sptaila distribution of weeds in arable crops: are current sampling and analytical methods appropriate? Weed Research 41:1-18.

Rew, L.J, B.D. Maxwell and R. Aspinall. 2005. Predicting the occurrence of non-indigenous species using environmental and remote sensed data. Weed Science 53:236-41.

RotorKraft. 2004. RotorKraft: Premium Radio Control Helicopters and Accessories. www.rotorkraft.com/index.htm.

Rouget, M., D.M. Richardson, S.J. Milton, and D. Polakow. 2001. Predicting invasion dynamics of four alien *Pinus* species in a highly fragmented semi-arid shrubland in South Africa. Plant Ecology 152:79-92.

Rowlinson, L.C., M. Summerton and F. Ahmed. 1999. Comparison of remote sensing data sources andtechniques for identifying and classifying alien invasive vegetation in riparian zones. Water SA 25:497-500.

Sharp, L.A., M. Hironaka, and E.W. Tisdale. 1957. Viability of medusahead seed collected in Idaho. Journal of Range Management 10:123-126.

Sheley, R. L. and J. K. Petroff, editors. (eds.). 1999. Biology and Management of Noxious Rangeland Weeds. Oregon State University Press. Corvallis.

Sheley, R., J. James, B. Smith, and E. Vasquez. 2010. Applying Ecologically Based Invasive-Plant Management. Rangeland Ecology and Management 63(6) 605-613.

Shih, F., Y. Chyang and O.R. Mitchell. 1992. A Mathematical Morphology Approach to Euclidean Distance Transformation. IEEE Transactions on Image Processing, 1(2):197-204.

Si, X., and Li J. 2008. Integrating agent-based modeling and GIS for realistically simulation of traffic control plan for emergency evacuation. Joint ISCRAM-China and Gi4DM Conference, Harbin, China, August 4-6, 8pp.

Smith, H. A., W. S. Johnson, J. S. Shonkwiler, and S. R. Swanson. 1999. The implications of variable or constant expansion rates in invasive weed infestations. Weed Science 47:62-66.

Sohn, Y., and R. M. McCoy. 1997. Mapping desert shrub rangeland using spectral unmixing and modeling spectral mixtures with TM data. Photogrammetry Engineering Remote Sensing 63:707-716.

Stafford, J. V., J. M. Le Bars and B. Ambler**.** 1996. A hand-held data logger with integral GPS for producing weed maps by field walking. Computers and Electronics in Agriculture 14 (2-3):235-247.

Strunz, G., W. Knpfle, and A. Roth. 1994. Automation of Tie Pointing Procedure for the Geocoding of Satellite Images. International Archives of Photogrammetry and Remote Sensing, 30(3):

Swenson, C.F., L. Duane and E.C. Lambert. 1964. Silica in medusahead. Weeds 12:16-18.

Swenson, C.F., L. Duane, E.C. Lambert. 1964. Silica in medusahead. Weeds. 12: 16-18.

Tang, L., Tian, L.H. Yao, and K. Thorp. 2001. A real-time in-field variability mapping system. ASAE Paper No. 011025. St. Joseph, MI: ASAE.

Tao, C.V. and Li J, 2007. Foreword: Advances in Mobile Mapping Technology. ISPRS Book Series, Vol. 4, Taylor & Francis, London, ISBN 978-0-415-42723-4, pp 11-14.

Theodore, M.W. and J. Cardina. 1997. Accuracy of a Global Positioning System (GPS) for Weed Mapping. Weed Technology. 11(4):782-786.

Torell, P.J., E.C. Lambert and H.H. Robert. 1961. The medusahead problem in Idaho. Weeds.9:124-131.

Torell, P.J. 1967. Dowpon-an aid to reseeding medusahead-infested rangeland. Down to Earth 23: 6-8.

Torell, P.J., E.C. Lambert and H.H. Robert. 1961. The medusahead problem in Idaho. Weeds 9:124-131.

Tripcevich, N. 2004. Mobile GIS in archaeological survey. The SAA Archeological Record, 4(3):17-22.

Tsou, M.H., 2004. Integrated mobile GIS and wireless internet map servers for environmental monitoring and management. Cartography and Geographic Information Science, 31(3):153-165.

Underwood, E., S.L. Ustin, and D. DiPietro. 2003. Mapping nonnative plants using hyperspectral remote sensing. Remote Sensing of Environment 86:150-161.

Ustin, S.L., D. DiPietro, K. Olmstead, E. Underwood, and G.J. Scheer. 2002. Hyperspectral Remote Sensing for Invasive Species Detection and Mapping. IEEE.

Van, W., E.C. Luschei, A.J. Bussan and B.D. Maxwell. 2002. Accuracy and cost effectiveness of GPS-assisted wild oat mapping in spring cereal crops. Weed Science. 50:120-129.

Webster, T.M. and J. Cardina. 1997. Accuracy of a global positioning system (GPS) for weed mapping. Weed Technology. 11:782-786.

Webster, T.M., J. Cardina and S.J. Woods. 2000. Spatial and temporal expansion patterns of *Apocynum cannabinum* patches. Weed Science. 48:728-733.

Wendy, W. 2006. Automated Georeferencing for Rapid Data Production. Photogrammetric Engineering & Remote Sensing, April 2006. pp 336-338

William G. 2000. Remote Sensing of Vegetation, Plant Species Richness, and Regional Biodiversity Hotspots. Ecological Applications 10(6)1861-1870.

Williams, A.P., E.R. Hunt Jr. 2002. Estimation of leafy spurge cover from hyperspectral imagery using mixture tuned matched filtering. Remote Sensing of the Environment 82:446-456.

Wood, S.D., R.L. Lawrence, R.L. Sheley. 2006. Mapping invasive plants using hyperspectral imagery, classification trees, and classification thresholds. ASPRS 2006 Annual Conference Reno, Nevada, May 1-5, 2006.

Xin, Y. 2006. Image Correction for Digital Mapping. Proceedings of the ASPRS Annual Conference, Reno, NV., USA.

Xin, Y. and D. Parent. 2004. Automated Procedure of a Prototype Mapping System. Proceedings of the ACRS Annual Conference, Chiang Mai, Thailand.

Xin, Y., J. Li, and Q. Cheng. 2007. Automatic generation of remote sensing image mosaicks for mapping large natural hazards areas. In Li, J., S. Zlatanova and A. Fabbri, (eds.) Geomatics Solutions for Disaster Management, Lecture Notes in Geoinformation and Cartography, Vol.18, Springer Verlag, Berlin, ISBN 978-540-72106-2, pp.61-73.

Yang, C., J.H. Everitt and H.B. Johnson. (2009). Applying image transformation and classification techniques to airborne hyperspectral imagery for mapping Ashe juniper infestations. International Journal of Remote Sensing 30 (11):2741-2758.

Yang, C., and J. H. Everitt. 2010. Mapping three invasive weeds using airborne hyperspectral imagery. Ecological Informatics 5(5):429-439.

Yang. C., J.H. Everitt, M.R. Davis and C. Mao. 2003. A CCD camera-based hyperspectral imaging system for stationary and airborne applications. Geocarto International Journal. 18:71-80.

Yehuda, A. and A. Brand. 1998. Mosaicking of Orthorectified Aerial Images Photogrammetric. Engineering and Remote Sensing 64(2) 115-125.

Yingen, X. and F. Quek. 2006. Automatic Aerial Image Registration Without Correspondence. ICVS '06: Proceedings of the Fourth IEEE International Conference on Computer Vision Systems, pp. 25-33.

Young, J. A. and R. A. Evans. 1970. Invasion of medusahead into the Great Basin. Weed Science 18:89-97.

Young, J. A. and R. A. Evans. 1971. Medusahead invasion as influenced by herbicide and grazing on low sagebrush sites. Journal of Range Management 24:451- 454.

Young, J. A., C. D. Clements, and G. Nader. 1999. Medusahead and clay: the rarity of perennial seedling establishment. Rangeland 6:19-23.

Yubin, X. Image correction for digital mapping. PCI Geomatics Inc. 50 West Wilmot St., Richmond Hill, Ontario L4B 1M5, Canada.

Zimmerman, J.R., W.S. Johnson and M.E. Eiswerth. Medusahead: Economic Impact and Control in Nevada. University of Nevada-Reno Fact Sheet FS-02-37. http://www.unce.unr.edu/publications/files/nr/2002/FS0237.pdf.

Zobrist, A.L., N.A. Bryant, and R.G. Mclead, 1983. Technology for Large Digital Mosaics of Landsat Data. Photogrammetric Engineering and Remote Sensing 49:1325-335

APPENDICES

Appendix 1: Aircraft direction, image error and offsets, and time displacement

X	Y	LAYER	Aircraft Direction	Corner	Image	Error (m)	Offset	PP Error (m)	Long Axis (m)	Short Axis (m)	Ofset Direction	Aircraft Speed (m/s)	Time Displacement	ABS Time Displacement
382963.8	4841173	Image Corner Theoretical	North Bound	NW	Img_136	94.5	95	109	1827	1179	S	69.66092216	1.564722	1.564722
384734.5	4841173	Image Corner Theoretical	North Bound	NE	Img_136	142.1	140				S	69.66092216		
384734.5	4839993	Image Corner Theoretical	North Bound	SE	Img_136	84.1	72				S	69.66092216		
382963.8	4839993	Image Corner Theoretical	North Bound	SW	Img_136	104.3	101				S	69.66092216		
381250.5	4833040	Image Corner Theoretical	South Bound	NW	Img_234	-98.7	-96.7	-106	1706	1092	N	67.16072216	-1.5783	1.578303
383021.2	4833040	Image Corner Theoretical	South Bound	NE	Img_234	-133.1	-125				N	67.16072216		
383021.2	4831859	Image Corner Theoretical	South Bound	SE	Img_234	-133.5	-106				N	67.16072216		
381250.5	4831859	Image Corner Theoretical	South Bound	SW	Img_234	-37.8	-5.1				N	67.16072216		
382897.2	4835887	Image Corner Theoretical	North Bound	NW	Img_121	116.7	73.3	95	1785	1217	S	69.45514438	1.367789	1.367789
384667.9	4835887	Image Corner Theoretical	North Bound	NE	Img_121	170	167				S	69.45514438		
384667.9	4834707	Image Corner Theoretical	North Bound	SE	Img_121	129	127.6				S	69.45514438		
382897.2	4834707	Image Corner Theoretical	North Bound	SW	Img_121	36.6	36.09				S	69.45514438		
386309.5	4839923	Image Corner Theoretical	North Bound	NW	Img_457	35.9	34.53	97	1779	1212	S	67.75233327	1.431685	1.431685
388080.2	4839923	Image Corner Theoretical	North Bound	NE	Img_457	150.2	145.5				S	67.75233327		
388080.2	4838743	Image Corner Theoretical	North Bound	SE	Img_457	177.3	139.3				S	67.75233327		
386309.5	4838743	Image Corner Theoretical	North Bound	SW	Img_457	37.2	9.8				S	67.75233327		
379098.7	4843520	Image Corner Theoretical	North Bound	NW	Img_304	58.1	50.3	64	1824	1183	S	69.31624438	0.923304	0.923304
380869.4	4843520	Image Corner Theoretical	North Bound	NE	Img_304	128	109.8				S	69.31624438		

380869.4	4842339	Image Corner Theoretical	North Bound	SE	Img_304	101.3	25.9				S	69.31624438		
379098.7	4842339	Image Corner Theoretical	North Bound	SW	Img_304	67.3	49.4				S	69.31624438		
379064.5	4838966	Image Corner Theoretical	North Bound	NW	Img_291	91.7	54.3	44	1703	1122	S	68.61659994	0.641244	0.641244
380835.2	4838966	Image Corner Theoretical	North Bound	NE	Img_291	117.5	47.6				S	68.61659994		
380835.2	4837786	Image Corner Theoretical	North Bound	SE	Img_291	9.34	8.9				S	68.61659994		
379064.5	4837786	Image Corner Theoretical	North Bound	SW	Img_291	131.8	109.9				S	68.61659994		
381250.3	4835050	Image Corner Theoretical	South Bound	NW	Img_228	-50.2	-49.7	-99	1747	1131	N	67.35106661	-1.46991	1.46991
383036.9	4835050	Image Corner Theoretical	South Bound	NE	Img_228	-142.7	-136.4				N	67.35106661		
383036.9	4833859	Image Corner Theoretical	South Bound	SE	Img_228	-156.5	-72.7				N	67.35106661		
381250.3	4833859	Image Corner Theoretical	South Bound	SW	Img_228	-31.9	-7.4				N	67.35106661		
381203.6	4838464	Image Corner Theoretical	South Bound	NW	Img_218	-130	-87.3	-104	2177	1192	N	67.25846661	-1.54627	1.546274
382990.3	4838464	Image Corner Theoretical	South Bound	NE	Img_218	-115.7	-51.6				N	67.25846661		
382990.3	4837273	Image Corner Theoretical	South Bound	SE	Img_218	-85.4	-31.4				N	67.25846661		
381203.6	4837273	Image Corner Theoretical	South Bound	SW	Img_218	-99.4	-87.9				N	67.25846661		
384708.8	4837946	Image Corner Theoretical	South Bound	NW	Img_65	-197	-81.9	-174	1839	1267	N	66.7131555	-2.60818	2.608181
386495.5	4837946	Image Corner Theoretical	South Bound	NE	Img_65	-179.8	-120				N	66.7131555		
386495.5	4836755	Image Corner Theoretical	South Bound	SE	Img_65	-175.9	-120				N	66.7131555		
384708.8	4836755	Image Corner Theoretical	South Bound	SW	Img_65	-244.9	-146.4				N	66.7131555		
384694.3	4838942	Image Corner Theoretical	South Bound	NW	Img_62	-116	-35.8	-107	1849	1246	N	65.94663328	-1.62252	1.622524
386480.9	4838942	Image Corner Theoretical	South Bound	NE	Img_62	-114	-99.2				N	65.94663328		
386480.9	4837751	Image Corner Theoretical	South Bound	SE	Img_62	-120	-104				N	65.94663328		
384694.3	4837751	Image Corner Theoretical	South Bound	SW	Img_62	-153.3	-90.2				N	65.94663328		
384773	4836558	Image Corner Theoretical	South Bound	NW	Img_69	-145	-17.2	-114	1819	1261	N	66.14726661	-1.72343	1.723427
386559.6	4836558	Image Corner Theoretical	South Bound	NE	Img_69	-119.4	-45.2				N	66.14726661		

386559.6	4835367	Image Corner Theoretical	South Bound	SE	Img_69	-117.9	-37	N	66.14726661	
384773	4835367	Image Corner Theoretical	South Bound	SW	Img_69	-188.3	-80.2	N	66.14726661	
										1.497942

Appendix 2: Table of 220 images collected over Buck mountain.

Table 1: 220 images collected over Buck mountain					
Flight Date	Flight Time	Image	ELEVATION	Present	Absent
08/15/2009	23:21:56	IMG_2449.JPG	2710		
08/15/2009	23:31:34	IMG_2563.JPG	2778		
08/15/2009	22:32:44	IMG_1867.JPG	2831		
08/15/2009	23:21:51	IMG_2448.JPG	2708		
08/15/2009	23:02:04	IMG_2214.JPG	2832		
08/15/2009	22:53:22	IMG_2111.JPG	2749		
08/15/2009	22:32:49	IMG_1868.JPG	2826		
08/15/2009	23:31:39	IMG_2564.JPG	2771		
08/15/2009	23:21:46	IMG_2447.JPG	2713		
08/15/2009	23:02:09	IMG_2215.JPG	2836		
08/16/2009	16:36:09	IMG_0276.JPG	2989		
08/15/2009	22:53:17	IMG_2110.JPG	2741		
08/15/2009	23:31:44	IMG_2565.JPG	2765		
08/15/2009	22:32:55	IMG_1869.JPG	2823		
08/15/2009	23:21:41	IMG_2446.JPG	2725		
08/15/2009	23:02:14	IMG_2216.JPG	2838		
08/16/2009	16:36:14	IMG_0277.JPG	2989		
08/15/2009	22:53:12	IMG_2109.JPG	2728		
08/15/2009	23:31:49	IMG_2566.JPG	2754		
08/15/2009	22:33:00	IMG_1870.JPG	2821		
08/15/2009	23:02:19	IMG_2217.JPG	2837		
08/16/2009	16:36:19	IMG_0278.JPG	2988		
08/15/2009	22:00:53	IMG_1490.JPG	2924		
08/15/2009	23:21:35	IMG_2445.JPG	2730		
08/15/2009	22:53:07	IMG_2108.JPG	2706		
08/15/2009	22:23:16	IMG_1755.JPG	2694		
08/15/2009	23:31:54	IMG_2567.JPG	2744		
08/15/2009	22:33:05	IMG_1871.JPG	2816		
08/15/2009	23:02:24	IMG_2218.JPG	2840		
08/15/2009	22:00:58	IMG_1491.JPG	2920		
08/16/2009	16:36:24	IMG_0279.JPG	2988		
08/15/2009	21:50:09	IMG_1363.JPG	2858		
08/15/2009	22:53:02	IMG_2107.JPG	2688		
08/15/2009	23:21:30	IMG_2444.JPG	2733		
08/15/2009	22:23:11	IMG_1754.JPG	2690		
08/15/2009	23:31:59	IMG_2568.JPG	2742		

08/15/2009	22:33:10	IMG_1872.JPG	2809		
08/15/2009	22:01:03	IMG_1492.JPG	2915		
08/16/2009	16:36:29	IMG_0280.JPG	2992		
08/15/2009	23:02:30	IMG_2219.JPG	2847		
08/15/2009	23:21:25	IMG_2443.JPG	2742		
08/15/2009	22:52:56	IMG_2106.JPG	2693		
08/15/2009	22:23:06	IMG_1753.JPG	2691		
08/15/2009	22:33:15	IMG_1873.JPG	2803		
08/15/2009	23:32:04	IMG_2569.JPG	2742		
08/15/2009	22:01:08	IMG_1493.JPG	2914		
08/15/2009	23:02:35	IMG_2220.JPG	2845		
08/16/2009	16:36:34	IMG_0281.JPG	2996		
08/15/2009	22:52:52	IMG_2105.JPG	2704		
08/15/2009	23:21:20	IMG_2442.JPG	2754		
08/15/2009	22:33:20	IMG_1874.JPG	2802		
08/15/2009	22:23:01	IMG_1752.JPG	2694		
08/15/2009	23:32:09	IMG_2570.JPG	2749		
08/15/2009	23:02:40	IMG_2221.JPG	2842		
08/15/2009	22:01:13	IMG_1494.JPG	2910		
08/16/2009	16:36:39	IMG_0282.JPG	2999		
08/15/2009	22:52:46	IMG_2104.JPG	2723		
08/15/2009	23:21:15	IMG_2441.JPG	2762		
08/15/2009	22:33:25	IMG_1875.JPG	2802		
08/15/2009	23:32:14	IMG_2571.JPG	2755		
08/15/2009	22:22:56	IMG_1751.JPG	2693		
08/15/2009	23:02:45	IMG_2222.JPG	2834		
08/15/2009	22:01:18	IMG_1495.JPG	2904		
08/16/2009	16:36:44	IMG_0283.JPG	2999		
08/15/2009	22:52:41	IMG_2103.JPG	2735		
08/15/2009	23:21:10	IMG_2440.JPG	2764		
08/15/2009	22:33:30	IMG_1876.JPG	2801		
08/15/2009	23:32:19	IMG_2572.JPG	2760		
08/15/2009	22:22:51	IMG_1750.JPG	2689		
08/15/2009	23:02:50	IMG_2223.JPG	2820		
08/15/2009	22:01:23	IMG_1496.JPG	2894		
08/16/2009	16:36:49	IMG_0284.JPG	2998		
08/15/2009	22:52:36	IMG_2102.JPG	2741		
08/15/2009	23:21:05	IMG_2439.JPG	2760		
08/15/2009	22:33:35	IMG_1877.JPG	2797		
08/15/2009	23:02:55	IMG_2224.JPG	2807		

08/15/2009	22:22:46	IMG_1749.JPG	2687		
08/15/2009	22:01:28	IMG_1497.JPG	2888		
08/15/2009	23:32:25	IMG_2573.JPG	2769		
08/15/2009	22:52:31	IMG_2101.JPG	2742		
08/15/2009	22:33:40	IMG_1878.JPG	2789		
08/15/2009	23:21:00	IMG_2438.JPG	2754		
08/15/2009	23:03:00	IMG_2225.JPG	2798		
08/15/2009	22:01:33	IMG_1498.JPG	2885		
08/15/2009	22:22:41	IMG_1748.JPG	2693		
08/15/2009	23:32:30	IMG_2574.JPG	2774		
08/15/2009	22:52:26	IMG_2100.JPG	2746		
08/15/2009	22:33:45	IMG_1879.JPG	2779		
08/15/2009	23:20:55	IMG_2437.JPG	2749		
08/15/2009	23:03:05	IMG_2226.JPG	2797		
08/15/2009	22:01:38	IMG_1499.JPG	2884		
08/15/2009	23:32:35	IMG_2575.JPG	2773		
08/15/2009	22:22:36	IMG_1747.JPG	2709		
08/15/2009	22:33:50	IMG_1880.JPG	2770		
08/15/2009	22:52:21	IMG_2099.JPG	2746		
08/15/2009	23:20:50	IMG_2436.JPG	2753		
08/15/2009	23:03:10	IMG_2227.JPG	2803		
08/15/2009	22:01:43	IMG_1500.JPG	2884		
08/15/2009	22:33:55	IMG_1881.JPG	2758		
08/15/2009	22:22:31	IMG_1746.JPG	2730		
08/15/2009	23:32:40	IMG_2576.JPG	2766		
08/15/2009	22:52:16	IMG_2098.JPG	2745		
08/15/2009	23:20:45	IMG_2435.JPG	2760		
08/15/2009	23:03:15	IMG_2228.JPG	2811		
08/15/2009	22:01:48	IMG_1501.JPG	2881		
08/15/2009	22:34:00	IMG_1882.JPG	2752		
08/15/2009	22:22:26	IMG_1745.JPG	2747		
08/15/2009	23:32:45	IMG_2577.JPG	2761		
08/15/2009	22:52:11	IMG_2097.JPG	2744		
08/15/2009	23:20:40	IMG_2434.JPG	2763		
08/15/2009	23:03:20	IMG_2229.JPG	2819		
08/15/2009	22:01:53	IMG_1502.JPG	2874		
08/15/2009	22:34:05	IMG_1883.JPG	2747		
08/15/2009	22:22:21	IMG_1744.JPG	2741		
08/15/2009	22:52:06	IMG_2096.JPG	2744		
08/16/2009	17:57:06	IMG_1233.JPG	2401		

08/15/2009	23:03:25	IMG_2230.JPG	2827		
08/15/2009	22:01:58	IMG_1503.JPG	2869		
08/15/2009	22:34:11	IMG_1884.JPG	2738		
08/15/2009	22:22:16	IMG_1743.JPG	2728		
08/15/2009	22:52:01	IMG_2095.JPG	2740		
08/15/2009	23:03:30	IMG_2231.JPG	2833		
08/15/2009	21:49:08	IMG_1351.JPG	2816	**20.4**	**79.6**
08/15/2009	22:02:04	IMG_1504.JPG	2872		
08/15/2009	22:34:16	IMG_1885.JPG	2734		
08/15/2009	22:51:56	IMG_2094.JPG	2733		
08/15/2009	22:22:10	IMG_1742.JPG	2719		
08/15/2009	23:03:35	IMG_2232.JPG	2841		
08/15/2009	21:49:03	IMG_1350.JPG	2825	46.1	53.9
08/15/2009	22:02:09	IMG_1505.JPG	2877		
08/15/2009	22:34:21	IMG_1886.JPG	2729		
08/15/2009	22:51:51	IMG_2093.JPG	2733		
08/15/2009	22:22:05	IMG_1741.JPG	2729		
08/15/2009	23:03:41	IMG_2233.JPG	2850		
08/15/2009	21:48:58	IMG_1349.JPG	2835	**35.3**	**64.7**
08/15/2009	22:02:14	IMG_1506.JPG	2877		
08/15/2009	22:34:26	IMG_1887.JPG	2723		
08/15/2009	22:51:46	IMG_2092.JPG	2737		
08/15/2009	23:03:46	IMG_2234.JPG	2846		
08/15/2009	22:22:00	IMG_1740.JPG	2745		
08/15/2009	22:34:31	IMG_1888.JPG	2713		
08/15/2009	22:02:19	IMG_1507.JPG	2873		
08/15/2009	21:48:53	IMG_1348.JPG	2836	**30.9**	**69.1**
08/15/2009	23:03:51	IMG_2235.JPG	2836		
08/15/2009	22:51:41	IMG_2091.JPG	2744		
08/15/2009	22:34:36	IMG_1889.JPG	2696		
08/15/2009	22:02:24	IMG_1508.JPG	2874		
08/15/2009	22:21:55	IMG_1739.JPG	2751		
08/15/2009	21:48:48	IMG_1347.JPG	2829		
08/15/2009	23:03:56	IMG_2236.JPG	2832		
08/15/2009	22:34:41	IMG_1890.JPG	2674		
08/15/2009	22:02:29	IMG_1509.JPG	2885		
08/15/2009	22:21:50	IMG_1738.JPG	2747		
08/15/2009	22:51:35	IMG_2090.JPG	2751		
08/15/2009	21:48:42	IMG_1346.JPG	2820	24.7	75.3
08/15/2009	21:31:38	IMG_1144_1.JPG	2807		

08/15/2009	23:04:01	IMG_2237.JPG	2841		
08/15/2009	22:34:46	IMG_1891.JPG	2658		
08/15/2009	22:02:34	IMG_1510.JPG	2895		
08/15/2009	22:21:45	IMG_1737.JPG	2740		
08/15/2009	22:51:30	IMG_2089.JPG	2759		
08/15/2009	21:31:43	IMG_1145_1.JPG	2812		
08/15/2009	21:48:37	IMG_1345.JPG	2809		
08/15/2009	23:04:06	IMG_2238.JPG	2859		
08/15/2009	22:02:39	IMG_1511.JPG	2902		
08/15/2009	22:34:51	IMG_1892.JPG	2648		
08/15/2009	21:31:48	IMG_1146_1.JPG	2811		
08/15/2009	22:51:25	IMG_2088.JPG	2773		
08/15/2009	22:21:40	IMG_1736.JPG	2733		
08/15/2009	21:48:32	IMG_1344.JPG	2796	**25**	**75**
08/15/2009	23:04:11	IMG_2239.JPG	2881		
08/15/2009	22:02:44	IMG_1512.JPG	2902		
08/15/2009	22:34:56	IMG_1893.JPG	2645		
08/15/2009	21:31:53	IMG_1147_1.JPG	2811		
08/15/2009	22:51:20	IMG_2087.JPG	2791		
08/15/2009	22:21:35	IMG_1735.JPG	2740		
08/15/2009	21:48:27	IMG_1343.JPG	2794		
08/15/2009	23:04:16	IMG_2240.JPG	2903		
08/15/2009	22:02:49	IMG_1513.JPG	2896		
08/15/2009	22:35:01	IMG_1894.JPG	2649		
08/15/2009	21:31:58	IMG_1148_1.JPG	2816		
08/15/2009	22:51:15	IMG_2086.JPG	2804		
08/15/2009	22:21:30	IMG_1734.JPG	2755		
08/15/2009	21:48:22	IMG_1342.JPG	2799	47.4	52.6
08/15/2009	22:02:54	IMG_1514.JPG	2891		
08/15/2009	22:35:06	IMG_1895.JPG	2647		
08/15/2009	21:32:03	IMG_1149_1.JPG	2824		
08/15/2009	22:51:10	IMG_2085.JPG	2807		
08/15/2009	22:21:25	IMG_1733.JPG	2767		
08/15/2009	21:48:17	IMG_1341.JPG	2803	19	81
08/15/2009	22:02:59	IMG_1515.JPG	2893		
08/15/2009	22:35:11	IMG_1896.JPG	2638		
08/15/2009	21:32:09	IMG_1150_1.JPG	2822		
08/16/2009	17:59:23	IMG_1260.JPG	2262		
08/15/2009	22:51:05	IMG_2084.JPG	2805		
08/15/2009	22:21:20	IMG_1732.JPG	2779		

08/15/2009	22:03:04	IMG_1516.JPG	2891		
08/15/2009	22:35:16	IMG_1897.JPG	2623		
08/16/2009	17:59:28	IMG_1261.JPG	2258		
08/15/2009	21:48:12	IMG_1340.JPG	2808	**46.8**	**53.2**
08/15/2009	21:32:14	IMG_1151_1.JPG	2814		
08/15/2009	22:51:00	IMG_2083.JPG	2805		
08/15/2009	22:03:09	IMG_1517.JPG	2889		
08/15/2009	22:21:15	IMG_1731.JPG	2788		
08/15/2009	21:48:07	IMG_1339.JPG	2809		
08/15/2009	21:32:19	IMG_1152_1.JPG	2808		
08/15/2009	22:50:55	IMG_2082.JPG	2812		
08/15/2009	22:21:10	IMG_1730.JPG	2798		
08/15/2009	22:03:15	IMG_1518.JPG	2896		
08/15/2009	21:32:24	IMG_1153_1.JPG	2800		
08/15/2009	21:48:02	IMG_1338.JPG	2812		
08/15/2009	22:50:50	IMG_2081.JPG	2820		
08/15/2009	22:03:20	IMG_1519.JPG	2906		
08/15/2009	21:32:29	IMG_1154_1.JPG	2793		
08/16/2009	17:58:58	IMG_1255.JPG	2288		
08/15/2009	21:47:57	IMG_1337.JPG	2822		
08/16/2009	17:58:52	IMG_1254.JPG	2302		
08/16/2009	17:58:47	IMG_1253.JPG	2311		
08/15/2009	22:50:45	IMG_2080.JPG	2826		
08/15/2009	22:50:40	IMG_2079.JPG	2833		

Appendix 3: Processed Images for the infestation analysis across Buck Mountain.

Image	Present	Absent	Image	Present	Absent	Image	Present	Absent	Image	Present	Absent	Image	Presen	Absen	Image	Present	Absent
IMG_1340.JPG	46.8	53.2	IMG_1515.JPG	10.9	89.1	IMG_1868.JPG	43.6	56.4	IMG_2089.JPG	40.9	59.1	IMG_2232.JPG	14.8	85.2	IMG_2570.JPG	27.1	72.9
IMG_1342.JPG	47.4	52.6	IMG_1516.JPG	49.1	50.9	IMG_1870.JPG	41.2	58.8	IMG_2091.JPG	46.3	53.7	IMG_2234.JPG	25.9	74.1	IMG_2572.JPG	27.7	72.3
IMG_1344.JPG	25	75	IMG_1517.JPG	50.3	49.7	IMG_1872.JPG	29	71	IMG_2093.JPG	41.6	58.4	IMG_2236.JPG	29.7	70.3	IMG_2573.JPG	33.1	66.9
IMG_1346.JPG	24.7	75.3	IMG_1522.JPG	42.1	57.9	IMG_1874.JPG	31.5	68.5	IMG_2095.JPG	11.9	88.1	IMG_2238.JPG	28	72	IMG_2575.JPG	12.8	87.2
IMG_1348.JPG	30.9	69.1	IMG_1730.JPG	34.6	65.4	IMG_1876.JPG	39.5	60.5	IMG_2097.JPG	48.8	51.2	IMG_2240.JPG	38.9	61.1	IMG_0275.JPG	28.2	71.8
IMG_1350.JPG	46.1	53.9	IMG_1732.JPG	26.7	73.3	IMG_1878.JPG	40.5	59.5	IMG_2099.JPG	32	68	IMG_2242.JPG	36.8	63.2	IMG_2577.JPG	16.8	83.2
IMG_1352.JPG	20.4	79.6	IMG_1734.JPG	38.1	61.9	IMG_1880.JPG	33.7	66.3	IMG_2101.JPG	29.4	70.6	IMG_2434.JPG	29.6	70.4	IMG_0278.JPG	9.2	90.8
IMG_1354.JPG	19	81	IMG_1736.JPG	33.6	66.4	IMG_1882.JPG	39.5	60.5	IMG_2103.JPG	33.6	66.4	IMG_2436.JPG	24.3	75.7	IMG_0279.JPG	3.3	96.7
IMG_1365.JPG	35.3	64.7	IMG_1737.JPG	31	69	IMG_1884.JPG	30.1	69.9	IMG_2105.JPG	40.8	59.2	IMG_2438.JPG	18.7	81.3	IMG_0282.JPG	11	89
IMG_1492.JPG	38	62	IMG_1738.JPG	9.9	90.1	IMG_1886.JPG	41.8	58.2	IMG_2107.JPG	49.4	50.6	IMG_2440.JPG	5.7	94.3	IMG_0284.JPG	20.5	79.5
IMG_1495.JPG	51.8	48.2	IMG_1739.JPG	16.5	83.5	IMG_1888.JPG	53.6	46.4	IMG_2109.JPG	45.5	54.5	IMG_2442.JPG	30.7	69.3	IMG_0287.JPG	9.2	90.8
IMG_1498.JPG	35.1	64.9	IMG_1741.JPG	46	54	IMG_1890.JPG	41	59	IMG_2111.JPG	44.2	55.8	IMG_2444.JPG	35.1	64.9	**Average Total**	**32.974**	**67.026**
IMG_1501.JPG	33.5	66.5	IMG_1743.JPG	30.7	69.3	IMG_1892.JPG	44.3	55.7	IMG_2212.JPG	38.4	61.6	IMG_2446.JPG	10.7	89.3			
IMG_1503.JPG	48.1	51.9	IMG_1745.JPG	49.4	50.6	IMG_1894.JPG	36.6	63.4	IMG_2214.JPG	38.9	61.1	IMG_2448.JPG	39	61			
IMG_1505.JPG	22.6	77.4	IMG_1747.JPG	30.4	69.6	IMG_1896.JPG	33.4	66.6	IMG_2216.JPG	40.7	59.3	IMG_2450.JPG	37.7	62.3			
IMG_1508.JPG	41.2	58.8	IMG_1749.JPG	15	85	IMG_1898.JPG	39.9	60.1	IMG_2220.JPG	39.7	60.3	IMG_2561.JPG	21.4	78.6			
IMG_1511.JPG	44.9	55.1	IMG_1751.JPG	32.2	67.8	IMG_2079.JPG	34.7	65.3	IMG_2222.JPG	41.4	58.6	IMG_2562.JPG	20.9	79.1			
IMG_1513.JPG	18	82	IMG_1753.JPG	20.1	79.9	IMG_2081.JPG	39.3	60.7	IMG_2224.JPG	49.7	50.3	IMG_2563.JPG	31.9	68.1			
IMG_1514.JPG	41.7	58.3	IMG_1754.JPG	23	77	IMG_2083.JPG	40	60	IMG_2226.JPG	46.7	53.3	IMG_2564.JPG	32	68			
IMG_1515.JPG	10.9	89.1	IMG_1755.JPG	20.3	79.7	IMG_2085.JPG	44	56	IMG_2228.JPG	38.7	61.3	IMG_2566.JPG	34.3	65.7			
IMG_1516.JPG	49.1	50.9	IMG_1866.JPG	51.4	48.6	IMG_2087.JPG	41.1	58.9	IMG_2230.JPG	32.1	67.9	IMG_2568.JPG	33.2	66.8	**Average Total**	**32.974**	**67.026**